CALIFORNIA ENERGY COMMISSION

California Energy Commission

CONSULTANT REPORT

Geothermal Exploratory Drilling, Surprise Valley

Prepared for: **California Energy Commission**
Prepared by: **Warner Mountain Energy Corporation for Modoc County**

September 2023 | CEC-300-2023-007

California Energy Commission

Primary Authors:

Lisa Safford Kuscu; Ismail Kuscu, Ph.D.; Leland Mink, Ph.D.; Curtis Rose
Warner Mountain Energy Corporation
67254 State Highway 299 East
Cedarville, CA 96104 www.warnermountainenergy.com

Nicholas Davatzes, Ph.D.
Temple University
1901 N. 13th Street
EES, Beury Hall, Rm. 307
Philadelphia, PA 19122 https://sites.temple.edu/ncdavatzes

Richard Holt
Geothermal Science, Inc.
19800 MacArthur Blvd. Suite 300
Irvine, CA 92612 www.geothermalscience.com

Contract Number: GEO-16-005

Prepared for:
California Energy Commission

Erica Loza (former manager, Elisabeth deJong)
Commission Contract Manager

Elizabeth Giorgi (former manager, Gina Barkalow)
Branch Manager

Armand Angulo
Deputy Director
Reliability, Renewable Energy & Decarbonization Incentives Division

Deana Carrillo
Director
Reliability, Renewable Energy & Decarbonization Incentives Division

Drew Bohan
Executive Director

ACKNOWLEDGEMENTS

Modoc County and Warner Mountain Energy Corporation kindly acknowledge Welsco Drilling Corporation, led by Augie Mariezcurrena, for all of its knowledge, cooperation, and diligence in drilling a successful well; David Anderson, head driller for Welsco Corporation; Virgil Welch of Welch Energy Services for his wealth of knowledge and experience leading to a successful drilling outcome; George Scheid for his drilling supervision, coordination, and dedication to the project during drilling; Jonathan Glen of the U.S. Geological Survey and Nick Davatzes of Temple University for their invaluable assistance in conducting geophysical logging, data analyses, and contributions to this report; Richard Holt of Geothermal Science for his guidance and knowledge in conducting a reservoir test and subsequent data analysis, reservoir modeling, and overall contributions to this report; Colog Inc. for its exceptional geophysical logging services; Well Analysis Corporation for its diligence in logging the well; Chester Robertson and the Modoc County Board of Supervisors for their continual support of geothermal exploration; and the Modoc County community for its participation in the team's public outreach events.

PREFACE

The California Energy Commission's (CEC) Geothermal Grant and Loan Program is funded by the Geothermal Resources Development Account and provides funding to local jurisdictions and private entities for a variety of geothermal projects.

Exploratory Geothermal Drilling, Surprise Valley is the final report for the Geothermal Grant and Loan Program Agreement Number GEO-16-005, conducted by Modoc County. The information from this project contributes to the goals of the Geothermal Grant and Loan Program to:

- Promote the use and development of California's vast geothermal energy resources.
- Address any adverse impacts caused by geothermal development.
- Help local jurisdictions offset the costs of providing public services necessitated by geothermal development.

For more information about the Geothermal Grant and Loan Program, please visit the Geothermal Grant and Loan Program Web page (https://www.energy.ca.gov/programs-and-topics/programs/geothermal-grant-and-loan-program) or contact the CEC's Reliability, Renewable Energy & Decarbonization Incentives Division at RREDIAnalytics@energy.ca.gov or at geothermal@energy.ca.gov

ABSTRACT

The Surprise Valley geothermal system in Cedarville (Modoc County) remains largely undeveloped but holds great potential for electrical energy production and direct use, given what is known about the resource. The California Energy Commission (CEC) funded this grant agreement to investigate the temperature and permeability of a deeper resource for energy production on the east side of the valley. Study methods included drilling an exploratory well to a targeted depth of 4,000 feet, mud logging, borehole geophysical logging, well testing, geochemical sampling, and reservoir modeling.

The research team initiated drilling May 15, 2019, and completed on June 8, 2019. The well, Warner Mountain Energy-Exploratory 1 (WME-E1), was drilled to a depth of 3,605 feet. WME-E1 is completed with 7" liner from 0-2,325 feet and 5" liner from 2,276 feet to 3,605 feet with 329 feet of perforated 5" liner placed in producing zones.

Reservoir testing and modeling show that WME-E1 can sustain the maximum artesian flow over 20 years or more. With additional production and injection wells, the Surprise Valley geothermal reservoir can sustainably support much higher levels of production. The productivity index of WME-E1 is among the highest level seen in the geothermal industry.

The reservoir supplying WME-E1 is a shallow and highly productive 230 °F high - temperature system, which makes it attractive in terms of production and injection drilling costs.

Geothermometry results indicate higher temperature potential. Deeper drilling could reveal a hotter, deeper reservoir and will help characterize the complex geological controls on the Surprise Valley geothermal system. A hotter resource will increase opportunities for Modoc County to apply the resource for economic development, build energy self-sufficiency and resiliency, and assist California in meeting its clean energy goals. Further, the study helps validate geothermal research methods and previous findings, build confidence and understanding about the geothermal potential, and, in turn, streamlines future exploration with reduced risk.

Keywords: Surprise Valley, geothermal, exploratory drilling, reservoir modeling, geophysical logging, geochemistry

Please use the following citation for this report:

Safford-Kuscu, Lisa, Leland Mink, Curtis Rose, Nicholas Davatzes, and Richard Holt. 2023. *Exploratory Drilling, Surprise Valley*. California Energy Commission. Publication Number: CEC-300-2023-007.

TABLE OF CONTENTS

LIST OF FIGURES

Page

LIST OF TABLES

Page

EXECUTIVE SUMMARY

Background

In 2014 the California Energy Commission (CEC) funded Modoc County to conduct geothermal exploration on the east side of Surprise Valley, including drilling temperature gradient holes and economic feasibility studies. The project is five miles east of Cedarville on private land owned by Warner Mountain Energy, a California-based company. The studies from this 2014 project included geologic, geochemical, geophysical, and thermal gradient drilling, which measures temperature and associated depth. The favorable results of the 2014 investigation resulted in the award of a second CEC grant in 2016 to conduct exploratory drilling and testing on the potential of Surprise Valley geothermal resource development.

Purpose and Need

Modoc County is identified as a disadvantaged community (DAC) according to the California Communities Environmental Health Screening Tool, CalEnviroScreen 3.0. The rate of unemployment in Modoc County as of February 2020 was 9.7 percent, whereas the overall California rate was 3.9 percent. Geothermal development has the potential to be an economic development opportunity for Modoc County.

Geothermal resources in Modoc County are used for space heating but not for electrical energy production. The project team sought to drill a geothermal exploratory well to obtain further knowledge about subsurface temperatures at various depths in the Surprise Valley geothermal field and estimate reservoir capacity and characteristics through well testing and reservoir modeling.

The need for this project was based on the following:

- Exploratory drilling is in the high-risk phase of geothermal development, and private investment is difficult to obtain in this high-risk phase of any geothermal project.
- Investors need confirmation of reservoir potential to invest in a project.
- Modoc County holds tremendous potential for renewable energy production using geothermal resources, but electricity is being supplied from out of state, largely from hydropower.
- Geothermal development means economic growth that could translate to economic development opportunities for Modoc County, which are very valuable given its DAC designation.
- Modoc County's energy supply reaches maximum capacity during summer irrigation season. Electrical power outages are traditionally a frequent occurrence throughout the year.
- Private investment is difficult to obtain in the high-risk phase of any geothermal project, the CEC grant provided the funding necessary to explore Geothermal development opportunities. Without this CEC grant, geothermal development in

Modoc County is not likely to advance in the foreseeable future. Exploratory drilling funding from other governmental sources is typically not available except for very specific project goals such as enhanced geothermal systems research.

Conclusions

The project drilled a geothermal exploratory well and obtained further knowledge of temperature and permeability with depth in the Surprise Valley geothermal field.

Warner Mountain Energy-Exploratory 1 (WME-E1) was drilled to a depth of 3,605 feet. The research team logged various subsurface characteristics during drilling — lithology, geophysical (temperature, caliper, natural gamma, acoustic borehole televiewer), pressure/temperature/spinner data logging after well stabilization, flow testing, brine and steam sample collection, and then reservoir testing and modeling after the well was completed. Maximum measured downhole temperature in WME-E1 is 230˚F (110˚C). The well flows under artesian pressure at nearly 500 gallons per minute meaning no pump is needed and showed no sign of slowing down after six hours of well testing.

The conditions of the geothermal reservoir that supply WME-E1 are shallow and highly productive which is promising for successful development. The well WME-E1 is capable of commercial-grade microgrid electrical energy production at a relatively shallow depth of roughly 2,300 feet.

The geothermal testing results indicate higher temperature potential. Geophysical testing reveals several prominent fault zones contributing to the prolific flow.

While this project is promising, the geothermal reservoir has lower temperatures than desired. The Surprise Valley geothermal system could be further characterized with deeper drilling in search for a hotter geothermal resource. A hotter resource will increase opportunities for Modoc County to develop the resource for economic development.

Public outreach and engagement conducted by primarily through public meetings, site tours, media releases, and newspaper articles helped inform the community about the project.

Benefits to California

Information gathered during this project provides flow and permeability data needed for preliminary geothermal resource development planning. Well testing reveals that the Surprise Valley geothermal system has the potential for large-scale direct use heating applications or electrical power supply development of a low- to medium-temperature resource. Without CEC funding, this information would not be known. As is, WME-E1 can produce about 0.5 megawatts of electrical power flowing under artesian conditions and has prolific direct-use potential, offsetting the need for other forms of energy.

This study indicates that resource development in Surprise Valley may help contribute to California's Renewables Portfolio Standards goals of 60 percent renewables by 2030, per California Senate Bill 100 (De León, Chapter 312, Statutes of 2016) or provide

micro-grid or other geothermal-related opportunities for this remote community. Many potential geothermal projects cannot continue because of the high risk associated with resource confirmation. This grant agreement provided a unique opportunity by reducing risk for further exploration and showing the potential to help meet California's renewable energy goals.

Private developers typically conduct geothermal exploration and keep exploration data private. Using CEC funding allows public access to the subsurface exploration data and methods that can help reduce risk in further exploratory efforts. Well drilling provided economic benefits to the local community both directly and indirectly. For example, nearly $70,000 was spent locally on various services and equipment.

Collaboration with the U.S. Geological Survey (USGS) provided an opportunity for the USGS to increase regional geologic information that builds on existing conceptual models of the valley. The study helps validate geothermal research methods and previous findings, build confidence and understanding about the geothermal potential, and, in turn, streamlines future exploration with reduced risk. Collaboration with Modoc County helps continue the synergy of geothermal development in the county and creates opportunities for public-private development partnerships. Geothermal development means economic development in terms of employment opportunities for Modoc County residents, increased spending in the local community, and increased tax revenues for the county. Additionally, energy security is becoming increasingly important, and this project provides data that support the creation of a local microgrid for community or private industry use to protect against.

CHAPTER 1: Introduction

Background

In 2014, the California Energy Commission (CEC) funded Modoc County to conduct geothermal exploration at the Surprise Valley site near Surprise Valley Hot Springs under Grant GEO-14-003. This project included geothermal exploration (two-meter probe temperature gradient survey, soil gas survey, shallow temperature probe augering, magnetotelluric survey, shallow seismic survey, geochemistry sampling and analysis, temperature gradient drilling of three wells, and well logging) and an economic feasibility study.

Temperature gradient drilling results showed favorable and consistent results among all three wells and therefore warranted a project to conduct deeper drilling and well testing.

Based on the results of the 2014 study, the CEC again funded Modoc County in 2016 under Grant GEO-16-005 to conduct exploratory drilling to further investigate the geothermal resource characteristics of the Surprise Valley geothermal field.

Project Purpose and Need

This project sought to drill a geothermal exploratory well to obtain further knowledge about subsurface temperature gradient with depth in the Surprise Valley geothermal field and estimate reservoir capacity and characteristics through well testing and reservoir modelling.

The need for this project was based on the following:

- Exploratory drilling is in the high-risk phase of geothermal development, and private investment is difficult to obtain in this high-risk phase of any geothermal project.
- Investors need confirmation of reservoir potential to invest in a project.
- Modoc County holds tremendous potential for renewable energy production using geothermal resources, but electricity is being supplied from out of state, largely from hydropower.
- Geothermal development means economic growth. Modoc County's economy is struggling and needs economic development opportunities. The rate of unemployment in Modoc County as of February 2020 was 9.7 percent, whereas the overall California rate was 3.9 percent.
- Modoc County's energy supply reaches maximum capacity during summer irrigation season. Blackouts are frequent throughout the year.

- Without this CEC project, geothermal development in Modoc County is not likely to move forward in the foreseeable future. Exploratory drilling funding from other governmental sources is typically not available except for very specific project goals, such as enhanced geothermal systems research.

Goals and Objectives

The goal of this exploratory drilling project was to generate well and reservoir data that can be used to attract geothermal development opportunities. Advancing the project to the stage of exploratory drilling reduces risk for geothermal development investors by adding value to the project. Ancillary goals included adding value to other potential geothermal development projects in Modoc County by proving the capabilities and extent of the resource, positioning Modoc County as a possible meaningful contributor to California's Renewables Portfolio Standard (RPS) requirements or, if unable to sell to an RPS-obligated entity, to contribute to the achievement of California's clean energy goals through a geothermal powered micro-grid or other geothermal-related opportunities. Further, the project goals included filling scientific data gaps existing on the east side of Surprise Valley, and creating economic growth opportunities for Modoc County.

Objectives of this project included: drilling to about 4,000 feet below ground surface (bgs); performing mud logging of the well cuttings, which helps identify zones and extent of mineral alteration in turn indicating geothermal activity; obtaining a geophysical borehole log to identify physical and chemical characteristics of the formation such as flow zones, fractures, resistivity, and permeability; and logging temperature gradients in the well. Reservoir modeling of the drilling data provided information for forecasting reservoir characteristics and performance.

Project Location

Modoc County's exploratory geothermal drilling project is the east-central Surprise Valley of Modoc County, town of Cedarville, near Surprise Valley Hot Springs (SVHS) in Township 42 N, Range 17 E, Section 06, Modoc County, Mount Diablo Meridian (Figure 1).

The location is about 5 miles east of Cedarville along State Highway 299 and is situated on 800 acres of private land owned by Warner Mountain Energy Corporation and Surprise Valley Hot Spring Resort, California-based companies.

Figure 1: Project Location

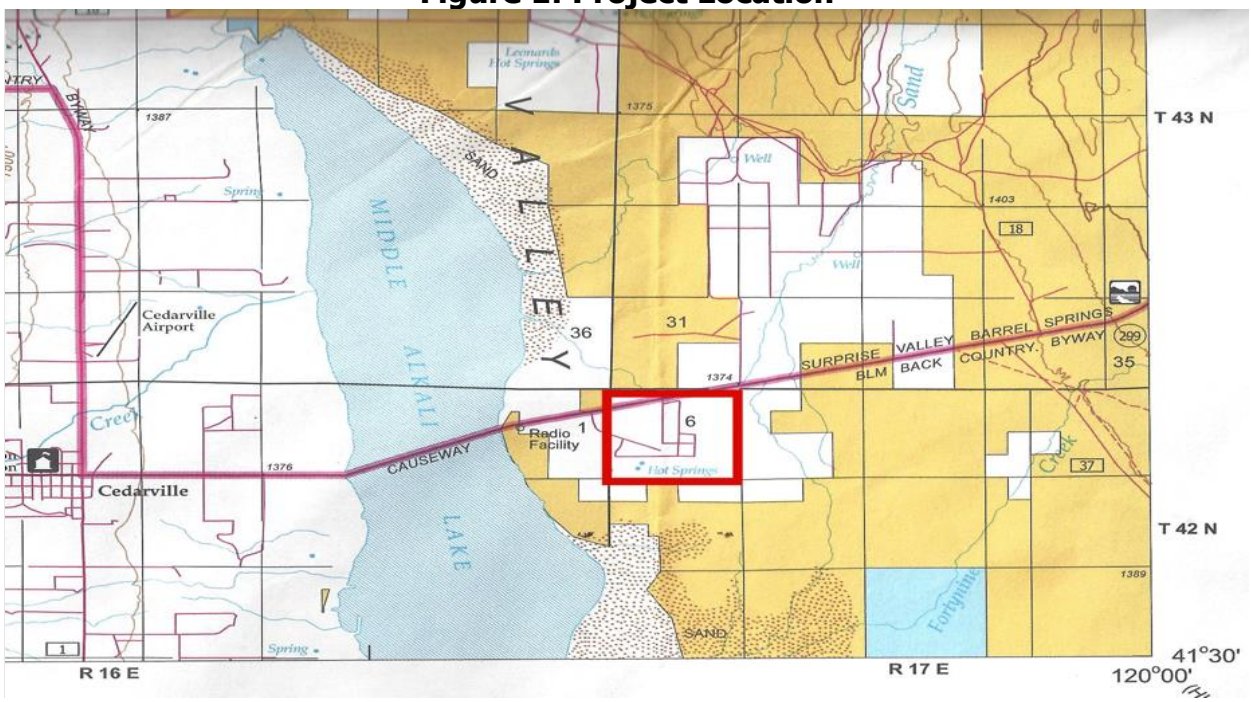

Source: U.S. Bureau of Land Management

CHAPTER 2:
Exploratory Drilling

Overview

Under GEO-16-005, Modoc County drilled an exploration well Warner Mountain Energy-Exploratory 1 (WME-E1) to further investigate the potential of geothermal development. Drilling operations commenced on May 15, 2019, and concluded on June 8, 2019, for a total of 25 days of drilling. The completed well is drilled to 3,605 feet bgs. The research team performed and completed mud, geophysical, and pressure/temperature/spinner logging.

Well-Drilling Collaborators

Well drilling requires many specialty companies that must coordinate to complete a drilling project successfully. For this project, Warner Mountain Energy Corporation (WME) managed and supervised all drilling. Welsco Drilling Corporation drilled the well; Horizon Well Logging performed mud logging; Colog performed downhole borehole geophysical logging (caliper, natural gamma, acoustic televiewer, and temperature); U.S. Geological Survey (USGS) oversaw and interpreted geophysical logging; and Well Analysis Corporation performed the pressure, temperature, spinner survey.

Well-Drilling Summary

Welsco Drilling worked with the California Division of Oil, Gas and Geothermal Resources on installation and testing of the blow out preventor (BOP) in getting the drilling started. Depth of surface 9-5/8" casing was cemented in at 616 feet bgs. Drilling activities proceeded as planned until 1,718–1,819 feet bgs, at which time the mud returns in the flow line reached 140˚F (60°C), a temperature threshold in the permit that required a mud cooling system to be brought on site and installed. Installation of the mud cooling system was completed and drilling continued. At around 1,835–1,900 feet bgs, minor losses of circulation occurred, but Welsco Drilling added drilling products to the well to effectively regain circulation. Drilling proceeded into basalt from 1,900–2,355 feet bgs. Depth of 7" casing was set and cemented at a depth of 2,325 feet bgs. At 2,355 feet bgs, total loss of circulation occurred. Several attempts to regain circulation of drilling fluids in the well were made without success. Blind drilling occurred from 2,355 feet to the bottom hole at 3,605 feet. Once the depth of 3,605 feet bgs was reached, Colog and the U.S. Geological Survey (USGS) began geophysical logging of the well (caliper, natural gamma, temperature, borehole) followed by data logs (caliper, temperature, natural gamma, and borehole [Figure 2]). Welsco Drilling initiated and completed the casing program upon final team decisions based on geophysical logging. A 5" slotted liner was hung from the 7" casing from 3,261 to 3,567 feet bgs. Welsco Drilling then rigged up to stimulate the well with air to conduct a well-cleanout test. Pressure and temperature measurements were recorded from the flow

line by Horizon Well Logging and monitored by Geothermal Science. During the well clean-out test, the well flashed and was flowing at about 450–500 gallons per minute (gpm) in Figure 3. Upon removal of the pipe, the well continued to flow under artesian conditions at about 450–500 gpm. After 1.5 hours of flowing, the well was shut in, testing equipment disconnected, and drilling operations ended.

Figure 2: Review of Geophysical Logs for Casing Program

Source: Curtis Rose, Warner Mountain Energy Corporation

Figure 3: WME-E1 Flashing During Well Clean-out Test

Source: Curtis Rose, Warner Mountain Energy Corporation

About one month after drilling activities ceased, Well Analysis Corporation conducted pressure, temperature, and spinner survey on WME-E1. The results of logging are discussed in the geophysical logging and reservoir model sections.

As a completed project, WME-E1 is shut in with access to being able to flow the well by a valve placed on the wellhead, and the vault in which the wellhead is placed is insulated and protected for security measures (Figure 4). WME and Welsco Drilling have removed all extraneous debris from the drill site.

Figure 4: WME-E1 Wellhead Flow Valve (left) and Secured Well (right)

Source: Curtis Rose, Warner Mountain Energy Corporation

The geographic coordinates of WME-E1 are latitude 41.535710 and longitude 120.073590. Site elevation is 4,516 feet above mean sea level.

Well Construction

Exploration well WME-E1 is completed as follows:

- 14” conductor casing from 0 to 81 feet
- 9-5/8” surface casing from 0 to 616 feet
- 7” casing (blank) from 0 to 2,325 feet
- 5” liner from 2,276 to 3,605 feet (perforated from 3,261 to 3,567. All other sections are blank.)

Well Logging

Parameters logged during drilling by Horizon Well Logging include drill rate, depth, lithology, fractures, mud loss, minerals, mud temperature, and gases. The drill rate, mud losses, mud temperatures, and gases contribute to the safety and oversight of drilling operations. Table 1 focuses on depth, lithology depth, fractures, and mineralogy.

Table 1: Well Lithology

Depth (ft. bgs)	Description
0–115	Gravel, clay, siltstone, sandstone, sand, and shale with quartz, calcite, pyrite, and hematite.
115–600	Andesite with quartz, calcite, pyrite, hematite, chlorite, and anhydrite. Fractures noted between 300 and 400 feet.
600–860	Welded tuff, clay, tuff, claystone, sandy clay, and claystone with minor quartz, pyrite, and chlorite.
860-1,070	Basalt with minor quartz, calcite, pyrite, hematite, and chlorite. Fractures noted between 920 and 970.
1,070–1,170	Andesite with clay. Quartz, calcite pyrite, chlorite.
1,170–1,380	Basalt with quartz, calcite, minor pyrite, hematite, chlorite.
1,380–1,430	Tuff, basalt, lithic tuff. Opal
1,430–1,460	Basalt
1,460–1,900	Tuff, lithic tuff, clay, rhyolite (1850-~1900). Fracture from ~1,840–1,900. Quartz, calcite, pyrite, hematite, chlorite, anhydrite. Losing mud circulation at 1,835–1,900.
1,900–2,355	Basalt with quartz, calcite, pyrite, hematite, chlorite, trace anhydrite
2,355–3,605	Total loss of circulation. Drill blind to bottom hole. Four 4,000-gallon water trucks running 24/7. Carbon dioxide gas present in varying levels. Drilling ceased at 3,605.

Source: Lisa Safford Kuscu, Warner Mountain Energy Corporation

Geological markers in WME-E1 include andesite (140 feet bgs), basalt (830 feet bgs), tuff (1,050 feet bgs), and basalt (1,900 feet bgs).

Although blind drilling occurred from 2,355 feet bgs to bottom-hole, a small rock chip (~1”x2” in size) was retrieved from the well in one of the geophysical logging tools when the tool was reeled back to the surface during well logging. The chip was analyzed by the USGS and determined to be of peridotite-serpentinite composition (Figure 5). The last known geologic unit prior to losing circulation was basalt. It is unknown where within the borehole the chip originated, presumably from the blind drilling zone. Peridotite is derived from the Earth's mantle, either as solid blocks and fragments, or as crystals accumulated from magmas that formed in the mantle. Peridotite is the dominant rock of the upper part of the Earth's mantle. Mantle material can be brought up as xenoliths in igneous bodies, country rock, and magma rising to

the surface. Xenoliths are different types of rock embedded in igneous rock bodies. Xenoliths are torn from deep cracks, or pipes, in the Earth's surface. Magma rises to the surface through these pipes between the Earth's crust and mantle. As the molten material rises, it tears off bits and pieces of the magma pipe in which it is traveling. These bits and pieces, trapped in the magma but not melting into it, become xenoliths. Given that drilling occurred within a dike system, it is possible that the chip was entrained in the dike material rising to the surface.

Figure 5: Peridotite-Serpentinite

Source: Lisa Safford Kuscu, Warner Mountain Energy Corporation

Geophysical Logging

Goals

The primary goals of geophysical logging were to measure (a) fracture population and (b) azimuth of the maximum horizontal compressive stress, S_{Hmax}. These measurements are correlated with the lithology and fluid entries along the well. Together, the natural fractures and constraints on the stress state provide a preliminary geomechanical model for the well.

Summary of Results

The population of natural fractures distributed along well WME-E1 was obtained from analysis of an acoustic image log of the borehole wall. The fractures display a wide range of attitudes in the imaged interval. Several prominent fault zones are encountered, which also coincide with zones of mud loss, anomalies in temperature gradient, and changes in natural gamma, including 810 meters (m) (2,657.5 ft), 894 m (2,933 ft), 1,001 m (3,284 ft), and 1,037 m (3402 ft) measured depth below the ground. Fractures and faults in the well display a wide range of attitude (or orientation), with the majority dipping 60°-90°.

Drilling induced structures including drilling induced tensile fractures (DITF) and break out (BO) document the local attitude of principal stresses. These constraints indicate the average direction of the maximum horizontal compressive stress, S_{Hmax}, is NNE-SSW (018.6 +/- 26.3º). This direction is slightly misaligned with the strike of the Surprise Valley fault, regional faults outside the valley, and dikes that outcrop to the southeast

(Athens et al., 2015). This may indicate a local stress state associated with a step in the magnetic anomaly where WME-E1 is located.

Detailed Results

Geophysical logs of WME-E1 were obtained by Colog geophysical field engineer Nolan Welsh in collaboration with Nick Davatzes of Temple University under the oversight of Lisa Safford Kuscu and Roy Mink of Warner Mountain Energy. Logging was conducted beginning the afternoon of June 5, 2019, and concluding midmorning of June 6, 2019. Prior to logging, no cuttings were obtained below 2360 ft bgs; the water level was approximately static and slowly rising. Within 24 hours after logging the well began to flow on its own. Table 2 shows key parameters for well WME-E1 and Table 3 shows a summary of geophysical logs obtained.

Table 2: WME-E1 Well Parameters

Parameter	Description
Wellhead Coordinates	(lat/lon) (41.535555,-120.07318333)
Elevation	4516 ft
Permanent Datum	Ground Level (GL)
KB (log ref depth)	10 ft + GL
Magnetic Declination	13.83˚
Drill Period	2019/05/18 to 2019/06/06
Casing Shoe depth (ft MD)	2314.4 (Image log)
Open Hole (ft MD)	2321.4 to 3554.2
Casing ID above open hole	6.538 in
Bit Size of open hole	6.125 in
Geophysical logs	Temperature, 3-Arm Caliper (unoriented), ABI43 Acoustic Borehole Televiewer (BHTV), Natural Gamma Ray
Run Date	Run 1: 2019/06/05-06
Deviation from vertical	Max: 39.1˚ (at base of hole), Median: 6.8˚
Mud log	Loss of returns below
Pressure history prior to logging	Prior to logging the well had not undergone lift or injection. However, loss of returns meant the water level had fallen below the surface.

Source: Nicholas Davatzes, Temple University

Caliper Log

Caliper logs use mechanical arms to measure the diameter of the borehole. The three-arm caliper in this study yields a single average measurement of borehole diameter derived from the radial measurements provided by each of the arms. In this analysis,

the caliper serves two purposes: (a) it indicates portions of the borehole that have expanded and (b) provides the calibration used to convert the two-way travel time of the acoustic pulse measured by the BHTV into a radial distance.

Natural Gamma Ray Log

The natural gamma ray tool measures the naturally occurring gamma radiation emanating from the rock comprising the borehole wall as the tool is pulled along the borehole. Gamma radiation is derived largely from the presence of potassium, as well as uranium and thorium. As a result, rock types rich in potassium such as felsic igneous rocks containing muscovite and feldspar or shale and mudstone containing clay minerals show relatively high count rates. Conversely, mafic dikes are associated with low gamma ray count rates.

Temperature Log

The temperature log is obtained by lowering and raising a thermistor within the borehole. This analysis includes temperature logs obtained in casing and the open-hole during or just after drilling. These measurements have been disturbed by circulation of drilling fluids and the ability of these fluids to leave along naturally occurring permeable and porous zones. Similarly, naturally occurring water may flow into the well. In this analysis, the primary use of the temperature logs is to identify the depth of major fluid exit and entry points along the well.

Image Log

Acoustic images of the WME-E1 borehole wall are obtained using the ABI43 Acoustic Borehole Televiewer. The ABI43 tool works by repeatedly sounding the borehole wall with an acoustic pulse, obtaining measurements of two-way travel time and amplitude ("loudness") from the resulting echo (Figure 6). About 144 pulses are generated per revolution, equivalent to 2.5º azimuthal resolution. For a borehole with an average diameter of 15.5575 cm (6.125 inches), this number is equivalent to 2 mm along the borehole circumference. Scans are completed every 0.1 ft (0.03058 m) along the borehole, providing a vertical resolution of 30.48 mm. A three-component magnetometer records the orientation of the image relative to magnetic north, while a three-component accelerometer records the tilt of the borehole in which the image is obtained and an orientation of the image relative to up (that is, the high side of the well).

Structures that roughen the borehole wall reduce the amplitude of the acoustic pulse. Structures that expand the diameter of the borehole wall lead to increased travel time and generally also decreased amplitude. These patterns provide the basis for interpreting the type of structure along the borehole, its position, and attitude.

Table 3: Summary of Geophysical Logs

Log type	Abbreviation	Tool	Logging Date	Depth Top (ft)	Depth Bottom (ft)
3-Arm Caliper	Cal	Comprobe Cal, 3ACC	2019/06/05	2315.5	3585.4
Natural Gamma	NG	Comprobe Gam, Hi-Temp	2019/06/05	2374.5	3585.4
Image	BHTV	ABI43	2019/06/06	2315.5	3553.9
Temperature	Temp	--	2019/06/05	0	3605.3

Source: Nicholas Davatzes, Temple University

Figure 6: Schematic Cross-Section Illustrating an Acoustic Borehole Televiewer (After Davatzes and Hickman, 2010)

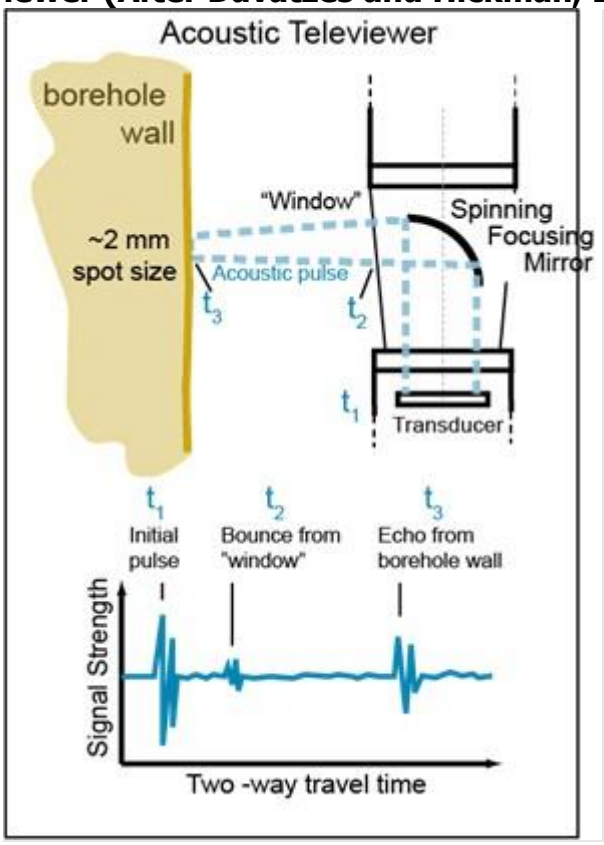

Image showing the method by which an acoustic borehole televiewer works. The instrument works by repeatedly sounding the borehole wall with an acoustic pulse, obtaining measurements of two-way travel time and amplitude ("loudness") from the resulting echo.

Source: Nicholas Davatzes, Temple University

Because of variation in borehole conditions, good images that can be interpreted are often not available throughout the logged interval. To avoid confusing regions of poor

image quality with the absence of interpretable structures, the quality of the image is mapped as summarized in Table 4.

Table 4: Image Quality

Quality Rank	Description
A	Highest quality with a clear and azimuthally complete image
B	Good image quality including greater than 80 percent image of the fracture wall
C	Less than 80 percent trace, image suffers from poor amplitude, repeated pixel traces where the tool was temporarily stuck (stick-slip) or decentralized image that distorts the fracture wall or a combination.
D	Uninterpretable image

Source: Nicholas Davatzes, Temple University

In WME-E1, the deeper section of the borehole includes extensive regions of poor image quality due to borehole expansion and stick-slip of the tool as it slid along the borehole, which distorts the image.

Image Log Interpretation

Two principal types of structures are evident in borehole image logs: (1) naturally occurring structures such as fractures or layering associated with bedding or foliation that constrain the geology and deformation history of the rock and (2) structures resulting from failure of the borehole wall that reflect the stress state acting on the walls of the well.

Natural Fractures

Planar structures intersecting the borehole such as fractures or layer boundaries form elliptical intersections. When the 360º image is unwrapped, these intersections are visible as sine waves (Figure 7). The low point of the wave indicates the dip direction. The dip is calculated from the diameter of the borehole and the amplitude of the sine wave. The diameter of the borehole is proportional to the velocity of the borehole fluid and the two-way travel time of the acoustic pulse. In this analysis, the diameter is obtained from the two-way travel time calibrated to (a) the average diameter provided by the caliper log and (b) the interior dimension of the casing.

Figure 7: Borehole Image Perspectives of Planar Structures

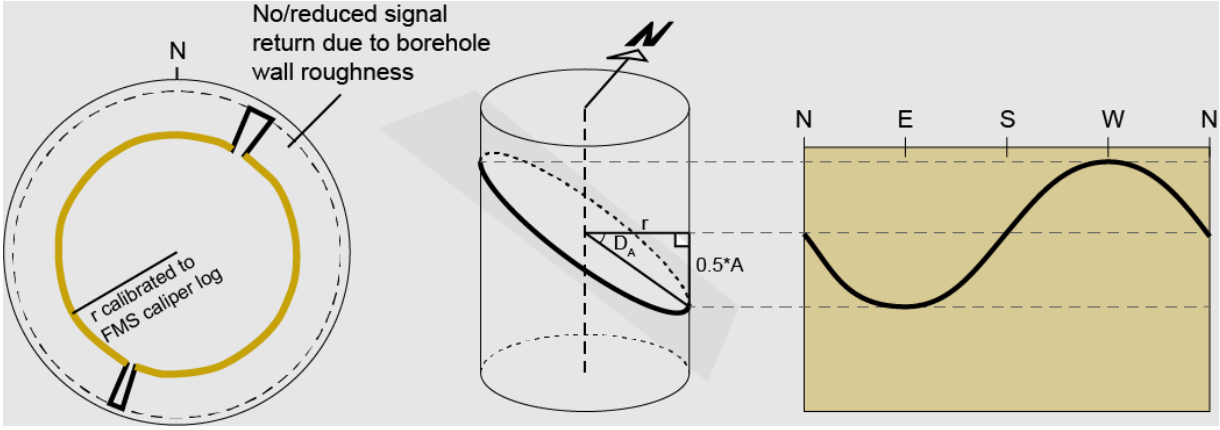

Left: Cross-section image of a borehole as imaged by a scan of acoustic pulses including where roughness scatters the pulse, leading to signal loss. Middle: Perspective view of the elliptical intersection of a planar structure imaged by a stack of scans. Right: Sine wave corresponding the planar structure in an unwrapped image of the borehole wall.

Source: Nicholas Davatzes, Temple University

Natural layering or the boundaries between rock types is typically evident in image logs (Figure 8). The planar boundaries form traces that separate regions of distinct image log character indicated by the textural uniformity (smoothness) and anisotropy (banding) of the image.

Figure 8: Borehole Image Logs

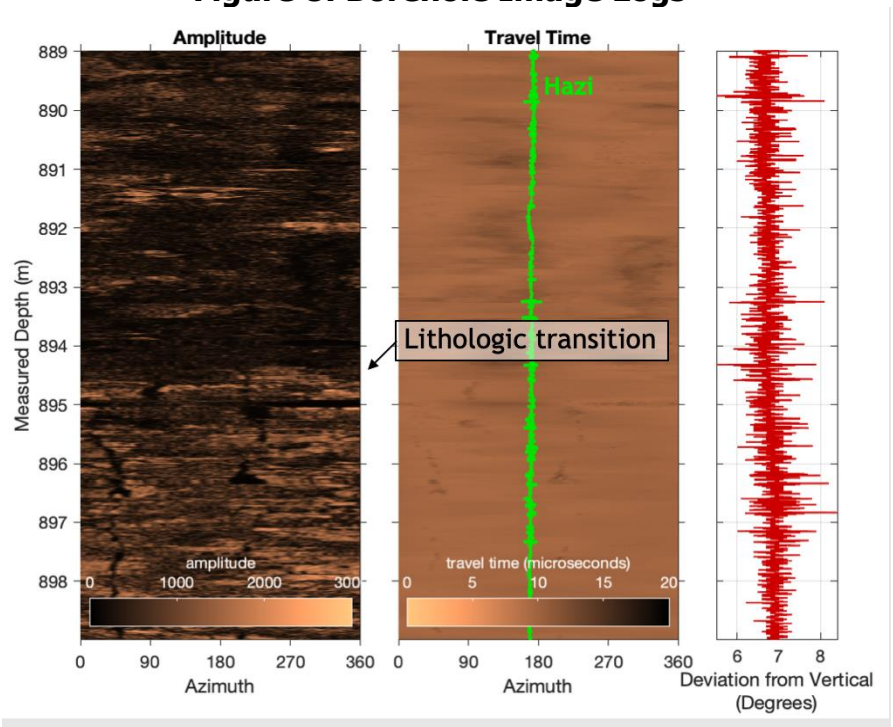

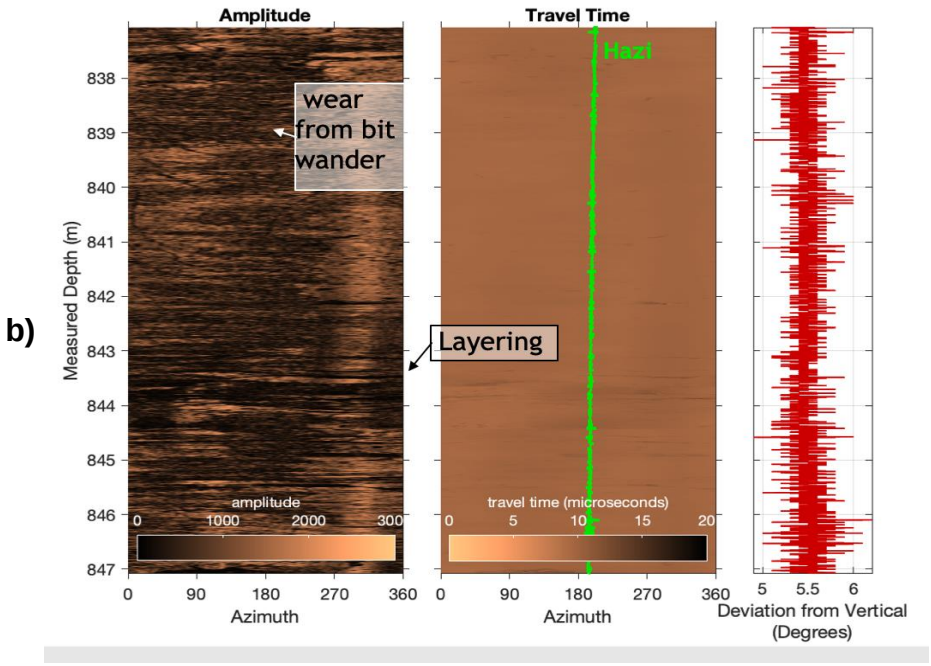

(a) Example of a lithologic transition (natural layering or boundaries between rock types) evident in the image log as noted on the image. Notice the difference in image quality above (quality B per Table 4) and below (quality C per Table 4) the lithologic transition. Also indicated is the azimuth in which the well deviations (Hazi) and the deviation of the well compared to vertical (Devi).

(b) Example of penetrative layering in the rock. Notice it has little to no effect on travel time although it is evident in the amplitude image.

Source: Nicholas Davatzes, Temple University

Fractures are discontinuities in the rock mass that appear as traces of low amplitude along the borehole wall (Figure 9). They accommodate opening or slip and typically display an increased in porosity (open space) that can focus fluid flow. This analysis distinguished small fractures, veins, and faults.

The trace of simple fractures appears as thin, continuous trace of low amplitude or signal loss along the borehole.

Veins show similar traces but show a central region of high amplitude.

Faults share one or more of the following features:

- Brecciation and locally high fracture density
- Offset of layering or other structures
- Thick traces at the borehole surfaces generally greater than a few millimeters and more irregular boundaries
- Expansion of the borehole diameter

Figure 9: Image Log Fractures

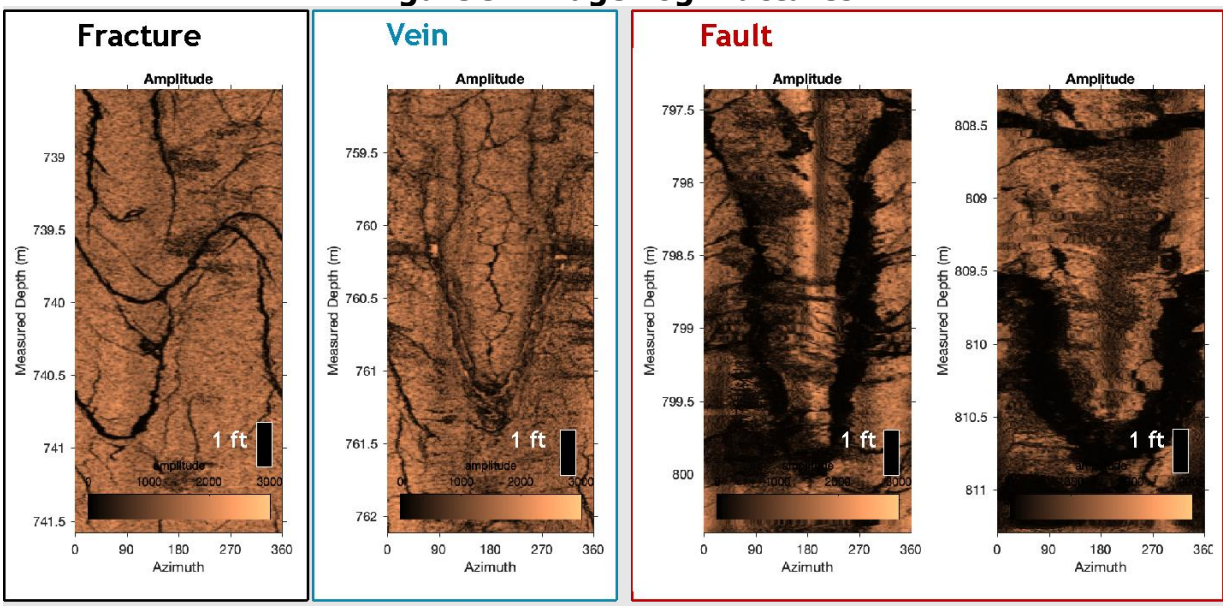

Typical natural fractures, veins (filled fractures), and faults evident in the image log of WME-E1 in the amplitude image obtained from the ABI43. See illustration in Figure 7.

Source: Nicholas Davatzes, Temple University

Attributes considered in interpretation of natural structures are show in Table 5.

Table 5: Attributes of Natural Structure Interpretation

Attribute	Description (Refer to Figure 7, Figure 8, and Figure 9)
Type	Primary Structure: rock type contact, internal layering Secondary Structure: fracture, vein, fault, brecciated fault, brecciated fault.
Attitude	Strike and dip of a plane fit to the sinusoidal trace.
Apparent Thickness	Thickness of trace along the borehole in mm. This is termed apparent as the structure may intersect the borehole at a non-90° angle and may be enhanced by erosion or damage at the intersecting; in either case, the thickness will exceed the true thickness of the structure.
Quality	Describes the reliability of the interpretation.

Source: Nicholas Davatzes, Temple University

In addition to interpreting the type of structure intersecting the well, the quality of that interpretation is assigned a grade of A, B, or C (Table 6).

Table 6: Quality Ranking of Natural Structure Interpretation

Quality Rank	Description
A	Unambiguous interpretation of type, complete trace, sine wave is well-constrained allowing accurate calculation of strike and dip

Quality Rank	Description
B	Unambiguous interpretation of type, greater than 75 percent trace, reliable strike and dip calculation because peak and trough of sign wave available for fitting
C	Less than 75 percent trace, increased uncertainty in attitude; still useful for analysis of fracture density

Source: Nicholas Davatzes, Temple University

Initially these structures are interpreted in the reference frame of the borehole defined by the borehole axis and magnetic north. Subsequently, the deviation direction recorded by the magnetometer and the deviation from vertical recorded by the accelerometer are used to transform these measurements to the east, north, and elevation geographic reference frame.

Borehole Indicators of Stress

The presence of a borehole intensifies the local stress state at the borehole wall to the point where it can overcome the rock strength and break the rock (for example, Zoback 2010) (Figure 10). The resulting damage to the borehole surface is typically visible in image logs or caliper logs (cartoon illustrated in Figure 11 with examples in Figure 12 and Figure 13). Since the amplification effect of the borehole is well-known, this damage provides a constraint on the direction in which the remote stresses act.

Assuming an Andersonian Stress state where the weight of rock corresponds to a principal stress (see discussion in Zoback, 2010), the remaining principal stresses are horizontal. Thus, in vertical wells (1) DITF of the borehole wall coincides with the azimuth of the maximum horizontal principal stress, S_{Hmax}, whereas (2) compressive failure leads to BO formation aligned with the azimuth of the least compressive horizontal principal stress, S_{Hmin} (Figure 10 and Figure 11). The characteristics of these structures is summarized in the Figure 11. Because the concentration of stress is symmetric, the borehole experiences the same concentration on opposite walls of the well. In general, if a borehole is in a relatively flat region and the borehole axis is less than 12°-15° from vertical, then this simple model applies (Peska and Zoback, 1995).

Combining these observations provides a summary of the stress directions. The average of all measurements along the borehole reflects the stress state in a volume that scales with the depth extent of the induced structures along the borehole. The standard deviation of this population describes the heterogeneity in the local stress state. In tectonically active regions, it is common for the local stress direction to oscillate because of slip and opening of natural fractures.

Figure 10: Stress State Around a Vertical Borehole

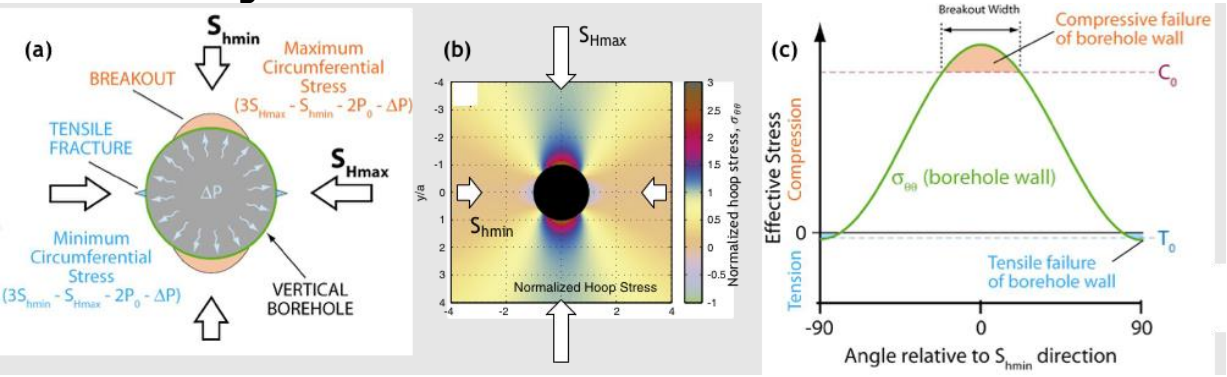

Stress state around a vertical borehole. (a) Stress at the borehole wall and in the surrounding volume results from the difference in the principal stresses, SHmax and SHmin, driving deformation, local temperature change and the balance of mud pressure to formation fluid pressure. (b) These stresses are amplified at and near the borehole so that the local stress components parallel to the borehole wall vary in magnitude as a function of the azimuth with respect to the remote principal stresses. (c) At the borehole wall, the azimuthal extent over which the hoop stress exceeds the uniaxial compressive strength of the rock leads to borehole breakout (orange); whereas tension can cause tensile failure. These failure sites occur in pairs 180° apart reflecting the symmetry of the borehole and stress state and uniquely define the azimuth of the remote principal stresses.

Source: Nicholas Davatzes, Temple University

Figure 11: Drilling Induced Tensile Fracture and Breakout Examples

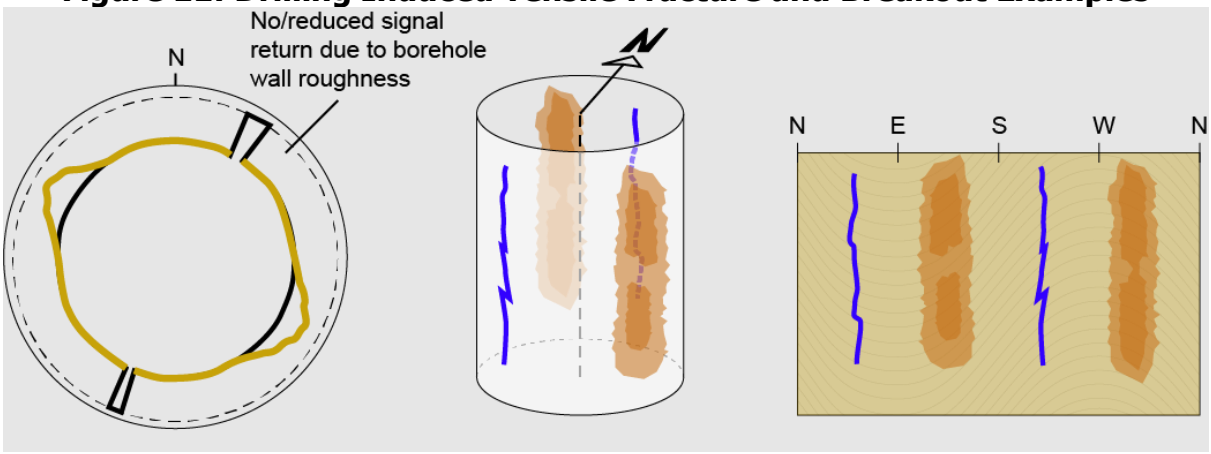

Illustration of the distribution and key geometric characteristics DITF in blue and patches of BO in orange resulting from uniaxial compressive failure in orange.

Source: Nicholas Davatzes, Temple University

Two other factors influence the stress state at the borehole wall: (a) temperature changes causing thermal strains and (b) the pressure of fluid in the borehole compared to the formation. Circulation of relatively cool water can induce thermal contraction along the borehole wall. This contraction induces tension which promotes DITF and suppresses BO (Figure 12 and Figure 13), whereas heating the well causes the complementary response. In WME-E1, prior to logging, water circulated for drilling exited the borehole at depth through loss zones; thus, the injection of relatively cool

water from the surface promoted thermal contraction of the borehole wall. Similarly, fluid pressure in the borehole pushes on its surface, stabilizing the borehole. If the pressure exceeds the pressure pushing back from the formation, it promotes expansion along the borehole wall and DITF while inhibiting BO. This difference is calculated as $\Delta P = P_m - P_f$, where P_m is the pressure of fluid in the borehole and P_f is the pressure of the fluid in the formation. However, if the fluid pressure in the well drops, then the borehole wall contracts, which promotes BO and inhibits DITF. In WME-E, loss of returns during drilling immediately before logging may indicate that the compressive stress along the borehole wall was enhanced, promoting breakout. However, the exact pressure history in the well is complicated by changes in the static water level during drilling and large changes in the fluid and rock temperatures.

These effects directly influence the magnitude of stress and thus failure of the borehole wall. Therefore, they must be considered when attempting to determine stress magnitude. Fortunately, these effects are uniform along the borehole wall and do not influence the relationship of BO and DITF azimuth with the directions the principal stresses act in the rock mass (example in Figure 13). This analysis is confined to the analysis of stress direction, which remains robust even for complicated borehole temperature and pressure history.

Figure 12: Examples of Breakouts Distributed Along the Borehole in Amplitude and Two-Way Travel Time

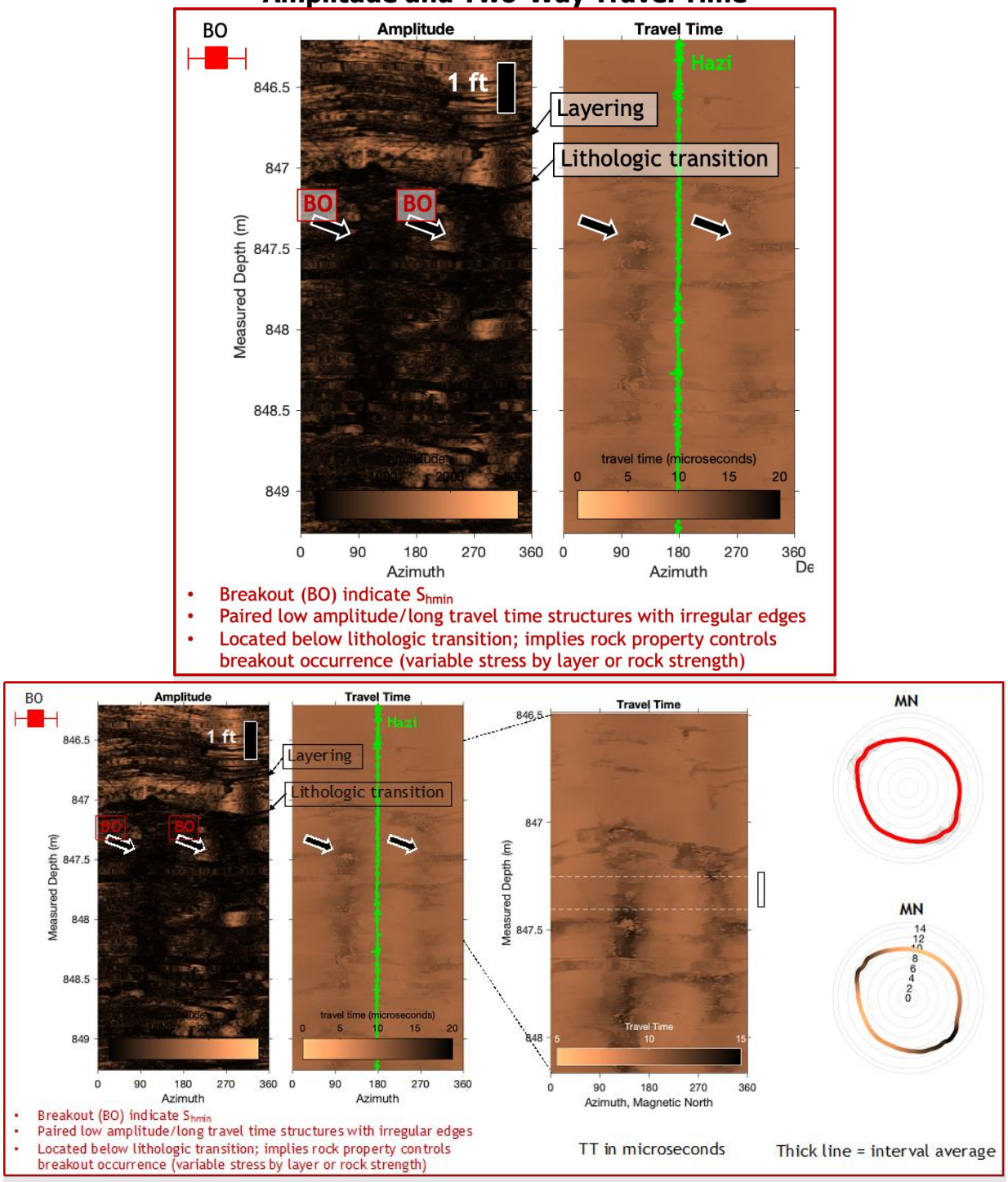

Examples of breakouts distributed along the borehole in amplitude (upper left) and two-way travel time (upper right). The breakouts are confined beneath a lithologic transition, consistent with a variation in rock strength controlling their distribution; see illustration in Figure 11. Image to right shows an expanded interval of two-way travel time and cross-sections of the borehole that clearly reveal characteristic breakout geometry.

Source: Nicholas Davatzes, Temple University

Figure 13: Examples of Drilling Induced Tensile Fracture

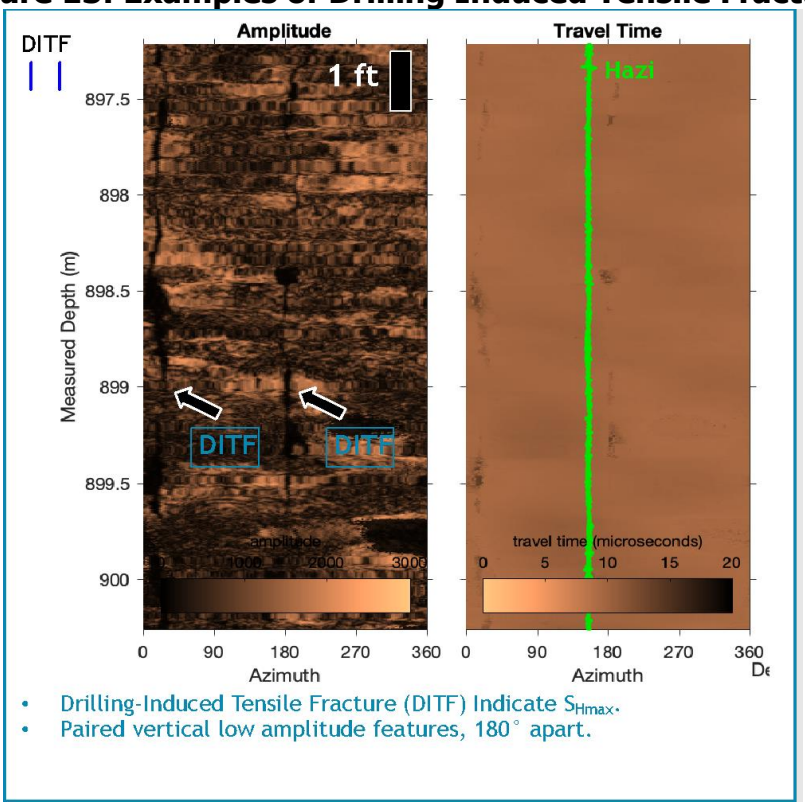

Example of DITF as pairs of cracks parallel to the borehole axis (vertical traces) in amplitude (left) and two-way travel time (right); see illustration in Figure 11.

Source: Nicholas Davatzes, Temple University

Table 7: Attributes of Drilling Induced Structures

Attribute	Description (refer to Figure 11, Figure 12, and Figure 13)
Type	BO: compressive failure of the borehole aligned with S_{hmin} DITF: tensile failure of the borehole wall
Attitude	Azimuth along the borehole wall
Quality	Describes the reliability of the interpretation.

Source: Nicholas Davatzes, Temple University

In addition to interpreting the type of drilling-induced structure along the well, the quality of that interpretation is assigned a grade of A, B, or C for quality assurance (Table 8 and Table 9) during the later analysis of the azimuth of the horizontal maximum compressive principal stress, S_{Hmax} .

Table 8: Quality Ranking of Drilling Induced Breakout of the Borehole Wall

BO Quality Rank	Description
A	Zones of low amplitude and long travel time (negative relief) aligned with the borehole axis, deepest in the center with irregular edges consistent with variation in rock strength along layering Occur in pairs 180° apart (These also provide a clear distinction from wear caused by the drill pipe.)
B	Single or poorly matched breakout, but which clearly demonstrates the other key geometric attributes
C	BO is compromised by proximity to another structure or image quality

Source: Nicholas Davatzes, Temple University

Table 9: Quality Ranking of Drilling Induced Tensile Fracture of the Borehole Wall

DITF Quality Rank	Description
A	Narrow cracks aligned with the borehole axis Occur in pairs 180° apart
B	Single or poorly matched breakout, but which clearly demonstrates the other key geometric attributes
C	DITF is compromised by proximity to another structure or image quality

Source: Nicholas Davatzes, Temple University

Geomechanical Analysis

Analysis of Natural Fractures

Fractures in WME-E1 show a wide range of attitude that loosely group around a representative Surprise Valley Fault (Figure 14). Fractures are abundant in the shallow, high-quality image log. At greater depth, fewer fractures were interpreted due to low image quality; this should not be taken as differing abundance of fractures along the well (Figure 15). In general, this analysis prioritizes interpretation quality over quantity and thus represents an underestimate of the fracture population. Most fractures are characterized by small apparent aperture (Figure 14, right) of a few millimeters or less, but a few prominent faults display larger apparent aperture up to nearly 100 millimeters. No association between attitude and aperture is apparent.

Figure 14: Stereograms of Natural Fractures

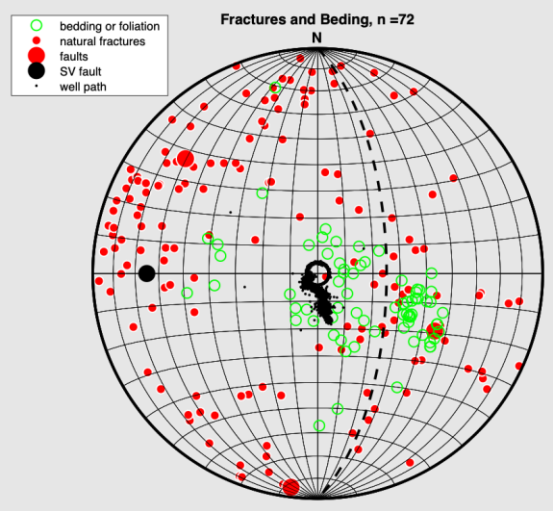

Stereogram of the natural fractures, faults, and layering interpreted from the image log. A representative Surprise Valley fault strike and dip are indicated by the heavy black circle and dashed great circle.

Source: Nicholas Davatzes, Temple University

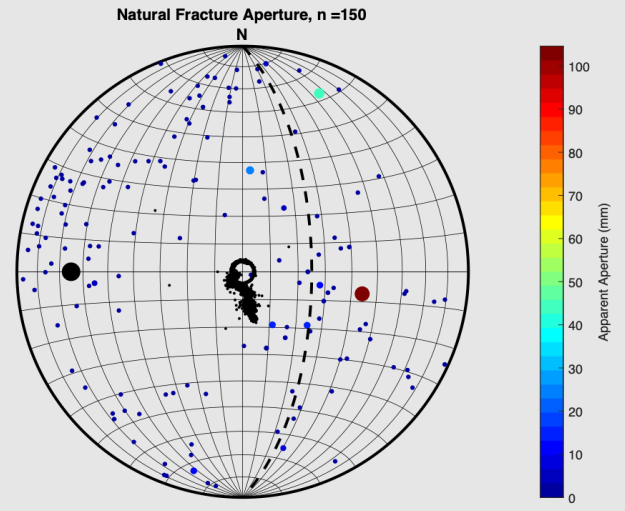

Stereogram illustrating the apparent thickness of natural fractures encountered along the well.

Source: Nicholas Davatzes, Temple University

Figure 15: Summary of Interpreted Natural and Induced Structures in a Modified Tadpole Plot

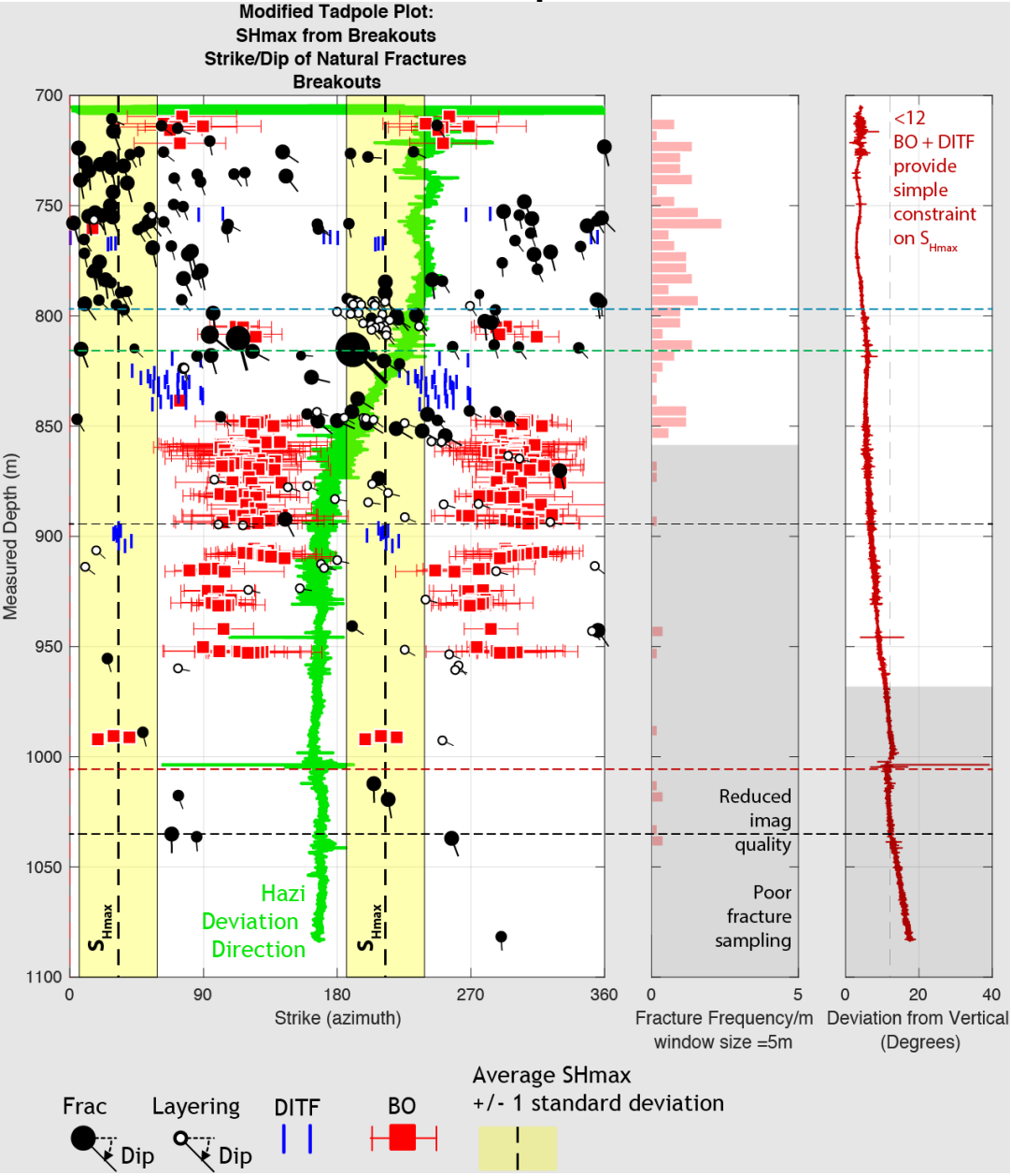

Summary of interpreted natural and induced structures in a modified tadpole plot.

Source: Nicholas Davatzes, Temple University

Analysis of Stress Indicators

Drilling induced structures indicate an average S_{Hmax} azimuth of 018.6 +/- 26.6° (Figure 16a). Notably, BO and DITF are distributed in distinct depth intervals distinguished by different rock types as implied by natural gamma and the quality of the image log (example in Figure 12, summarized in Figure 15). The relatively large rotations of up to 40° in proximity to large faults (Figure 15 and Figure 16), imply an actively deforming basin (Day-Lewis et al., 2010, Schoenball and Davatzes, 2017).

Figure 16: Rose Diagram and Depth Distribution of Structures

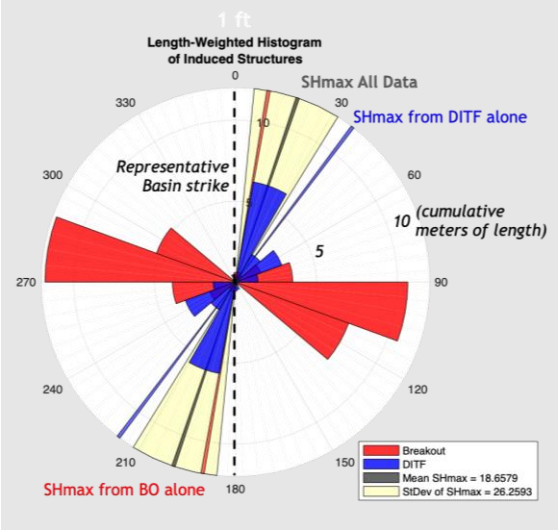

Rose diagram illustrating the azimuth of each interpreted drilling induced structure. The circular mean and standard deviation are indicated: BO (red), DITF (blue), all data (yellow).

Source: Nicholas Davatzes, Temple University

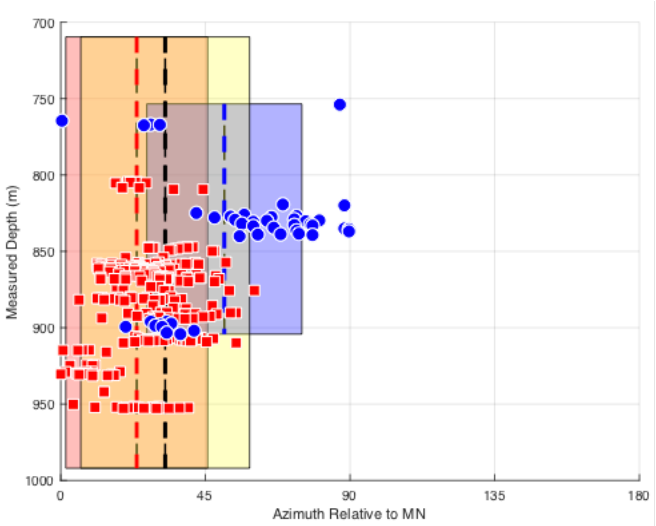

Analysis of the depth distribution of each drilling induced structure and the implied azimuth of SHmax (zero indicates true north). Each vertical dashed line indicates the circular mean and the width of the box is the circular standard deviation from BO (red), DITF (blue), all data (yellow). The analysis suggests significant depth heterogeneity.

Source: Nicholas Davatzes, Temple University

Borehole Condition

Caliper and image logs indicate the borehole is largely in gauge with only minor borehole enlargement. Several faults are associated with borehole enlargement (Figure 15) and degraded image quality due to stick-slip during the logging run below about 990 meters (m) measured depth (MD) and ground level (GL). The stick-slip also affected the temperature, natural gamma, and caliper logging runs. The stick-slip appears to result from the combination of a roughened borehole surface and increased

deviation from vertical; this portion of the hole is now behind a series of slotted and blank liners.

Deviation from vertical in the borehole begins in the region of extensive breakout from 850 to 950 m MD GL and again at 1000 m MD GL at a prominent enlargement in the borehole associated with a fault and water entry (Figure 15, Figure 17). Breakouts are promoted when the rock is relatively weak. In WME-E1, breakouts are confined within lithologic units (Figure 12) and typically occur in intervals of poor image log quality even outside the breakout footprint. Together, these relationships imply a reduction in rock strength influencing borehole deviation. At 1000 m MD GL, the BHTV became stuck on a large structure. The reduction image quality means the attitude of this structure is not known, but it is likely the structure is responsible for the change in borehole deviation.

Geomechanical Synthesis

The nonequilibrium temperature logs reveal several exit points presumably responsible for the loss of returns in WME-E1 (Figure 17). These points are indicated by inflections in the temperature distribution. Images at each major zone indicate the presence of large structures or lithologic transitions, which are further supported by variation the natural gamma ray count and the magnetic field strength recorded by the magnetometer in the BHTV. The panel plot (Figure 17) indicates that these exit points are consistently associated with faults that strike approximately parallel to S_{Hmax}, consistent with normal faulting.

The azimuth of S_{Hmax} at WME-E1 is misaligned with azimuth expected from geologic indicators including the Surprise Valley normal fault, recent fault scarps, the surrounding regional faults (Egger and Miller, 2010; Egger et al., 2011; 2014), and dikes (personal comm. J. Glen; Athens et al., 2015) (Figure 18). However, if recently active, both fault slip and dike dilation can affect the stress conditions at depth. This situation provides a potential explanation for both the measured S_{Hmax} azimuth and the wide range in measured fracture attitude.

Figure 17: Temperature Logs Showing Exit Points for Loss of Returns

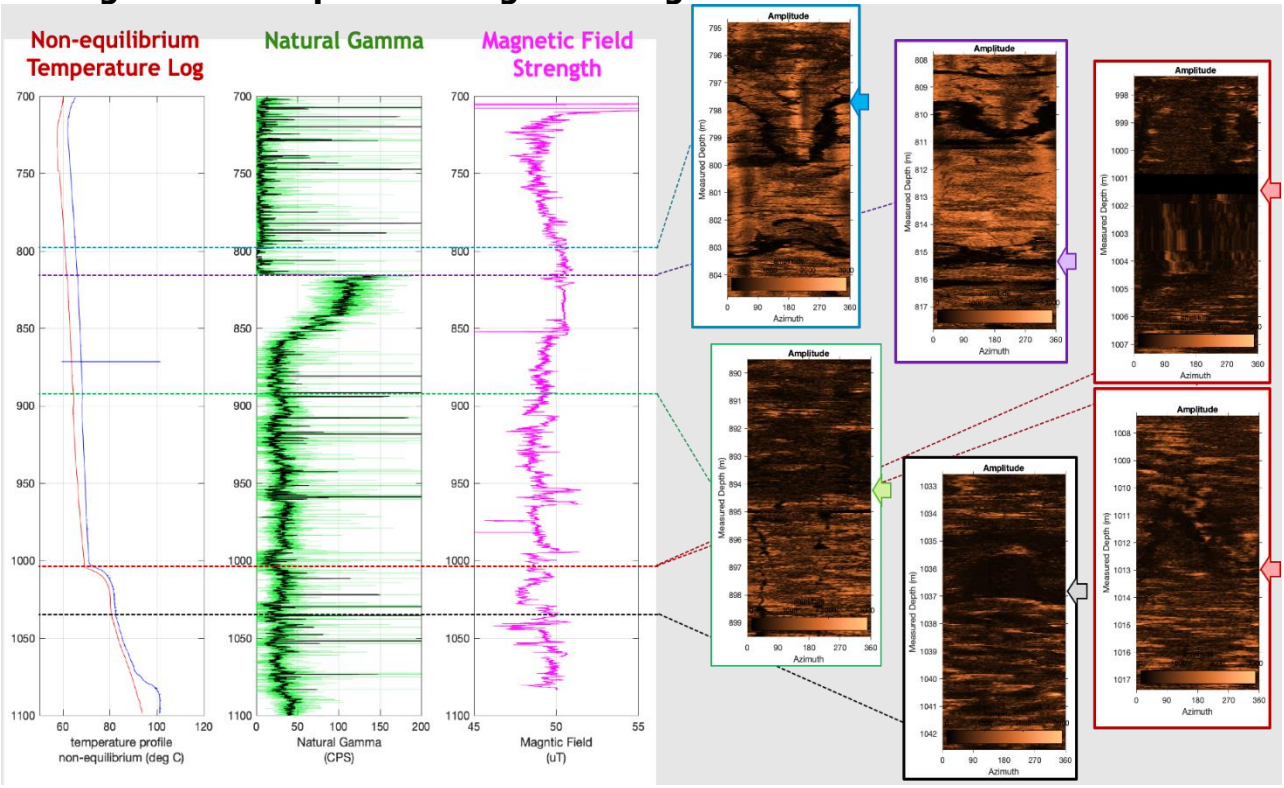

Figure 17 includes logs for non-equilibrium temperature, natural gamma, and magnetic field strength data with more detailed images of exit points for loss of returns during drilling. Temperature logs reveal several exit points, indicated by arrows on the borehole images, presumably responsible for the loss of returns in WME-E1.

Source: Nicholas Davatzes, Temple University

Figure 18: Geologic Map and Magnetic Survey

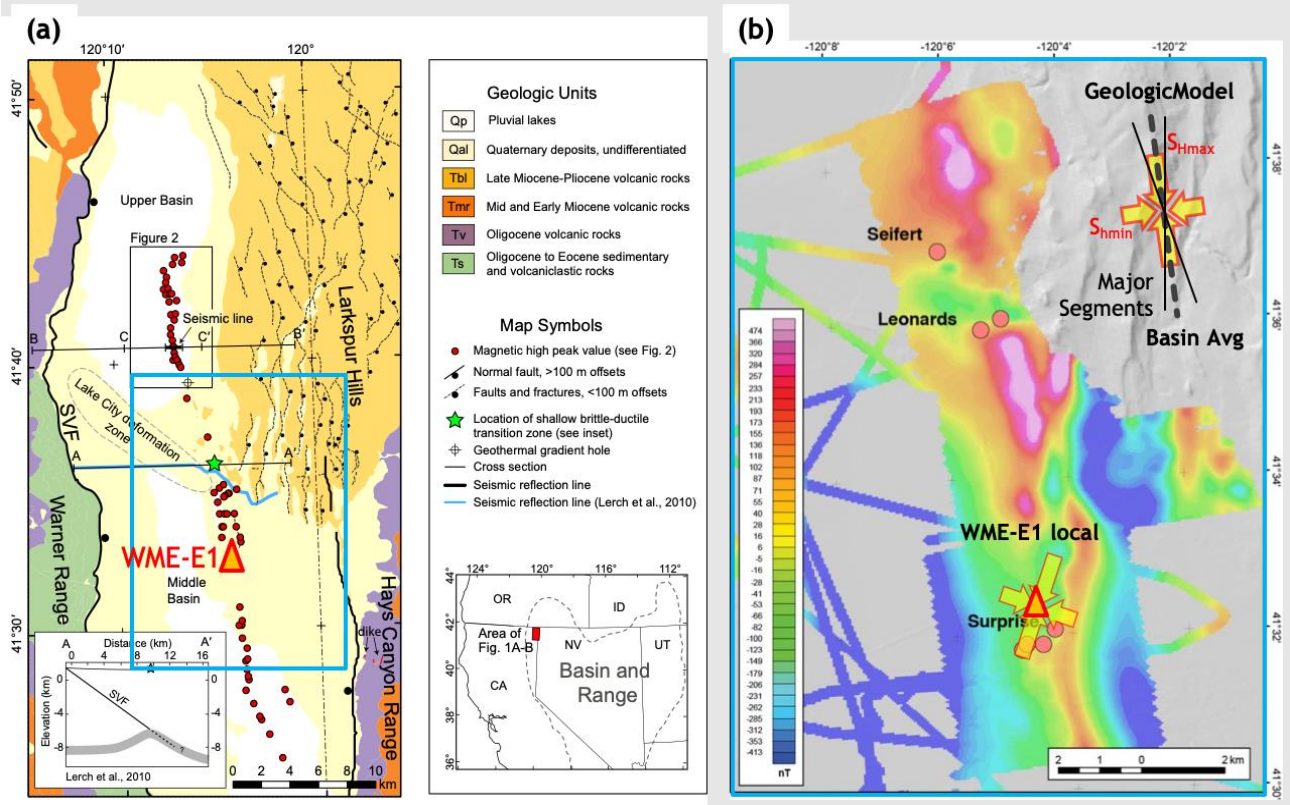

Geologic map of Surprise Valley including major faults and a series of local magnetic anomalies attributed to an array of sub-cropping dikes (Athens et al., 2015; (b) Detailed magnetic survey in the vicinity of WME-E1. The local stress state inferred from borehole wall failure is plotted. Inset is the regional geological model for inferred from the strike of major regional structures including the Surprise Valley Fault.

Source: Nicholas Davatzes, Temple University

Geochemistry

Methods

Brine and steam samples were collected from WME-E1 on July 13, 2019, in clean plastic and glass bottles. Field pH and conductivity measurements were not obtained. Samples for cation and trace element analysis were filtered and acidified in the field. Samples for stable isotope, anion, pH, and conductivity analyses were filtered in the field but not acidified. Samples were refrigerated pending analysis. Samples were later analyzed by the USGS laboratory.

The well had been purged of more than eight volumes of water and was flowing under artesian conditions at about 450-500 gpm when the samples were collected. The fluids were clear and no odor detected. Geothermal fluid temperature at the time of sample collection was 208˚F.

Fluid was collected with a beaker taped onto a stick to be able to safely reach the hot flow, filtered and transferred to sample containers. Water quality parameters were not collected on site. Sample point was from discharge of flash chamber into the weir.

Brine samples were collected directly from the discharge point of the flash chamber into the weir and then into the mud sump. Steam samples were collected via coiled copper tubing (Figure 19) plumbed into a flash chamber being used to divert water to the weir and then the mud sump. The copper tubing was situated in a bucket with ice to allow the fluids to condense for collection of the steam component.

Figure 19: Steam Collection Through Copper Tubing

Left: Copper tubing plumbed into flash chamber. Right: Blue tarp covering bucket with copper tubing filled with ice and plumbed into flash chamber.

Source: Lisa Safford Kuscu, Warner Mountain Energy Corporation

Results

Geochemistry parameters for WME-E1 brine and steam are shown in Table 10. For a point of reference, results of the SVHS well and the Warner Mountain Energy temperature gradient #2 (WME-TG2) well are provided.

Table 10: Geochemistry Parameters

Parameter	Units	WME-E1 Brine	WME-E1 Steam	SVHS Well	WME-TG2
Easting	UTM	744152	744152	743766	744152
Northing	UTM	4602360	4602360	4602055	4602360
Elevation	m	1376	1376	1373	--
Temperature	°C	98	--	97	~50
Conductivity (Field)	mS	--	--	1.372	--
Conductivity (Lab)	mS	1.45	--	--	--
pH (Field)	pH	--	--	8.46	--
pH (Lab)	pH	8.6	--	8.64	8.6

Parameter	Units	WME-E1 Brine	WME-E1 Steam	SVHS Well	WME-TG2
Stable Isotopes					
δ^2H	VSMOW	-117	-149	-119.2	-116.4
$\delta^{18}O$	VSMOW	-13.4	-19.4	-14.3	-14
Major Elements (ICP-MS)					
Si	mg/L	110	--	44.8	44.6
Na	mg/L	280	--	266	282
K	mg/L	6.5	--	5.2	5.4
Ca	mg/L	26.7	0.3	16.7	19.2
Mg	mg/L	0.1	0.03	0.03	0.12
Major Elements					
B (Soluble)	mg/L	6	--	5.9	5.8
Cl	mg/L	190	0.05	178	186
SO_4	mg/L	343	0.13	327	333
NO_3	mg/L	0.03	--	<	<
HCO_3	mg/L	67.3	--	36.6	48.8
CO_3	mg/L	--	--	9	9
Trace Elements					
Al	ug/L	100	0	51.7	163
As	ug/L	288	1	191	71
Ba	ug/L	20	0	5.8	6.1
Cd	ug/L	0	1	0.05	0.02
Co	ug/L	0	0		--
Cr	ug/L	0	0	0.05	0.23
Cs	ug/L	--	--	9.4	11.8
Cu	ug/L	0	577	0.17	0.31
Fe	ug/L	0	0	1.08	2682
Li	ug/L	110	0	85.1	90.8
Mn	ug/L	0	3	0.6	110.4
Mo	ug/L	34	0	33	20.9
Ni	ug/L	0	2	--	--
NO3	ug/L	30	0	--	--
P	ug/L	--	--	8.1	52.7
PO4	ug/L	30	110	--	--
Pb	ug/L	--	--	<	2.3
Rb	ug/L	0	0	18.8	21
Sb	ug/L	--	--	3.5	2.7
Se	ug/L	0	0	2.7	--
Sr	ug/L	259	1	219	155
U	ug/L	--	--	<	0.01
V	ug/L	--	--	0.39	0.89

Parameter	Units	WME-E1 Brine	WME-E1 Steam	SVHS Well	WME-TG2
Zn	ug/L	0	113	1.1	82

Source: Richard Holt, Geothermal Science

Temperature Gradient Logging

WME logged WME-E1 for temperature gradient (Table 11) on August 10, 2019. WME-E1 had stabilized for 60 days before this logging event. Temperature gradient logging shows the well heating up rapidly in the first 300 feet bgs, going isothermal for about 200 feet, then indicating a second heating trend to about 2,262 feet. After 2,262 feet, the well shows a slight reversal and then becomes isothermal. The highest temperature recorded in logging is 230.5˚F from 2,000 to 2,100 feet bgs.

Figure 20: Temperature Gradient Log of WME-E1

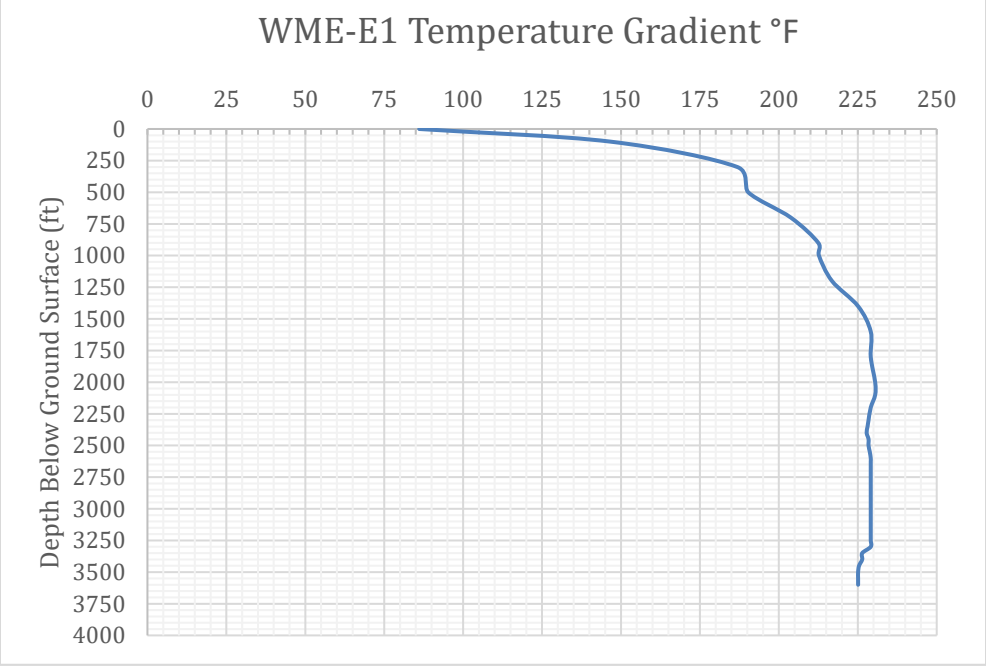

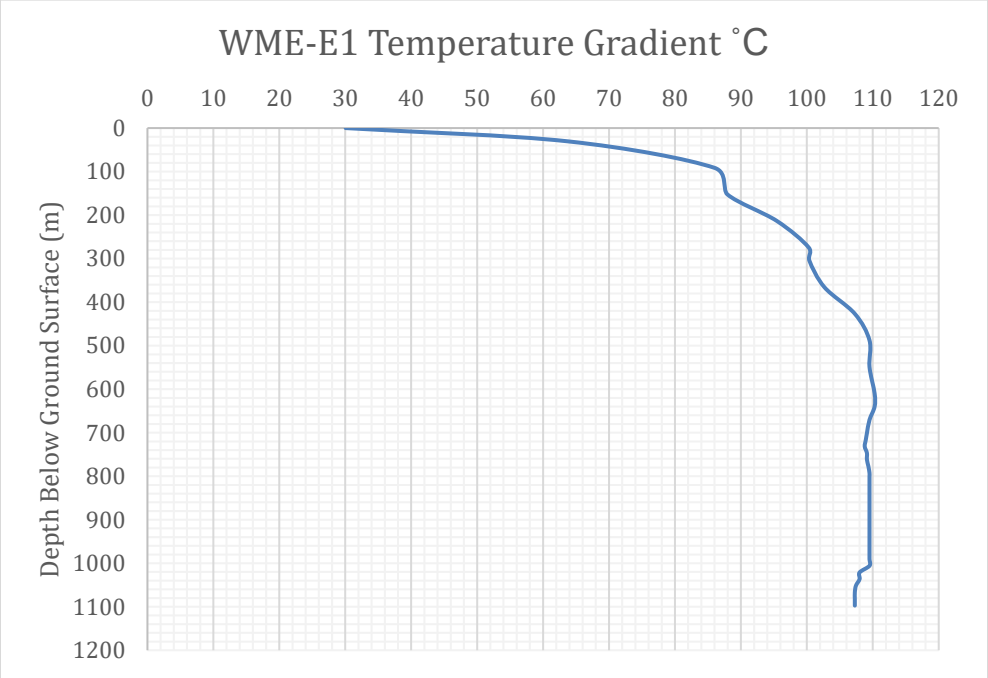

Source: Richard Holt, Geothermal Science

Geothermometry Results

Geothermometry estimates are presented in Table 12. For a point of reference, previous geothermometry estimates from the WME-TG2 and the SVHS well are presented. Maximum measured downhole temperature in WME-E1 is 230.5 ˚F (110°C); maximum temperature in WME-TG2 is 215 ˚F (101.7°C); and maximum temperature in SVHS well is 217 ˚F (102.8°C).

The Na-K-Ca and Na-K-Ca Mg geothermometry values are lower than measured temperatures in the wells but are similar to measured spring temperatures located near the wells.

The Na/K (Fournier, 1979) and chalcedony conductive geothermometers result in equilibrium temperatures similar to measured downhole temperatures in all three wells.

Table 12: Geothermometer Estimates

Geothermometer	WME-E1 (3600 ft) (°F)	WME-E1 (3600 ft) (°C)	WME TG2 (929 ft) (°F)	WME TG2 (929 ft) (°C)	SVHS Well (~200 ft) (°F)	SVHS Well (~200 ft) (°C)
Chalcedony conductive (Fournier, 1977)	241	116	241	116	226	107.8
Quartz conductive (Fournier and Potter, 1982)	289	142.8	275	135	275	135
Quartz adiabatic (Fournier, 1977)	279	137.2	266	130	268	131.1
Na-K-Ca (Fournier and Truesdell, 1973)	194	90	196	91.1	198	92.2
Na-K-Ca Mg corr (Fournier, 1978)	194	90	196	91.1	198	92.2
Na/K (Fournier, 1979)	243	117.2	225	107.2	226	107.8
Na/K (Giggenbach, 1988)	280	137.8	262	127.8	264	128.9
K/Mg (Giggenbach, 1986)	241	116.1	226	107.8	268	131.1

Source: Warner Mountain Energy Corporation

CHAPTER 3:
Reservoir Testing

Data Organization and Project Initiation

The reservoir testing involved first performing tests on well WME-E1 to gather pertinent data needed to characterize the resource. The goal of the testing was to gather the engineering data needed for the development of a numerical simulation model for the Surprise Valley geothermal reservoir. Once developed, the project team used the numerical simulation model to analyze the reservoir testing data and forecast the response of the resource to a production scenario. The analysis and forecast provide long-term predictions of the pressure and temperature response of the resource to production. The testing consisted of two flow periods on WME-E1, a clean-out flow in June 2019, and a later flow test with downhole survey in July 2019. The team took a further static temperature survey in August 2019.

Clean-Out Flow June 2019

The drilling of well WME-E1 was completed June 8, 2019. With the drilling rig still on the well, the well was flowed on June 8, 2019. While flowing, the well was entered with an open-ended drill pipe to inject air into the well with an air compressor to displace the well fluids and force them to rise up the casing and discharge from the well. The wellhead was configured with a wellhead "T," which was connected to a flowline. The flowline discharged wide open into an atmospheric flash vessel from which steam discharged vertically from three pipes while the liquid phase discharged horizontally. The liquid from the flash vessel flowed into a square-notch weir box, allowing the liquid flow to be metered through standard weir-flow equations. The configuration is shown in Figure 20, the photo taken while the well was undergoing air lift.

The goals of the WME-E1 clean out flow were to:

- Air lift to induce stronger flow and better cleanout.
- Accelerate heat-up to assure complete heat-up before the later flow test.
- Flow out cold fluids introduced to the reservoir during drilling.
- Flow out drilling mud and rock cuttings to clean out well.
- Determine if well will flow under artesian conditions without initiation.
- Collect surface data on the flow rate (via weir box measurements).

Figure 21: Well WME-E1 Clean-Out Flow, June 2019

Source: Richard Holt, Geothermal Science

Geothermal Science, Inc. staff members were on-site to guide the flow operations, witness the flow, and collect data directly on the flow parameters during the clean-out flow. When the well was opened to flow, artesian flow initiated immediately. The initial flow, as expected, was warm muddy water, which cleared up and heated up over two and a half hours. The flow was then stopped briefly to rig up the air compressor to the drill pipe. The well was air lifted for one hour during which the rate increased, and the produced water cleared up. After the air lift, the well was producing nearly clear fluid that had heated up to (210.2 ºF) 99˚C at the surface (boiling point). The surface liquid flow rate during the cleanout flow is shown in Figure 21.

Results of clean-out flow:

- WME-E1 flowed immediately under artesian conditions.
- Muddy brown water cleared up during air lift.
- Liquid flow at surface heated up during test (45.4 ºF [63ºC] to 210.2 ºF [99ºC]).
- The flow was 89 tonnes per hour (tph) of liquid to surface (with flow restricted due to drill pipe in the well).

- The temperature: 210.2°F (99°C) (boiling point as evidenced by steam from flash vessel)

Figure 22: WME-E1 Flow During June 2019 Cleanout Flow

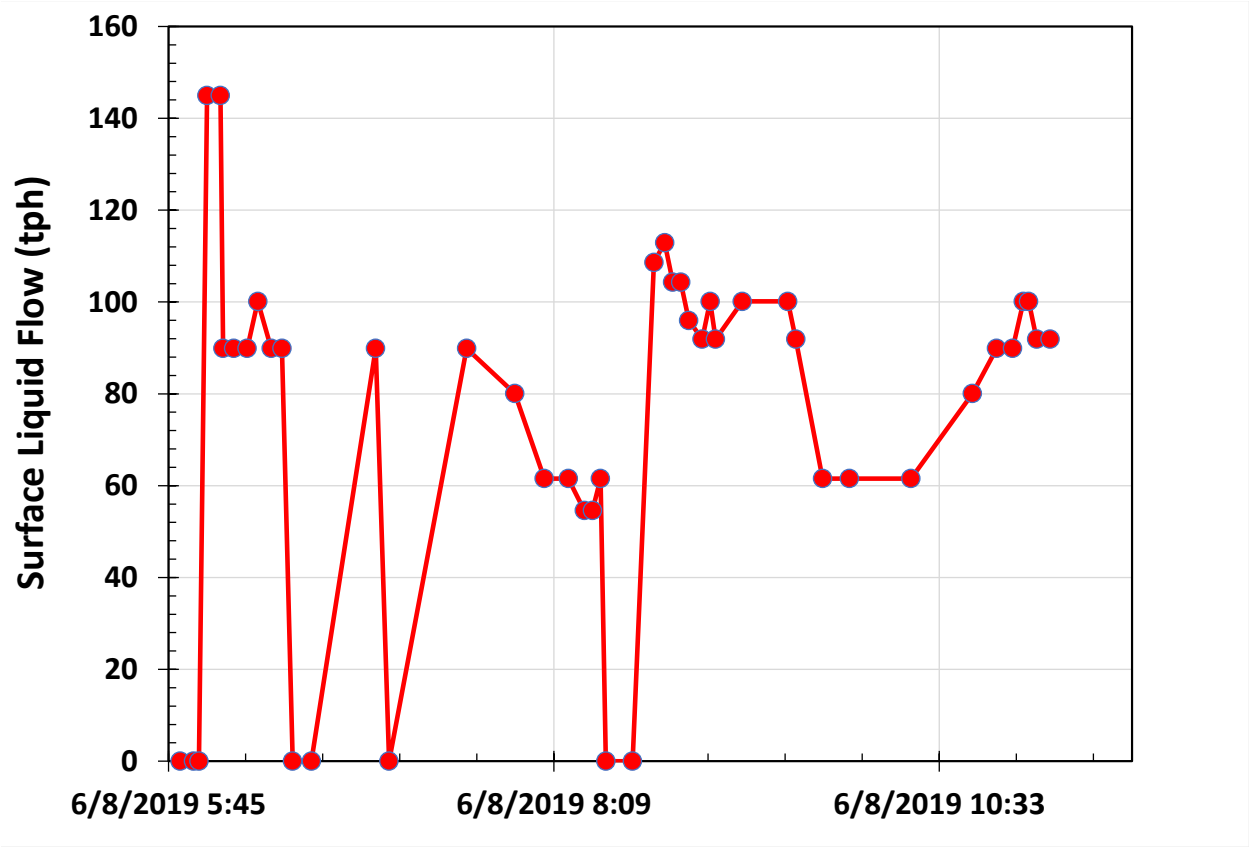

Source: Richard Holt, Geothermal Science

WME-E1 Flow Test July 13, 2019

After the cleanout flow, the drilling rig was moved off site, and the well WME-E1 was left idle to allow time for further reservoir heat up and planning a flow test. The flow test was conducted July 13, 2019.

July 13, 2019 flow test data collection goals:

- Quantify wide-open flow with likely near-complete heat up and without - restriction of drill pipe in the hole.
- Perform a multi-pass dynamic pressure, temperature, spinner (PTS) survey.
- Perform static pressure and temperature surveys 24 hours after end of flow (pressure recovery).
- Perform a static temperature survey 30 days after end of flow (temperature recovery August 10, 2019).

The test was designed to test flow without the restriction caused by having drill pipe in the hole, running a downhole dynamic multipass PTS survey, and running a static

pressure-temperature survey the day after the flow test. The program followed is listed below:

PTS Program for dynamic PTS with 24-hour recovery static PTS survey:

- While well is flowing, dynamic PTS
- Log down with PTS from surface to total depth (TD) at 0.5 m/s
- Log up with PTS from TD to surface at 0.25 m/s
- Log down with PTS from surface to TD at 0.25 m/s
- Log up with PTS from TD to fracture depth at 0.5 m/s
- Hold PTS at fracture depth, continuing flowing well for 5 minutes
- Log up with PTS from TD to fracture depth at 0.5 m/s
- Rig down PTS, shut-in well for 24 hours
- Rig up PTS
- Log down from surface to TD at 0.5 m/s (static survey) (well remains shut-in)
- Hold PTS at fracture depth, continuing logging static well for 2 hours
- Log up with PTS from TD to surface at 0.75 m/s

The flow equipment and configuration for the July 13, 2019 flow test is shown in Figure 23. Some minor modifications were made to the flash vessel to accommodate the absence of the drilling rig and have the connections needed for the survey company to attach its equipment and enter the well. The flow test was conducted in accordance with the PTS program identified above.

Figure 23: July 13, 2019, Flow Test Configuration

Source: Richard Holt, Geothermal Science

Following the PTS program, the chronology of testing was as follows:

Flow test chronology July–August 2019:

- July 13, 2019: Flowed well wide open through test equipment for four hours
- July 13, 2019: While flowing ran multipass dynamic PTS surveys from surface to total depth 3600 feet
- July 14, 2019: Static PTS survey
- August 8, 2019: Static temperature survey
- Log up with PTS from TD to fracture depth at 0.5 m/s

The flow test operations were carried out successfully, and the results are summarized below.

Flow test of July 13, 2019, results:

- Well achieved stabilized wide-open flow of 110 tph, (Figure 23), which was higher than the stabilized flow of 89 tph achieved in the cleanout flow in June 2019. The increase in flow is due to the well being flowed without being restricted by drill pipe in the hole and from the additional heat up of the well.
- In the flowing survey, the wide-open flow was at 110 tph.
- At 224.6°F (107°C), water enters well at about 975 meters but is flowing down behind pipe from 700 meters (Figure 24).
- The project team encountered a high-permeability, highly prolific reservoir at about 700 meters containing water at 224.6°F (107°C) to 230°F (110°C), the

zone at 700 meters continued to heat up after the flow test and reached 230°F (110 °C) by the August 10, 2019, static temperature survey.

- The team also encountered a less prolific reservoir zone at 1,000 meters that contributes less than 20 percent of the total flow and is about 222.8°F (106°C).
- As shown in Figure 26, there was 0.3 bar of pressure drawdown for 110 tph of flow, making the productivity index (PI) 360 tph/bar among the highest level seen in the geothermal industry.

Figure 24: WME-E1 Flow Test July 13, 2019

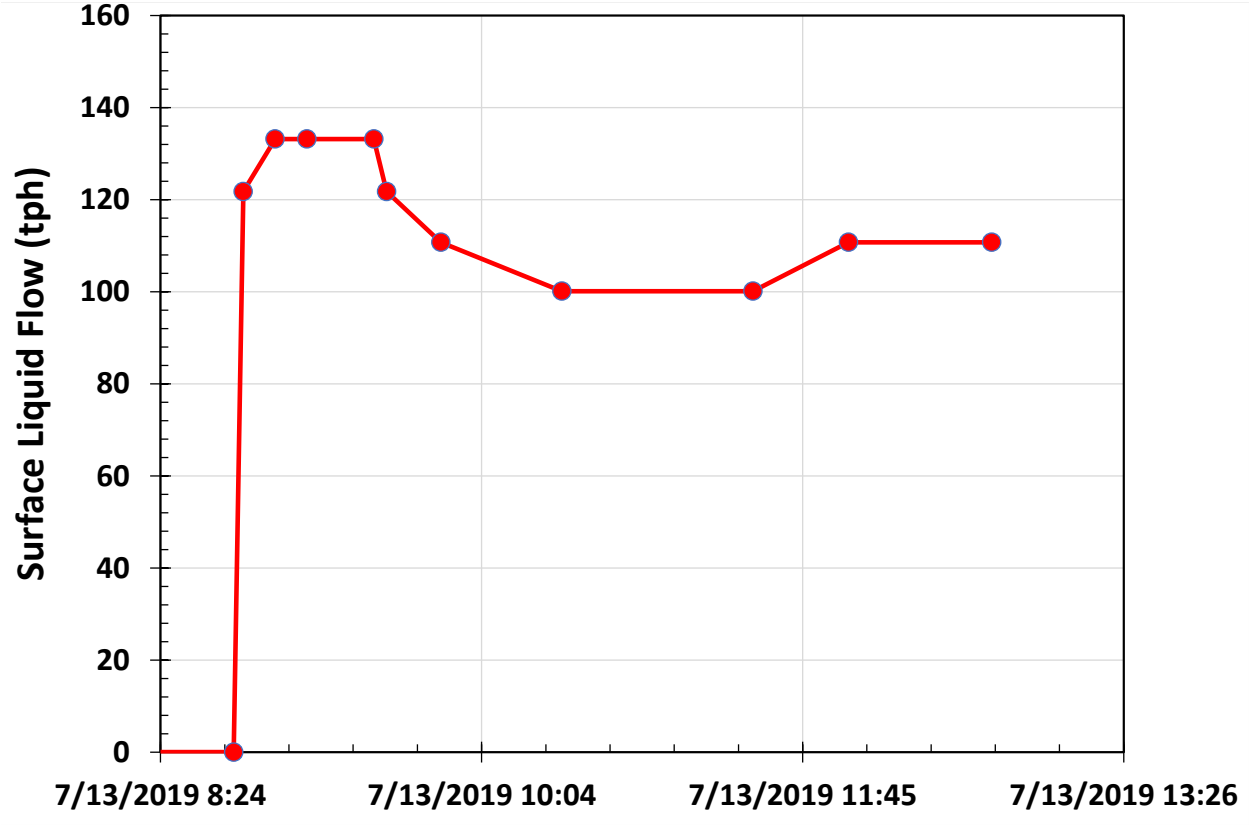

Source: Richard Holt, Geothermal Science

Figure 25: WME-E1 Flowing Temperature Survey July 13, 2019

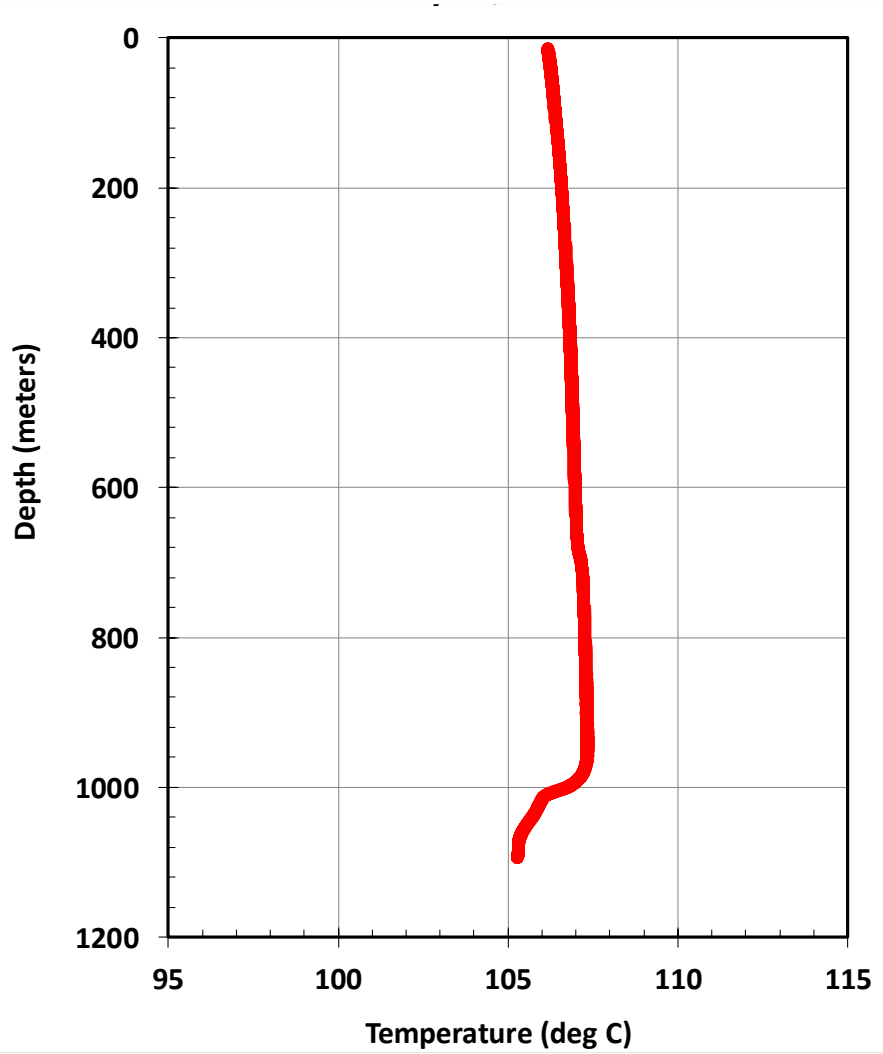

Source: Richard Holt, Geothermal Science

Figure 26: WME-E1Static and Dynamic Temperature Surveys 2019

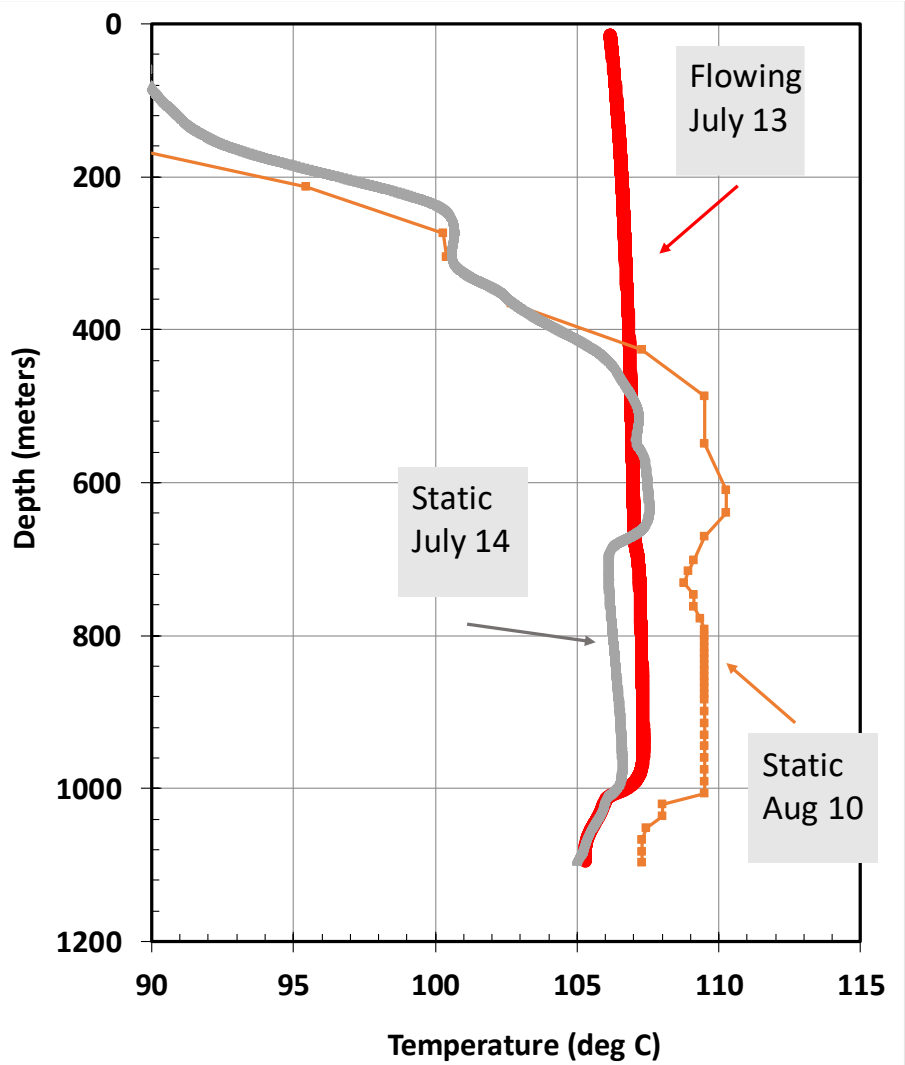

Source: Richard Holt, Geothermal Science

Figure 27: WME-E1 Static and Dynamic Pressure Surveys (Drawdown)

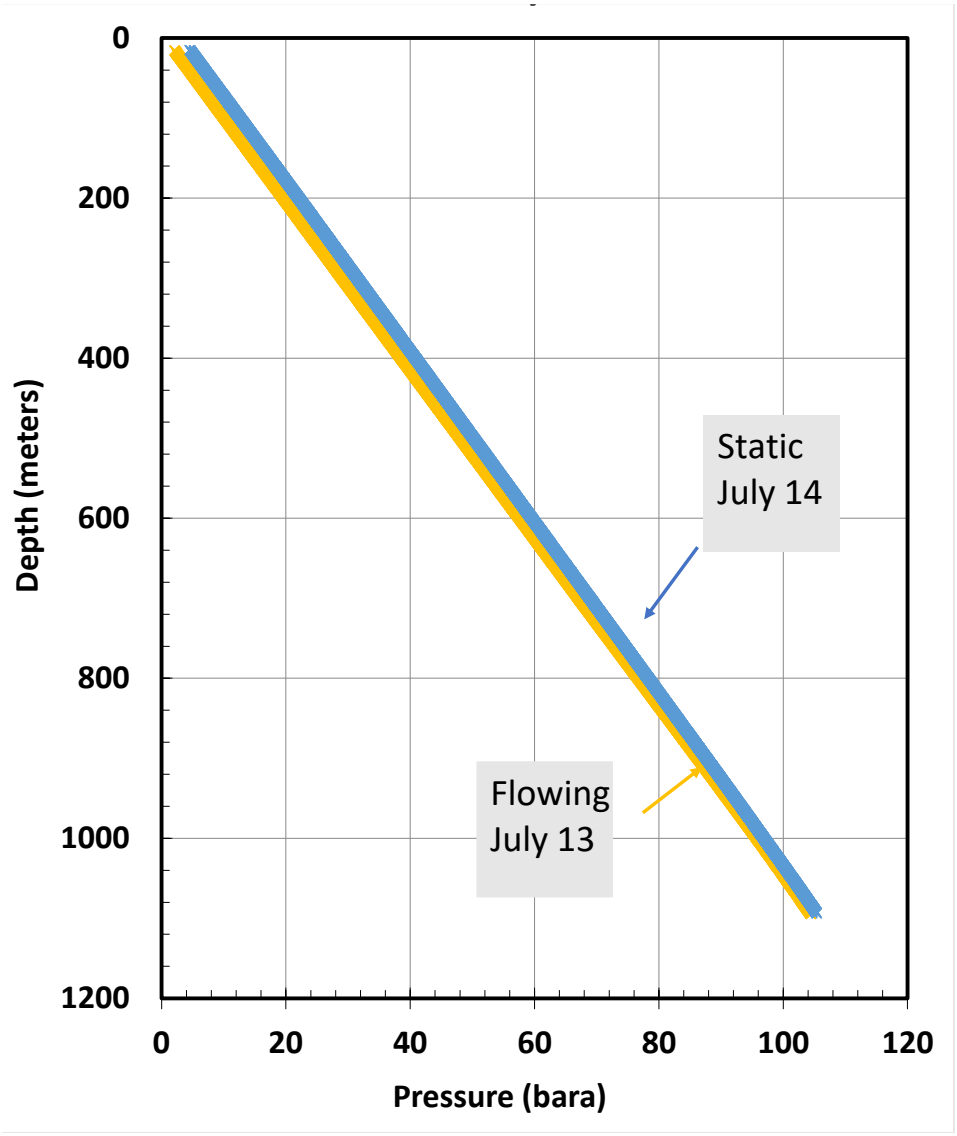

Source: Richard Holt, Geothermal Science

Applicability of Numerical Simulation at Surprise Valley

A reservoir study primarily forecasts reservoir conditions and production characteristics for various development options. At Surprise Valley, as with all geothermal reservoirs, the reservoir properties are known to vary within and around the reservoir in a three-dimensional manner. Because there is only one deep well, a numerical model had to be built using data collected and filling in data gaps using analogy to similar geothermal systems.

Reservoir simulation is a technique that allows theses variations to be represented more rigorously than other analysis techniques (Aziz and Settari, 1979). The simulation software can digitally represent the entire reservoir, including the variations in rock properties described in the conceptual model and flows into (deep source) and out of

the geothermal system (surface discharges). The locations of existing and proposed wells, production flows, and reinjection flows are also represented digitally. The simulation software is used to predict the effects of different development options.

Over the past three decades, reservoir simulation has become the predominant method by which geothermal reservoirs are analyzed and predictions about the future state of a reservoir are made. The published literature contains hundreds of successful case studies of the application of geothermal simulation to geothermal reservoirs. The geothermal industry has accepted reservoir simulation as the best practice in analyzing geothermal reservoirs. The application of reservoir simulation at Surprise Valley is believed the best method in generating forecasts of future reservoir behavior.

The reservoir simulation software TETRAD was selected and used for the numerical modeling of Surprise Valley. TETRAD is a three-dimensional, single- or dual-porosity, multiphase, multicomponent, thermal, finite-difference simulator (Vinsome and Shook, 1993). In the geothermal industry, TETRAD is widely used by operating companies, consulting firms, and research organizations. Furthermore, a published research study by a U.S.-based national laboratory concluded that TETRAD provides valid solutions to the complex equations in geothermal applications (Shook and Faulder, 1991).

Numerical Model Grid Design

Figure 28 shows the extent of the Surprise Valley numerical model simulation grid domain within a topographic map. The model covers an area of 8 by 8 kilometers and is centered on the surface location of well WME-E1. The model grid is aligned north to south (that is, it is not rotated), making the grid in approximate alignment with the predominate fracture orientation in the region (generally north-south). Figure 29 shows an aerial view of the numerical model grid with a satellite image of the region.

The area of the model was chosen by balancing two considerations. First, the model domain was made large enough to enclose an area such that modeling of the edges (boundary conditions) of the model would not have a significant effect. Second, the model domain and individual grid divisions were made so that the number of cells was not so large that computational times became unreasonably large. The model contains 18 layers extending from ground surface +1,370 meters above sea level (mASL) to a depth of -1,500 mASL. Each layer contains 3,200 gridblocks. The surface was modeled as flat because the topography of the area surrounding the area is nearly flat. The complete simulation grid has 57,600 gridblocks. Figure 30 shows a three-dimensional view of the numerical model grid.

Figure 28: Extent of Numerical Model Grid

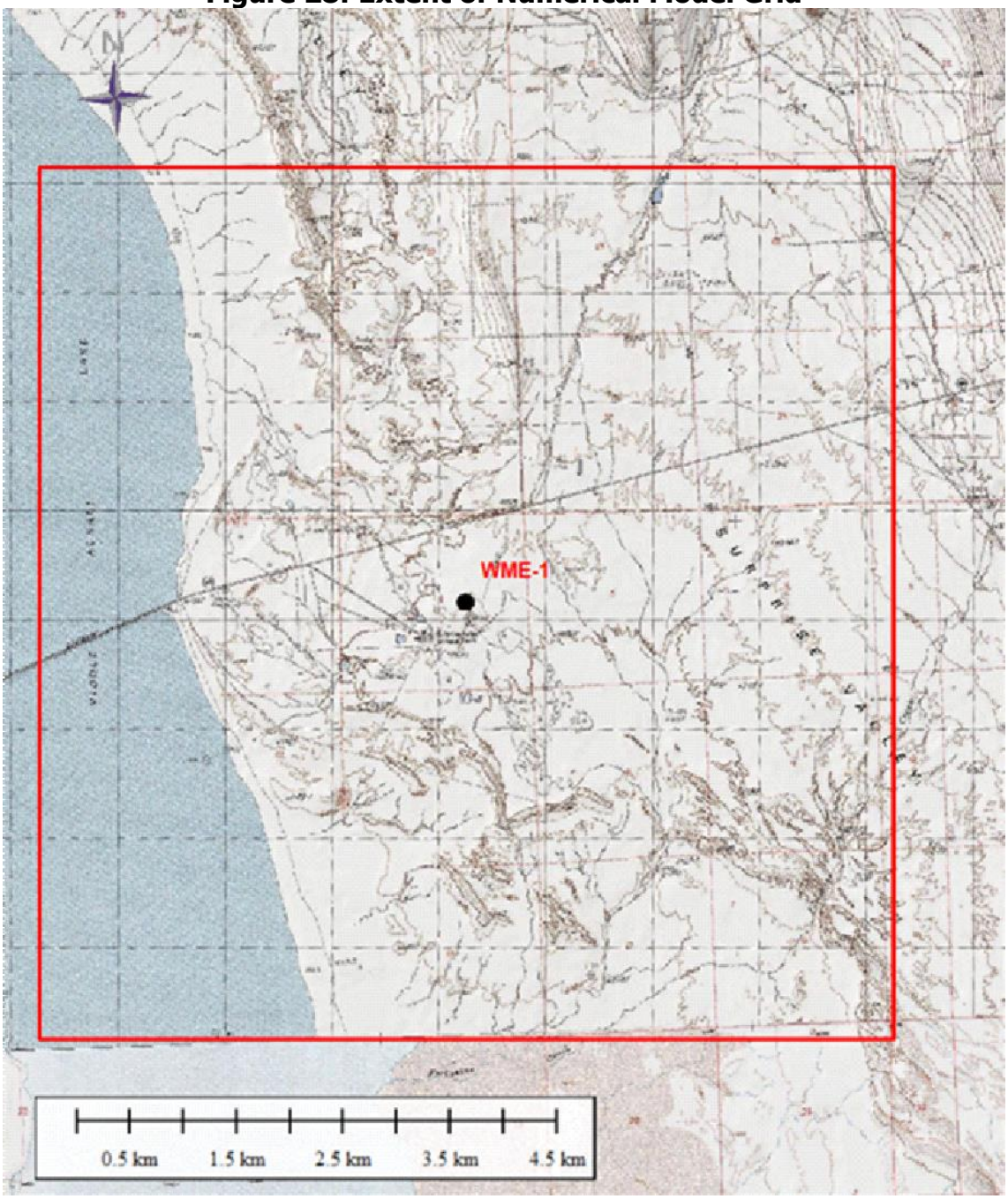

Source: Richard Holt, Geothermal Science

Figure 29: Aerial View of Numerical Model Grid With Satellite Image

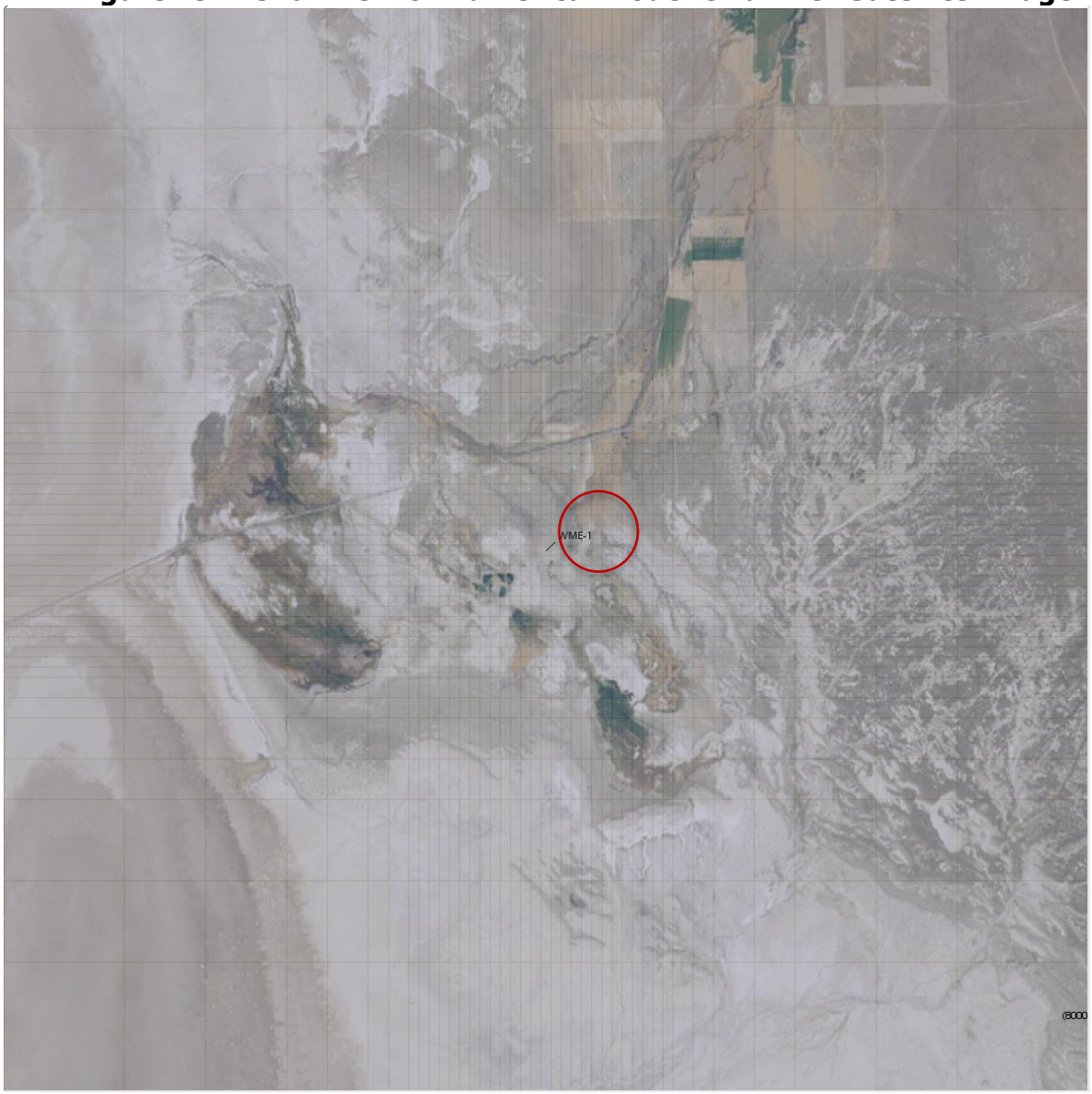

Source: Richard Holt, Geothermal Science

Figure 30: Three-Dimensional View of Simulation Grid

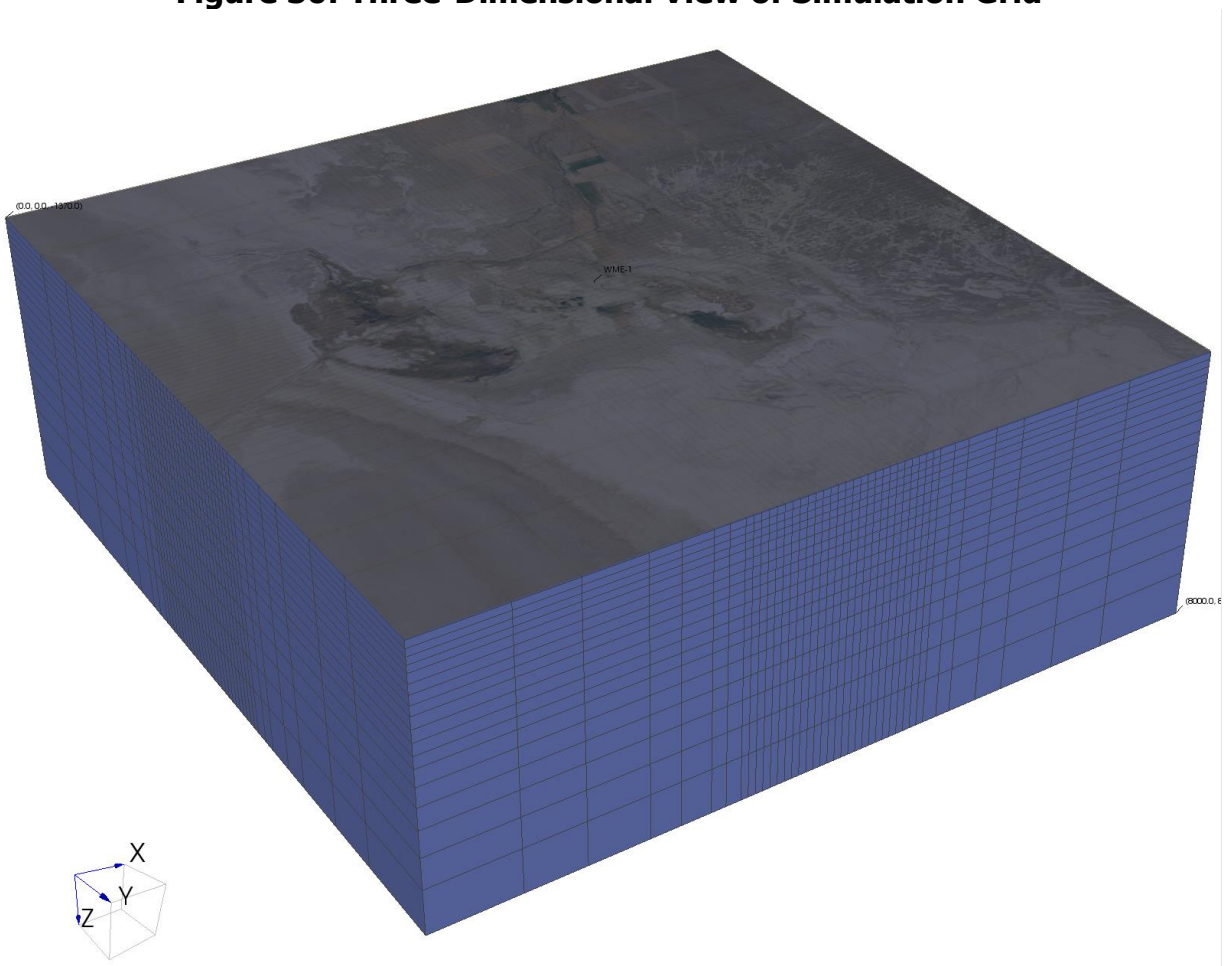

Source: Richard Holt, Geothermal Science

Conceptual Model Converted to Numerical Model

The starting point and fundamental basis for the Surprise Valley numerical model is a conceptual model of the overall geothermal resource. Because the flow within the reservoir is believed associated with faulting or open fractures or both, the reservoir rock is modeled using a dual-porosity formulation. The concepts of single porosity and dual porosity have been described in the literature (Warren and Root 1963).

In a single porosity model, there is a computational grid covering the space within the model. In dual-porosity models, there are two computational grids covering the same space within the model. One computational grid represents the "fractures," which tend to have higher permeability but limited capacity to store heat and fluid. The second computational grid covers the "matrix," which tends to have a higher capacity to store heat and fluids but has lower permeability. The third component of a dual-porosity formulation is a function that calculates the flow from the matrix blocks into the fracture blocks.

TETRAD contains a built-in option for implementing dual porosity, and that was used in the Surprise Valley reservoir model. Throughout the Surprise Valley model, the fracture

domain is 1 percent of the total block volume, and the matrix domain occupies the remaining 99 percent. The matrix permeability is a uniform 0.05 MD across the entire grid, whereas the fractures have permeabilities up to 100,000 MD. These ratios are calibrated to match the measured data at Surprise Valley. Listed below are summaries of each component of the conceptual model:

Primary permeability: Distribution of primary permeable zones is related to the texture and mode of formation of the geological unit (for example, low-permeability mudstones or high- permeability volcanics). Wells drilled thus far at Surprise Valley have not encountered geologic units with significant primary permeability; permeability is associated to faults or fracture zones.

Secondary permeability: Distribution of secondary permeable zones is related to brittle faulting and fractures generated by earthquakes or regional strain or both. In the Surprise Valley region wells that contain significant permeability, it is related entirely to faulting and fracturing within a background rock of low primary permeability.

Deep heat inflow: The Surprise Valley resource is in an area of high regional heat flow, and significant heat probably exists extensively at great depths within impermeable rocks. Local faulting at Surprise Valley provides a vertically permeable pathway for fluid migration to bring heated fluid to the ground surface convectively (active hot springs).

Discrete fault: The Surprise Valley geothermal field consists primarily of a discrete fault zone. This fault is a discrete segment of permeability at depth which extends north and south. This fault was partially interpreted using well losses and measured production zones in addition to geophysical methods.

Permeability distribution: A dual-porosity formulation was used across the entire model, which means there is a permeability and porosity value for each of the two domains, fracture and matrix. Taken together, overall permeability and porosity distribution in the model was changed iteratively to attain a match to the static and flowing temperature of WME-E1 and the pressure response at WME-E1 measured in response to the July 13, 2019, flow test.

Boundary conditions: The boundary conditions for the Surprise Velley numerical model are based on the natural state temperature profile of WME-E1, spring locations, geothermometry, and the geologic conceptual model. Based on these sources, GSI implemented an elongated hot upflow on the bottom of the model, extending along a north-south fault, which exists in a background of high background heat flow. The fluid outflows at the intersection of the fault system with the ground surface in the area of the hot springs southwest of well WME-E1.

Rock type distribution: Figure 31 is a west-east cross-section through the numerical model showing the distribution of materials used in the model.

Figure 31: Model Grid Showing Material Distribution on West-East Cross-Section

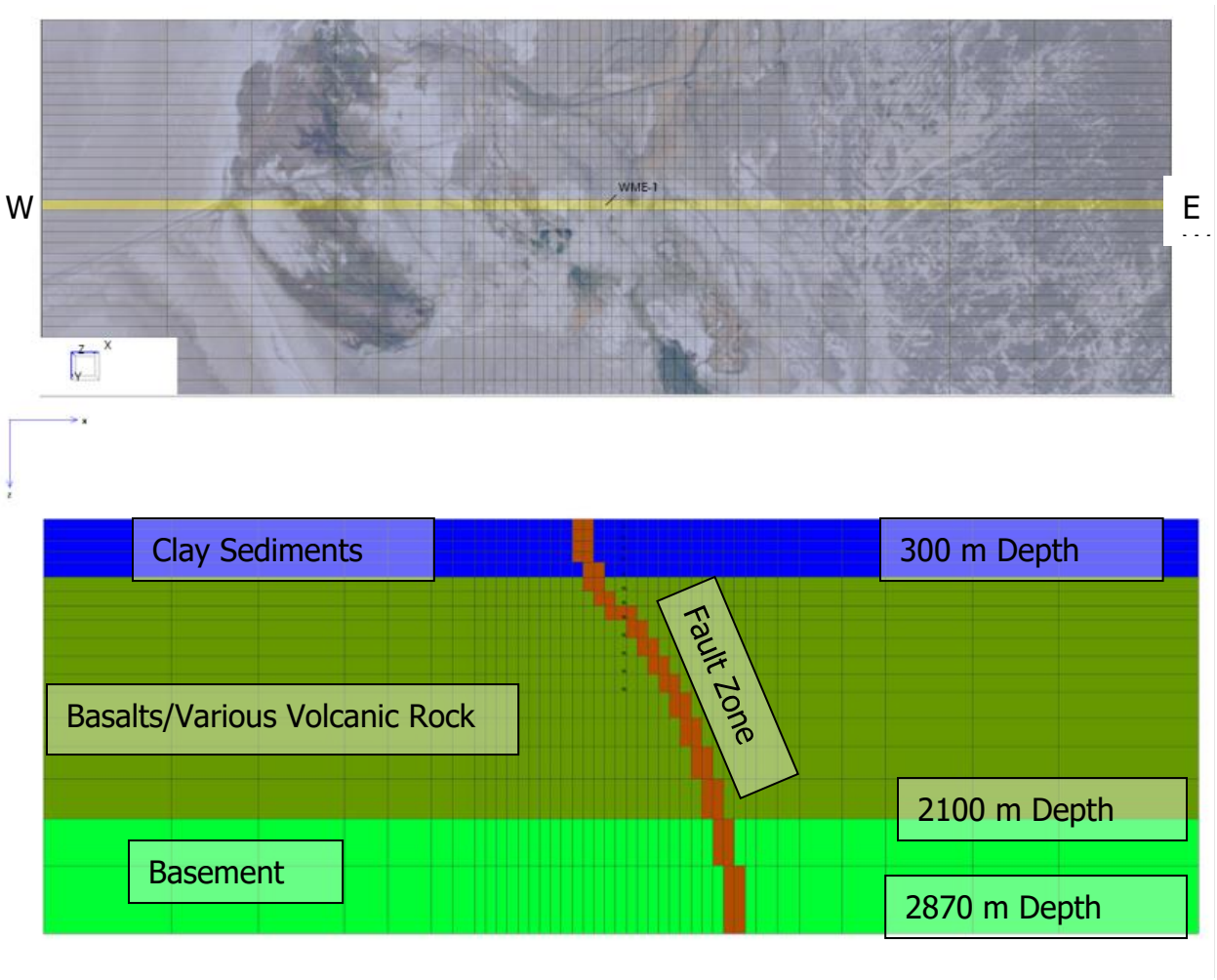

Source: Richard Holt, Geothermal Science

Natural State Model

In a natural state model, the boundary conditions are fixed, and the model is run for a period simulating geologic time. The model code is run until it comes to stable conditions where the pressures and temperatures are not changing with additional simulation time. The goal is to represent the preproduction natural state of the reservoir with its initial distribution of temperature and pressure. Heterogeneity in the permeability structure causes the fluid to flow preferentially in certain regions. Changes to this permeability structure, the inflow conditions, outflow locations, and the constant temperature boundaries resulted in the match to natural state conditions. Figure 32 shows simulated natural state temperatures on a west-east cross-section, and Figure 33 shows temperature isosurfaces across the entire grid. Figure 34 shows a direct match of measured static temperature at WME-E1 with simulated temperatures. The match between measured and simulated temperatures is good, indicating the quality of the calibration of the model is high, which adds confidence to forecasts made with the model.

Figure 32: Simulated Natural State Temperatures on West-East Cross-Section

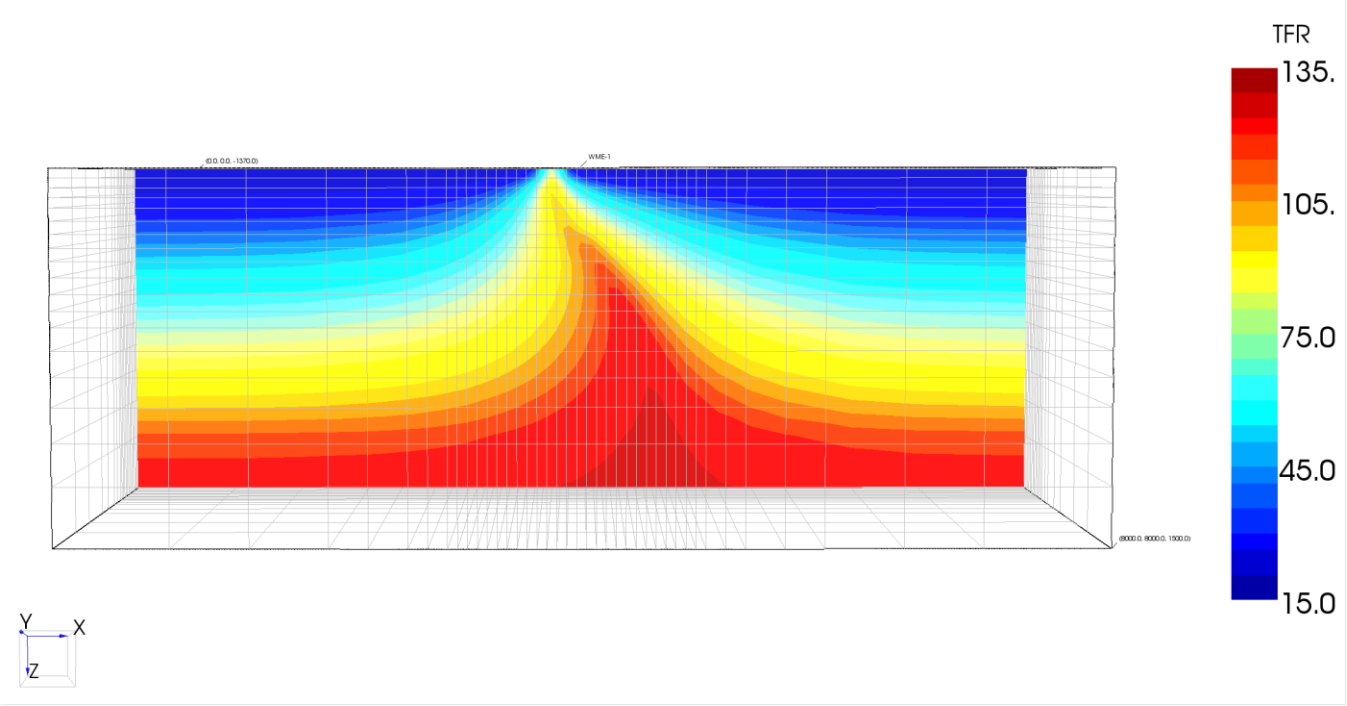

Source: Richard Holt, Geothermal Science

Figure 33: Simulated Temperature Isosurfaces

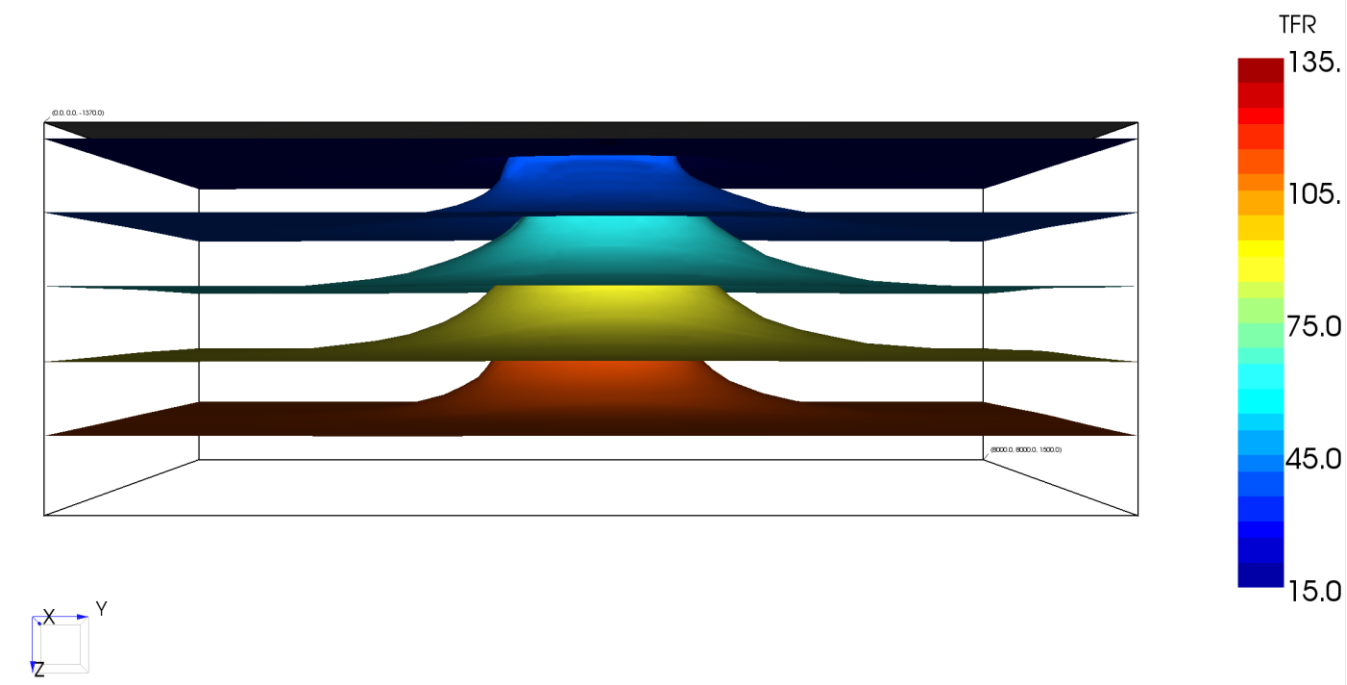

Source: Richard Holt, Geothermal Science

Figure 34: WME-E1 Natural State History Match

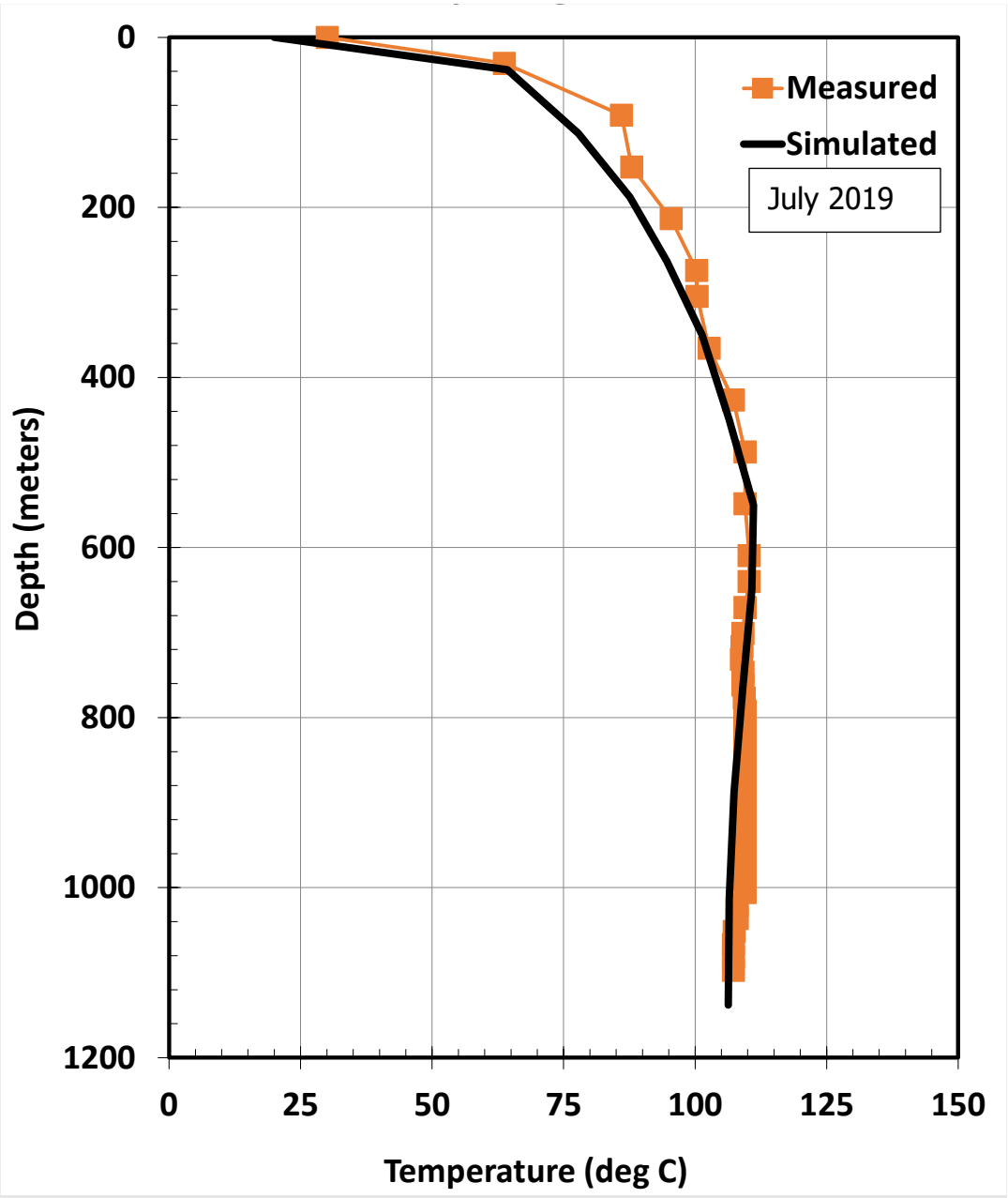

Source: Richard Holt, Geothermal Science

Production History Match

The Surprise Valley numerical model was calibrated to well measurements under pressure transient conditions. Specifically, the downhole flowing pressure during the end of the July 13, 2019, flow test and the static pressure recovery survey from July 14, 2019, was used to calibrate the model. Using the final model, a good match was obtained between measured and simulated data (Figure 20). The following element of the calibration results is important for reservoir management because it increases confidence in the model forecasts.

Figure 35: Match to Flow Test Pressure Transient

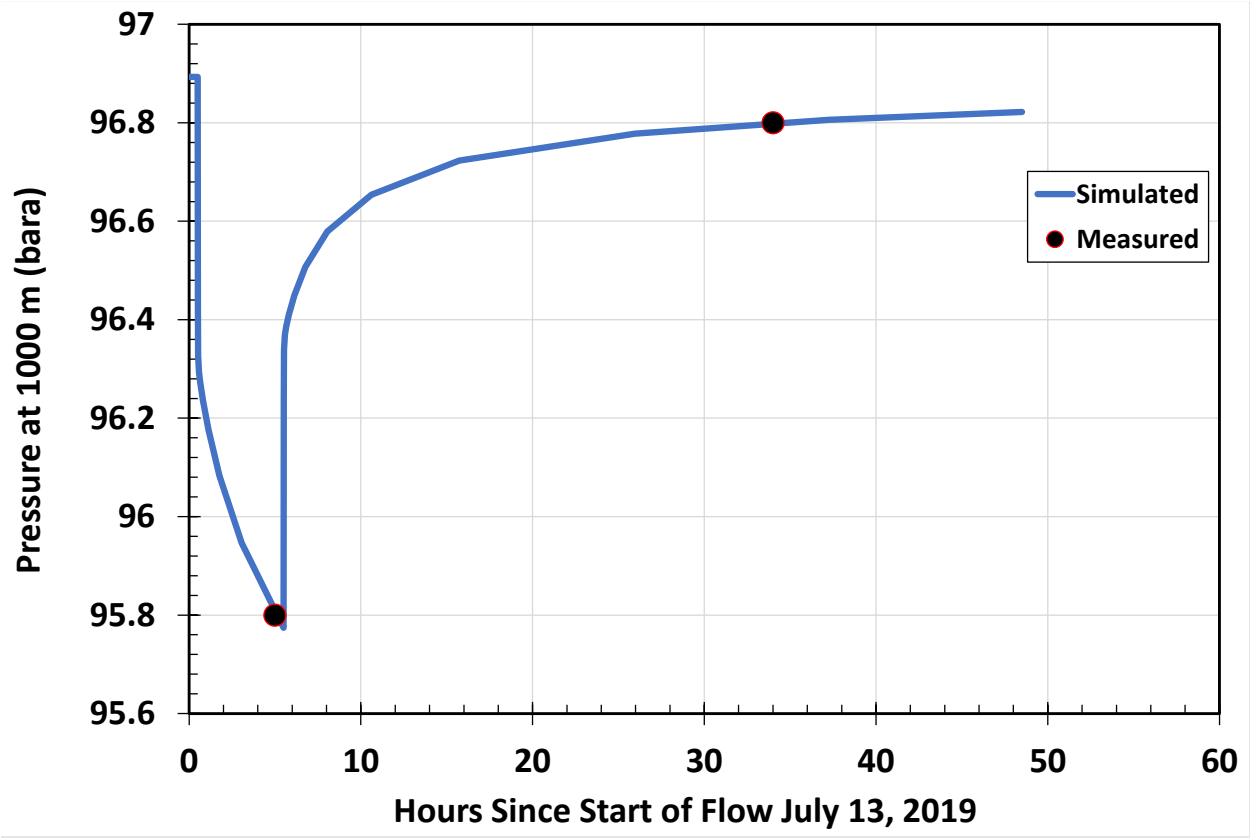

Source: Richard Holt, Geothermal Science

Long-Term Forecast

The calibrated model was used to make a forecast of the reservoir response to long-term production of well WME-E1 at artesian flow capacity (110 tph). To calculate gpm, multiply tph by 4.583.

Figure 36 shows the forecasted downhole pressure at WME-E1 for long-term production of 110 tph. As shown, the model predicts an initial drawdown of about 5 bars, followed by long-term stability with negligible further pressure drop. This stability represents favorable, sustainable production because pressure support from injection was included in the simulation. Figure 36 shows the forecasted downhole flowing temperature at WME-E1 for long-term production of 110 tph. As shown, the forecasted temperature shows a negligible long-term temperature decline and is consistent with long-term sustainability.

Figure 36: Downhole Pressure Forecast WME-E1 (at 110 tph)

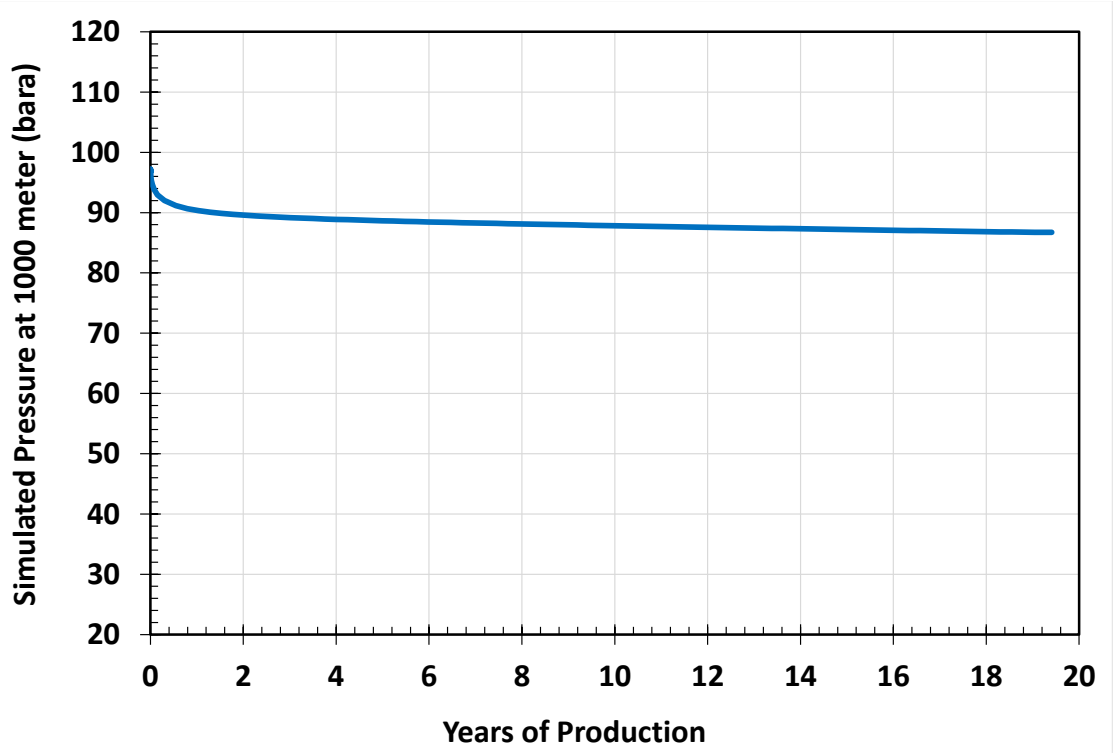

Source: Richard Holt, Geothermal Science

Figure 37: Downhole Flowing Temperature Forecast WME-E1 (at 110 tph)

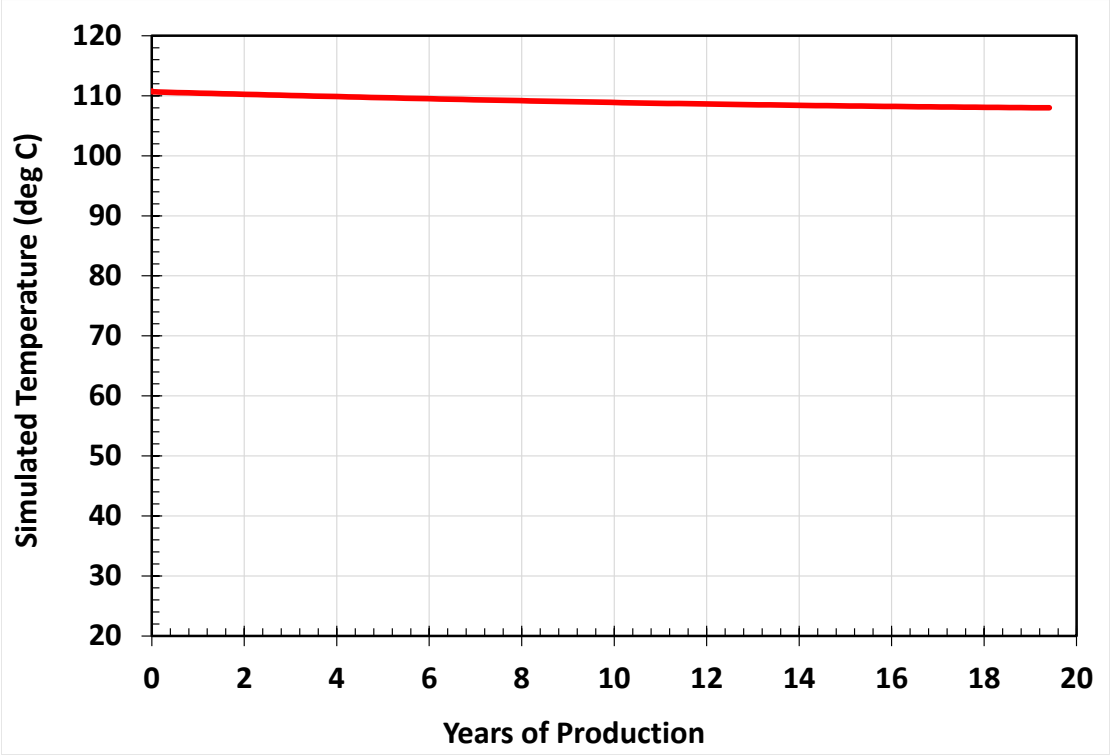

Source: Richard Holt, Geothermal Science

CHAPTER 4:
Public Outreach

The public outreach and communication goals included (1) keeping the public and project stakeholders apprised of project activities and geothermal development progress and (2) helping create a synergistic community economic development environment supported by geothermal energy use and development. Public outreach strategies included educational outreach, project updates/public gatherings, and spontaneous activities. Table 13 lists the activities undertaken by Modoc County and WME for public outreach.

Table 13: List of Public Outreach Activities

Description	Date
Newspaper article published in Modoc Record, project update	May 30, 2019
Public meeting, Cedarville Senior Center: Community meeting to introduce project, team and solicit input. WME and Modoc County made a presentation to the public.	May 30, 2019
Publish advertisement of public meeting in Modoc Record	June 2, 2019
Newspaper article published in the Modoc Record, project update	June 4, 2019
Press release ad for community meeting published in Modoc Record	September 25, 2019
Public meeting, Whalen's Public House: Provide project findings and describe activities. Provided Webex link for offsite participants. WME, Modoc County, USGS, and CEC provided discussion at the meeting.	October 2, 2019
Newspaper article published in the Modoc Record, project update	October 3, 2019
Paper on reservoir modeling submitted and accepted to Stanford Geothermal Conference	November 1, 2019
Provide educational geothermal handout to Cedarville High School science teacher for curriculum	May, 2019
Conduct tour of geothermal drilling activities for Modoc County Board of Supervisors	May, 2019
Publish notices of meetings on Modoc County website	May, June, 2019
Distribute flyers of meeting notices in Cedarville, Lake City, Eagleville, Ft. Bidwell Reservation, Canby, Likely, Alturas, Cedarville Indian Rancheria, Pitt River Tribe.	May, June, 2019
Media release submissions: Modoc Record, Redding Search Light, NPR Radio, Jefferson public radio, KIXE Channel 9 (PBS), KRCR TV, KOTI TV, Sacramento Bee, Fresno Bee, Intermountain News, Northstate News (Burney, Fall River, McArthur, Round Mountain, Big Bend), AP News, Action News Now, Enterprise Record, LA Times, San Francisco Chronicle, San Diego Union, Orange County Register, Chico News and Review, Lassen County Times. WME contacted media outlets by phone and/or email for submission information.	Completed
Provide project briefing to Geothermal Resource Council, North American Clean Energy, Renewable Energy World, Ruralite Magazine, EnergyBiz, Think GeoEnergy Newsletter, International Geothermal Energy Association, U.S. Department of Energy, National Renewable Energy Laboratory, Surprise Valley School District, Alturas School District, Modoc High School. WME contacted media outlets by phone and/or email for submission information. Some contacts were made in person.	Completed
Project updates: Ongoing communication, verbal and electronic, to Modoc County Board of Supervisors. WME provides summary of economic benefits to Modoc County.	Completed

Source: Warner Mountain Energy Corporation

CHAPTER 5: Conclusions

The project succeeded in drilling a geothermal exploratory well, obtaining further knowledge about subsurface temperature gradient with depth in the Surprise Valley geothermal field, and estimating reservoir capacity and characteristics through well testing and reservoir modeling.

The exploratory geothermal well was drilled to a total depth of 3,605 feet on the east side of Surprise Valley to investigate the potential for electrical energy development. The project team performed mud logging, geophysical logging (temperature, caliper, natural gamma, acoustic borehole televiewer), pressure/temperature/spinner logging after well stabilization, flow testing, brine and steam sample collection, and reservoir modeling.

Geophysical studies, based on borehole logging, reveal the presence of several prominent fault zones. The fault zones have a wide range of attitude, mostly dipping 60°–90°, typical of Basin and Range structures. Fractures below ~ 2300 feet bgs are associated with increasing temperature gradient in WME-E1. WME-E1 is highly permeable, and borehole logs confirm fractures are the primary control on hydrothermal flow. Fractures observed in WME-E1 at these depths were well-aligned with the stress state to accommodate normal faulting. Well-aligned fractures were more likely to create a permeable zone. However, the preferred orientation of the fractures was slightly misaligned with the strike of the Surprise Valley Fault on the west side of the valley and localized dike structures. This misaligned orientation can indicate a recently active tectonic system, and the fracture misalignment may be one of the key factors explaining why hydrothermal flow was present on the east side of the valley at the WME-E1 site.

Geothermometry based on water chemistry in WME-E1 indicated reservoir temperatures ranging from 194°F (90°C) to 289°F (143°C). However, the measured flowing temperature (225°F [107°C]) and maximum borehole temperature (230.5°F [110°C]) in WME-E1 were higher than some of the geothermometer estimates. WME-E1 flowed under artesian conditions at ~500 gpm in the 5” liner with no drawdown for six hours during flow testing. This result indicated a highly permeable system. Reservoir modeling indicates that Well WME-E1 can sustain an artesian flow over 20 years or more, and the geothermal reservoir on the east side of Surprise Valley can sustainably support higher levels of production with reinjection. Flow test results show the productivity index of WME-E1 is very high, among the highest level seen in the geothermal industry.

The reservoir supplying WME-E1 is a shallow and highly productive high-temperature system, making it attractive in terms of production and injection drilling costs. Based on the project results, WME-E1 appears capable of commercial grade electrical energy production and direct use applications at a relatively shallow depth of ~2,300 feet bgs.

Benefits to California

Information gathered during this project provides flow and permeability data needed for preliminary geothermal resource development planning. Well testing reveals that the Surprise Valley geothermal system has the potential for large-scale direct use or electrical power supply development of a low- to medium-temperature resource. Without CEC funding, this information would not be known. As is, WME-E1 can produce about 0.5 megawatts of electrical power flowing under artesian conditions and has prolific direct-use potential.

This study indicates that resource development in Surprise Valley may help to contribute to California's RPS goals or provide micro-grid or other geothermal-related opportunities for this remote community. Many geothermal projects cannot continue due to the high risk associated with resource confirmation. This grant agreement provided a unique opportunity to validate geothermal research methods and previous findings, build confidence and understanding about the geothermal potential, and to reduce risk for further exploration stages that can help meet California's renewable energy goals.

Private developers typically conduct geothermal exploration and keep exploration data private. Using CEC funding allows public access to the subsurface exploration data and methods, which can help reduce risk in further exploratory efforts. Well drilling provided economic benefits to the local community in terms of direct, indirect, and induced multiplier effects. About $70,000 was spent locally on various services and equipment.

Collaboration with the USGS provided an opportunity for the USGS to expand on regional geologic information that builds on existing conceptual models of the valley. The study findings help validate geothermal research methods and previous study findings. This validation streamlines future exploration while reducing risk. Collaboration with Modoc County helps continue the synergy of geothermal development in the county and creates opportunities for public-private development partnerships. Geothermal development means employment opportunities for Modoc County residents, increased spending in the local community, and increased tax revenues for the county. Energy security is becoming increasingly important, and this project provides data the supports creation of a local microgrid for community or private industry usage.

Recommendations

Geothermometry results indicate higher temperature potential. Deeper drilling could reveal a hotter, deeper reservoir and will simplify characterization of the complex geological controls on the Surprise Valley geothermal system. A hotter resource will increase opportunities for Modoc County to use the resource for economic development. Further, exploring the viability of a local microgrid could lead to long-term benefits, including energy security in an economically depressed part of California, increased economic development, and help in realizing California's clean energy goals.

REFERENCES

Athens, N.D., J.M.G. Glen1, S.L. Klemperer2, A.E. Egger3, and V.C. Fontiveros (2015) Hidden intrabasin extension: Evidence for dike-fault interaction from magnetic, gravity, and seismic reflection data in Surprise Valley, northeastern California. Geosphere, v 12(1), p. 15-25.

Aziz, K. & Settari, A. 1979. Petroleum Reservoir Simulation. Elsevier Applied Science Publishers, 1: 1-4.

Davatzes, N. C., and S. H. Hickman (2010b), Stress, fracture, and fluid-flow analysis using acoustic and electrical image logs in hot fractured granites of the Coso Geothermal Field, California, USA., in Dipmeter and Borehole Image Lsog Technology, AAPG Mem., vol. 92, edited by M. Poppelreiter, C. Garcia-Carballido, and M. Kraaijveld, pp. 259–293, Am. Assoc. Pet. Geol., Tulsa, Okla., doi:10.1306/13181288M923134.

Day-Lewis, A., M. D. Zoback, and S. H. Hickman (2010), Scale-invariant stress orientations and seismicity rates near the San Andreas Fault, Geophys. Res. Lett., 37, L24304, doi:10.1029/2010GL045025.

Egger, A.E., and Miller, E.L., 2011, Evolution of the north- western margin of the Basin and Range: The geology and extensional history of the Warner Range and environs, northeastern California: Geosphere, v. 7, no. 3, p. 756–773, doi:10.1130/GES00620.1.

Egger, A.E., 2014, Paleoearthquake magnitudes derived from lidar-based mapping of fault scarps in the northwestern Basin and Range: Geological Society of America Abstracts with Programs, v. 46, no. 6, paper 323-5, p. 777.

Egger, A.E., and Miller, E.L., 2011, Evolution of the northwest- ern margin of the Basin and Range: The geology and extensional history of the Warner Range and environs, northeastern California: Geosphere, v. 7, p. 756–773, doi: 10.1130/GES00620.1.

Egger, A.E., Glen, J.M.G., and Ponce, D.A., 2010, The north- western margin of the Basin and Range province part 2: Structural setting of a developing basin from seismic and potential field data: Tectonophysics, v. 488, p. 150–161, doi:10.1016/j.tecto.2009.05.029.

Egger, A.E., Glen, J.M.G., and McPhee, D.K., 2014, Structural controls on geothermal circulation in Surprise Valley, California: A re-evaluation of the Lake City fault zone: Geologi- cal Society of America Bulletin, v. 126, p. 523–531, doi:10 .1130/B30785.1.

Glen, J.M.G., Egger, A.E., Ippolito, C., and Athens, N., 2013, Correlation of geothermal springs with sub-surface fault terminations revealed by high-resolution, UAV-acquired magnetic data, *in* Proceedings of the 38th Workshop on Geothermal

Reservoir Engineering: Stanford Geothermal Program Workshop Report SGP-TR-198, p. 1233–1242.

Peška, P., and M. D. Zoback (1995), Compressive and tensile failure of inclined well bores and determination of in situ stress and rock strength, J. Geophys. Res., 100(B7), 12,791–12,811, doi:10.1029/95JB00319.

Shook, M. & Faulder, D. 1991. Validation of a Geothermal Simulator, EG & G Report #EP-9851, October 1991.

Vinsome, K.W & Shook M.1993, Multi-Purpose Simulation, Journal of Petroleum Science and Engineering, vol 9, pages 29-38, 1993.

Vinsome, K.W. & Shook M. "Multi-Purpose Simulation," Journal of Petroleum Science and Engineering, Vol. 9 (1993), 29-38.

Warren, J.E., Root, P.J. "The Behavior of Naturally Fractured Reservoirs." Fall Meeting of the Society of Petroleum Engineers, Los Angeles, CA (1962).

Zoback, M. D. (2010), Reservoir Geomechanics, 461 pp., Cambridge Univ. Press, Cambridge.

GLOSSARY

Abbreviation or Acronym	Term	Definition
	acoustic borehole televiewer	An acoustic probe that generates an image of the borehole wall by transmitting ultrasonic pulses from a fixed transducer with rotating mirror and recording the amplitude and travel time of the signals reflected at the interface between borehole fluid and the formation (borehole wall).
bgs	below ground surface	self explanatory
BHTV	borehole televiewer	Equipment used in geophysical logging to capture images in a well borehole.
BO	Breakout	Enlargements and elongation of a borehole in a preferential direction and are formed by spalling of fragments of the wellbore in a direction parallel to the minimum (least) horizontal stress (Sh).
BOP	blow out preventor	A specialized valve or similar mechanical device, used to seal, control and monitor oil, gas, and geothermal wells to prevent blowouts, the uncontrolled release of crude oil, natural gas, or geothermal fluids from a well.
caliper		A tool for measuring the diameter and shape of a borehole which has 2, 4, or more extendable arms. The arms can move in and out as the tool is withdrawn from the borehole, and the movement is converted into an electrical signal by a potentiometer.
CEC	California Energy Commission	self explanatory
DITF	drilling induced tensile fractures	Fractures initiated in deviated wellbores when the minimum effective stress tangential to the wellbore is less than the tensile strength of the rock.
ft	feet	self explanatory
gpm	gallons per minute	self explanatory
lithology		The study of the general physical characteristics of rocks.
m	meters	self explanatory

mASL	meters Above Sea Level	self explanatory
natural gamma		A penetrating form of electromagnetic radiation arising from the radioactive decay of atomic nuclei. Different types of rock emit different amounts and different spectra of natural gamma radiation.
PI	productivity index	A measure of the well potential or ability to produce.
SHmax	maximum horizontal principal stress	One of the principle stresses in the reservoir that is used in assessing the geometry and fracture propagation, barrier zones, safe mud window determination, reservoir production behavior, and the wellbore stability.
Shmin	minimum horizontal principal stress	One of the principle stresses in the reservoir that is used in assessing the geometry and fracture propagation, barrier zones, safe mud window determination, reservoir production behavior, and the wellbore stability.
SVHS	Surprise Valley Hot Springs	self explanatory
TD	total depth	self explanatory
TFR	temperature field reconstructed	Use of modeling tools to reconstruct a temperature field.
tph	tonnes per hour	self explanatory
PTS	pressure, temperature, spinner survey	A geophysical survey performed to measure the pressure, temperature, and flow characteristics of a well.
VSMOW	Vienna-Standard Mean Ocean Water	self explanatory
WME	Warner Mountain Energy	self explanatory
WME-E1	Warner Mountain Energy Exploratory-1 well	self explanatory

APPENDIX A:
WME-E1 Geophysical Field Print

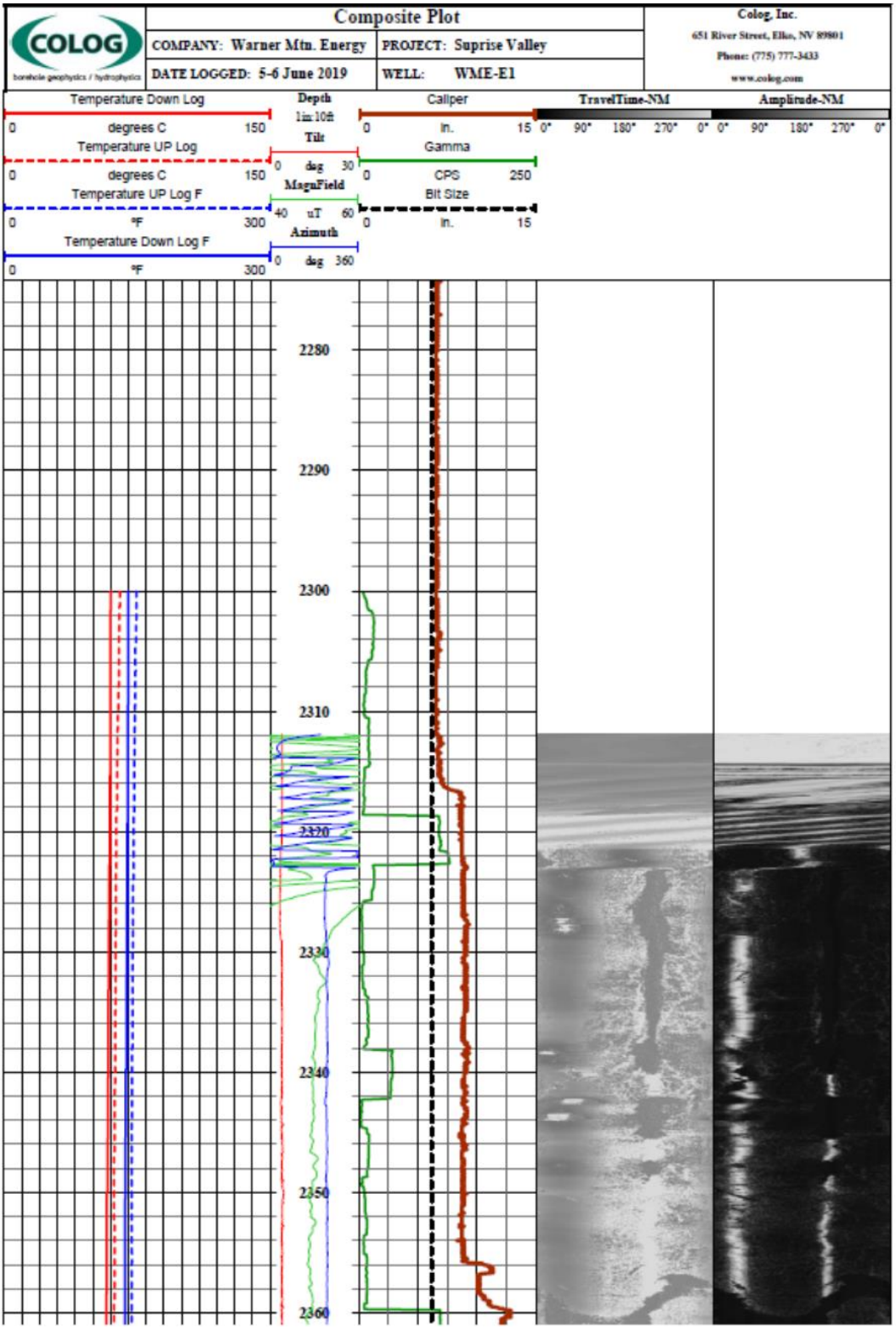

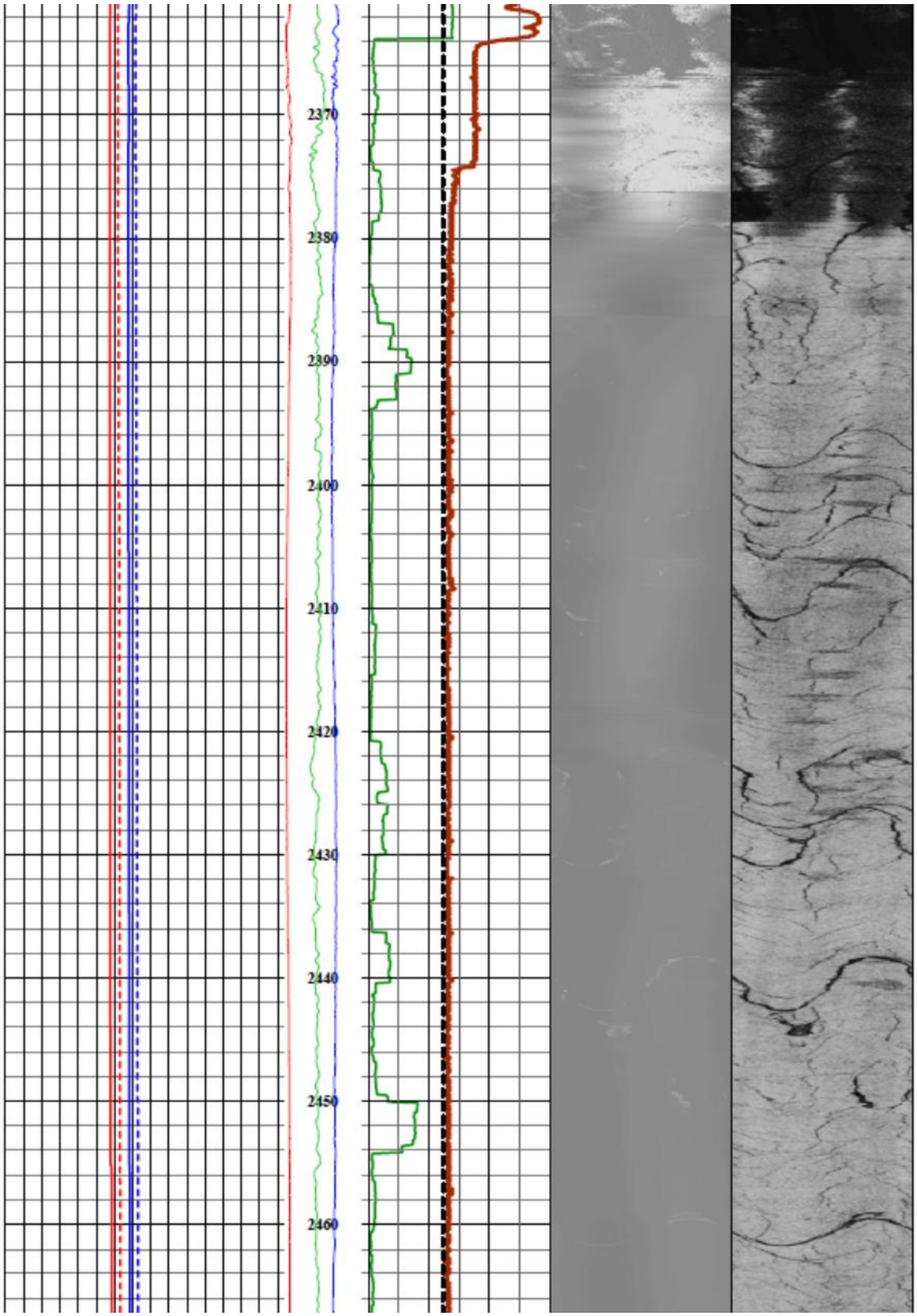
2370
2380
2390
2400
2410
2420
2430
2440
2450
2460

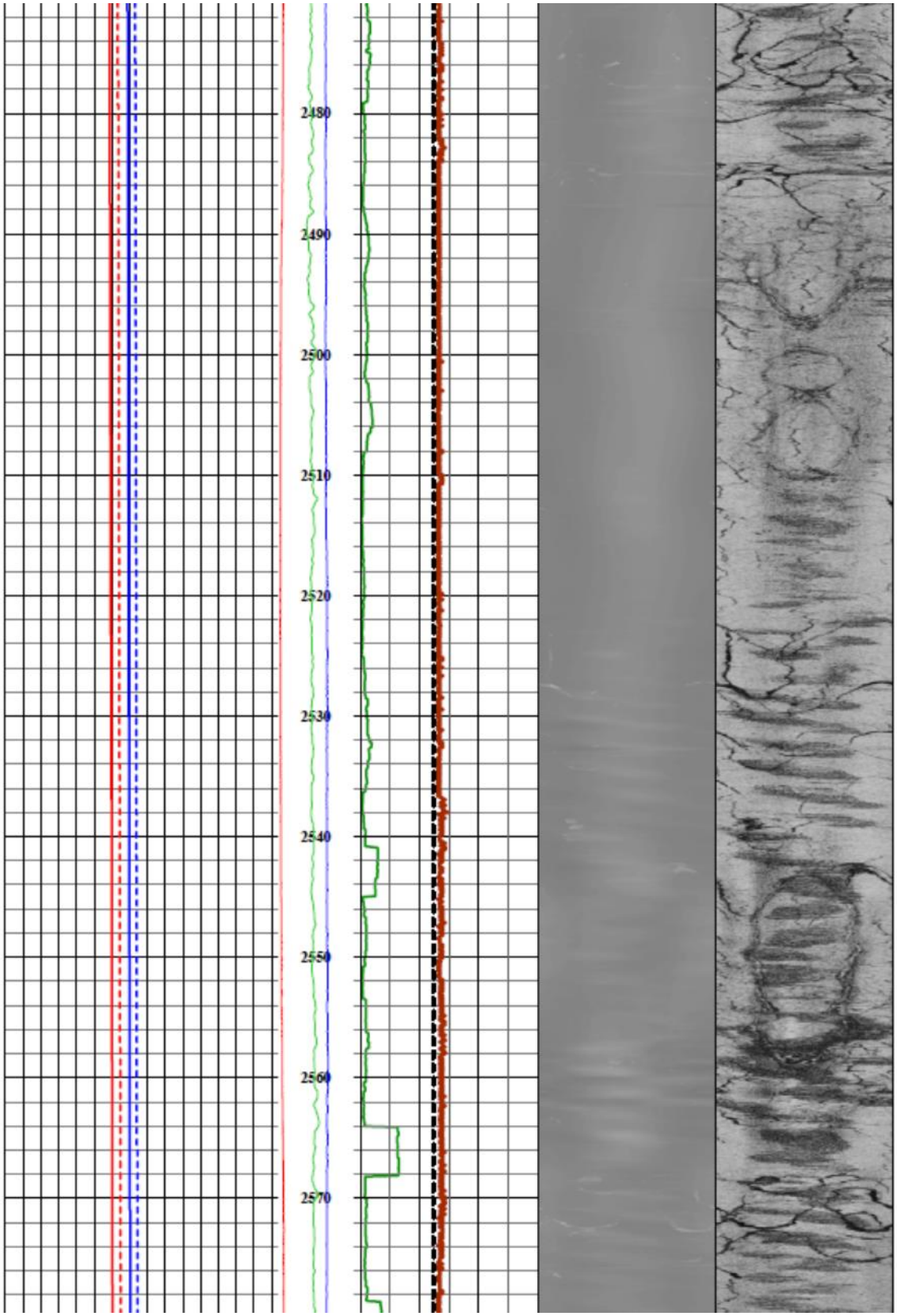
2480
2490
2500
2510
2520
2530
2540
2550
2560
2570

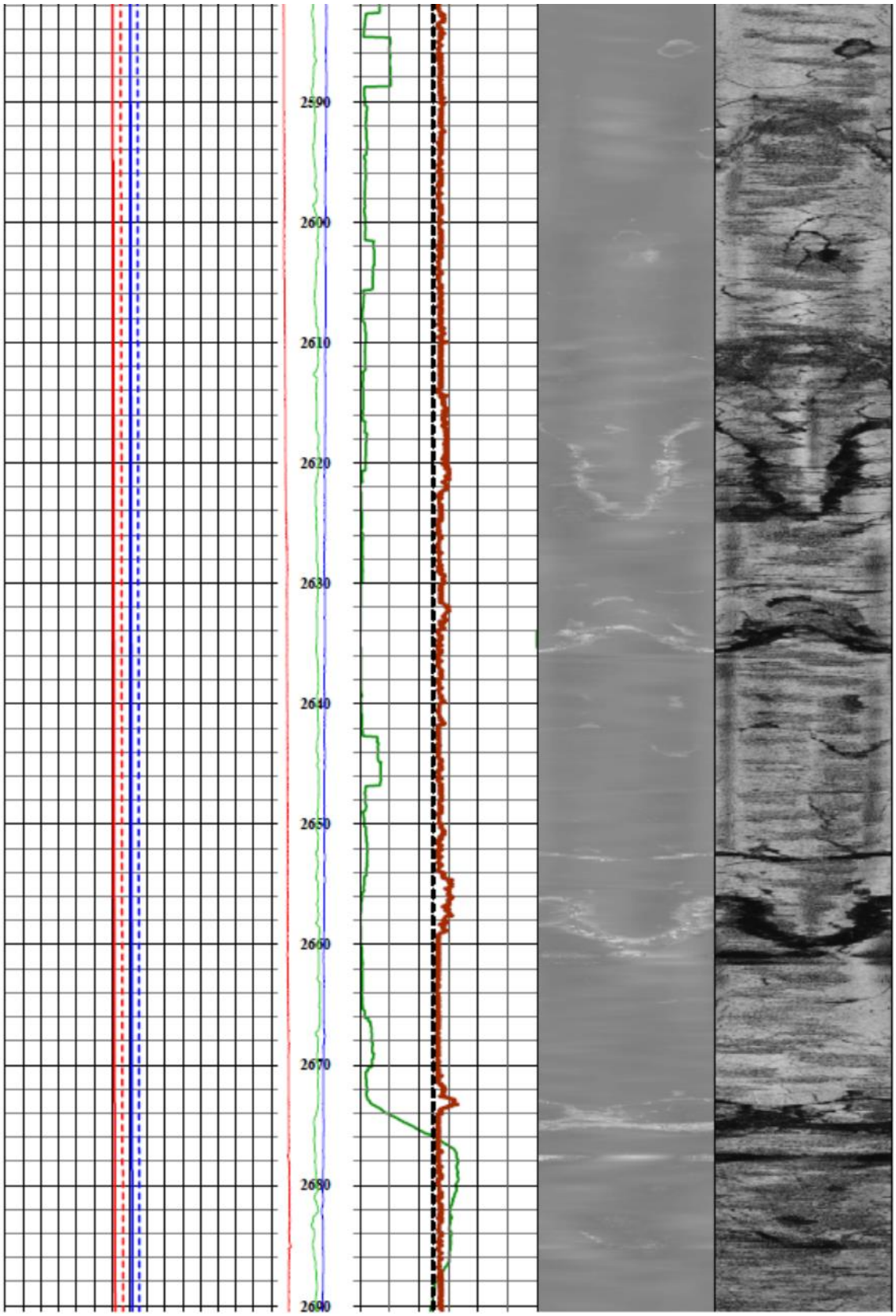
2590
2600
2610
2620
2630
2640
2650
2660
2670
2680
2690

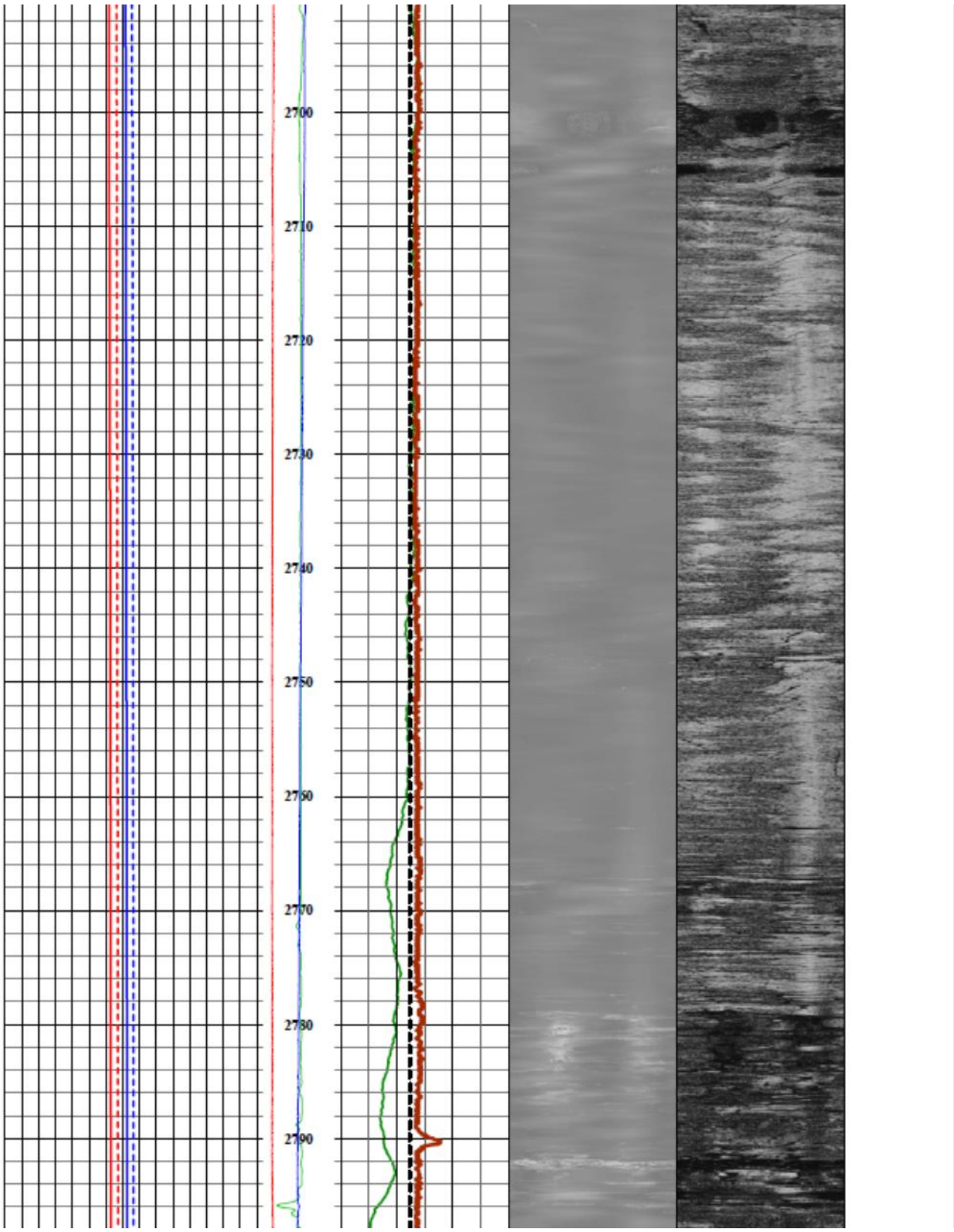
2700
2710
2720
2730
2740
2750
2760
2770
2780
2790

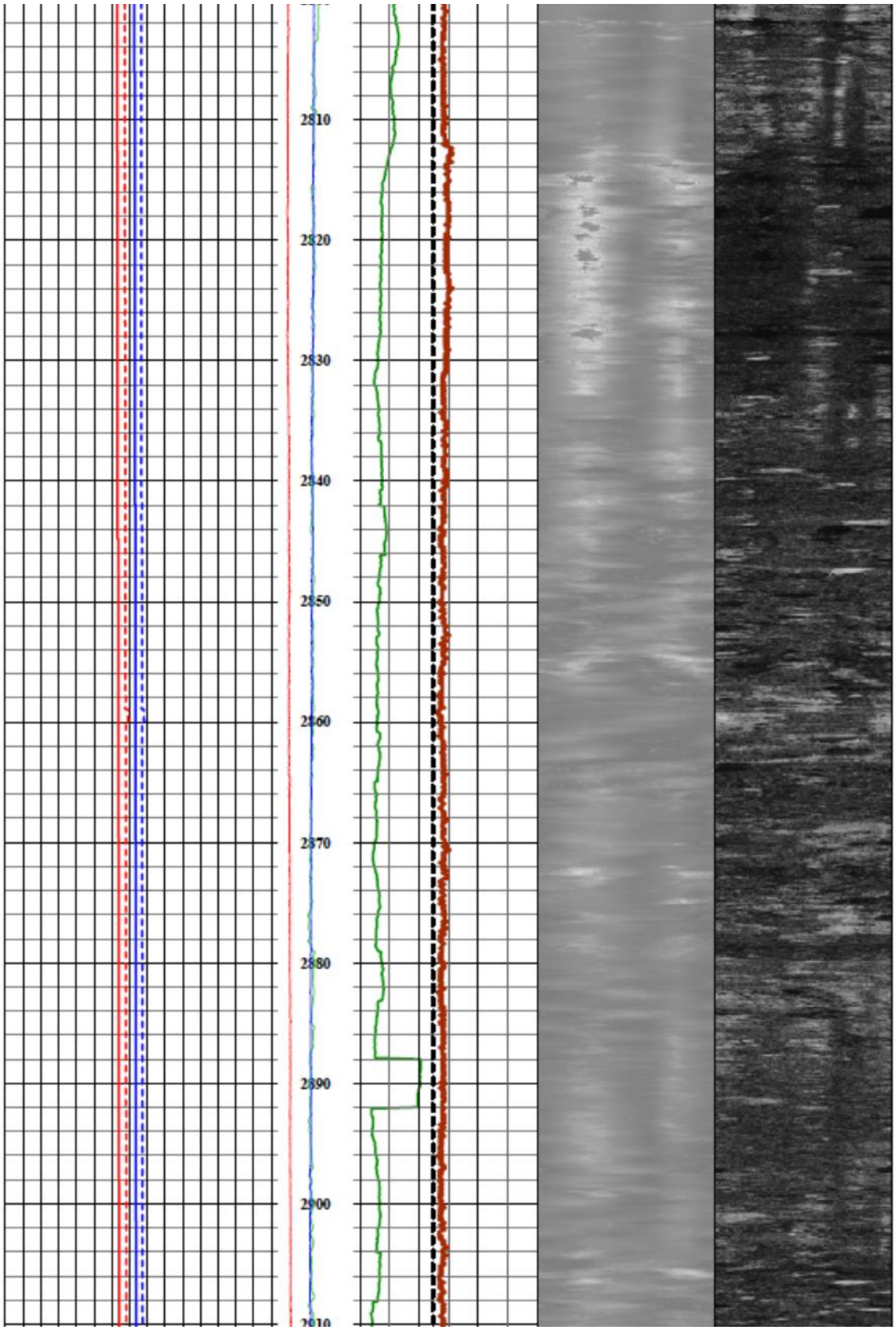
2510
2520
2530
2540
2550
2560
2570
2580
2590
2600

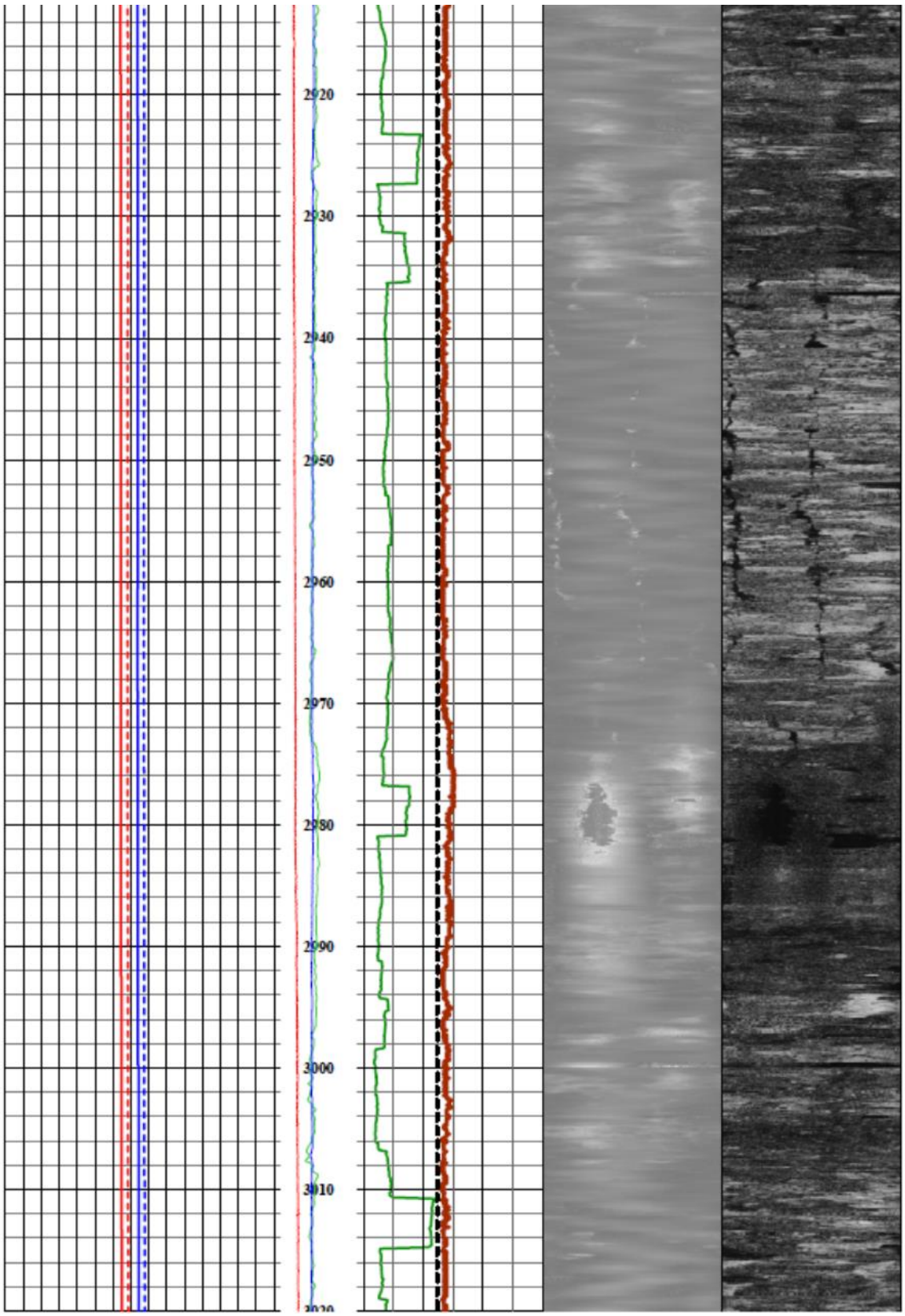
2920
2930
2940
2950
2960
2970
2980
2990
3000
3010

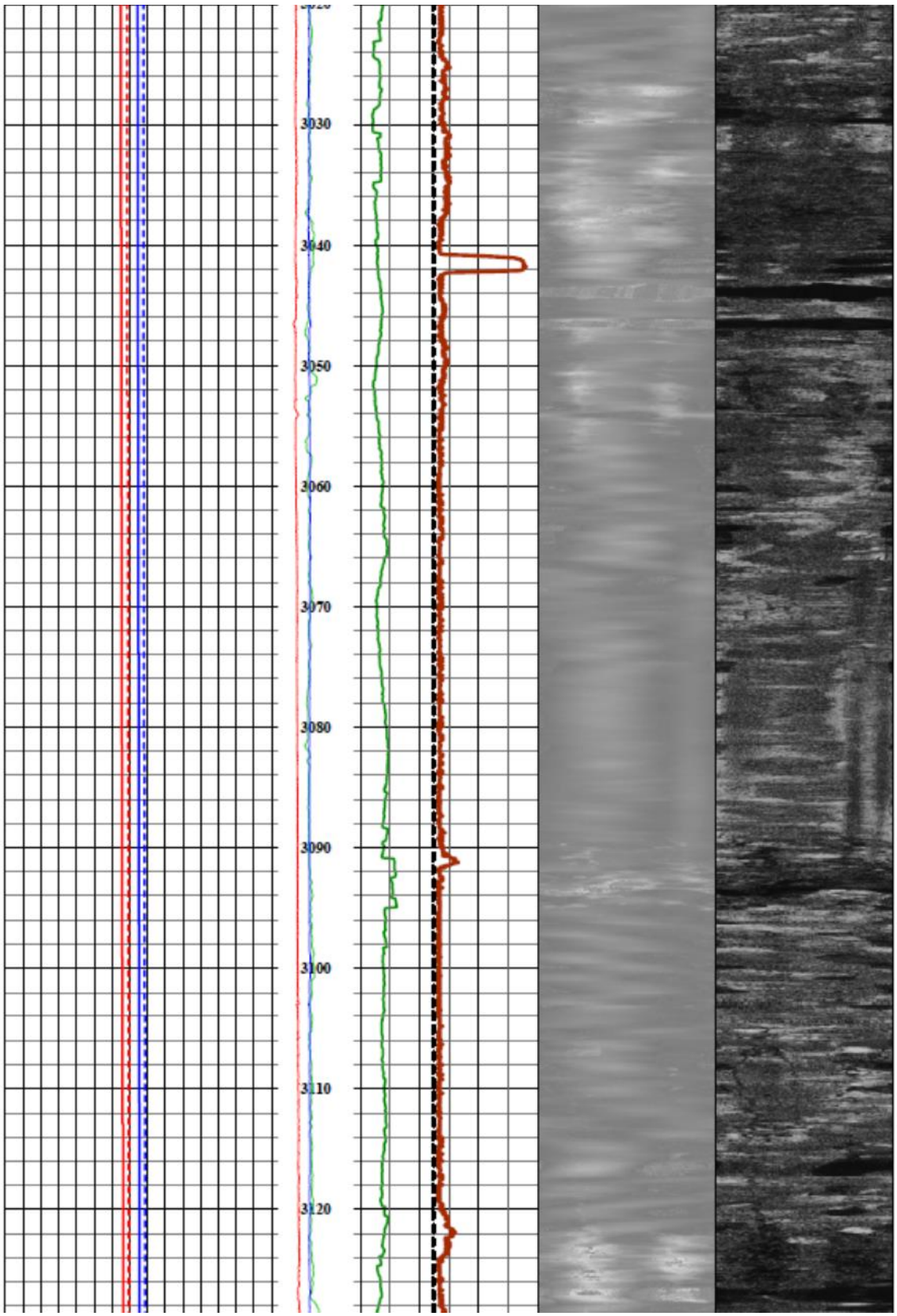
3030
3040
3050
3060
3070
3080
3090
3100
3110
3120

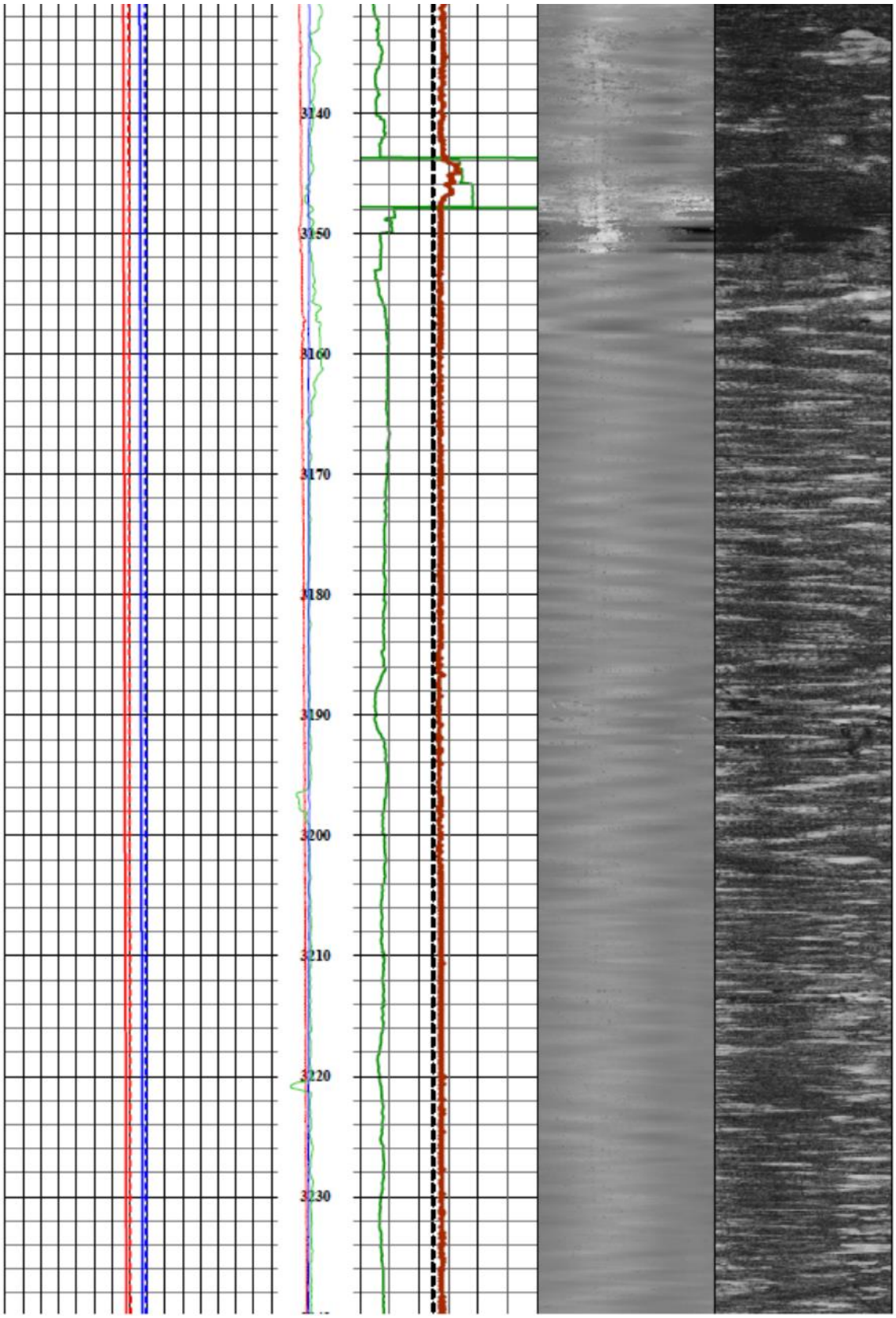
3140
3150
3160
3170
3180
3190
3200
3210
3220
3230

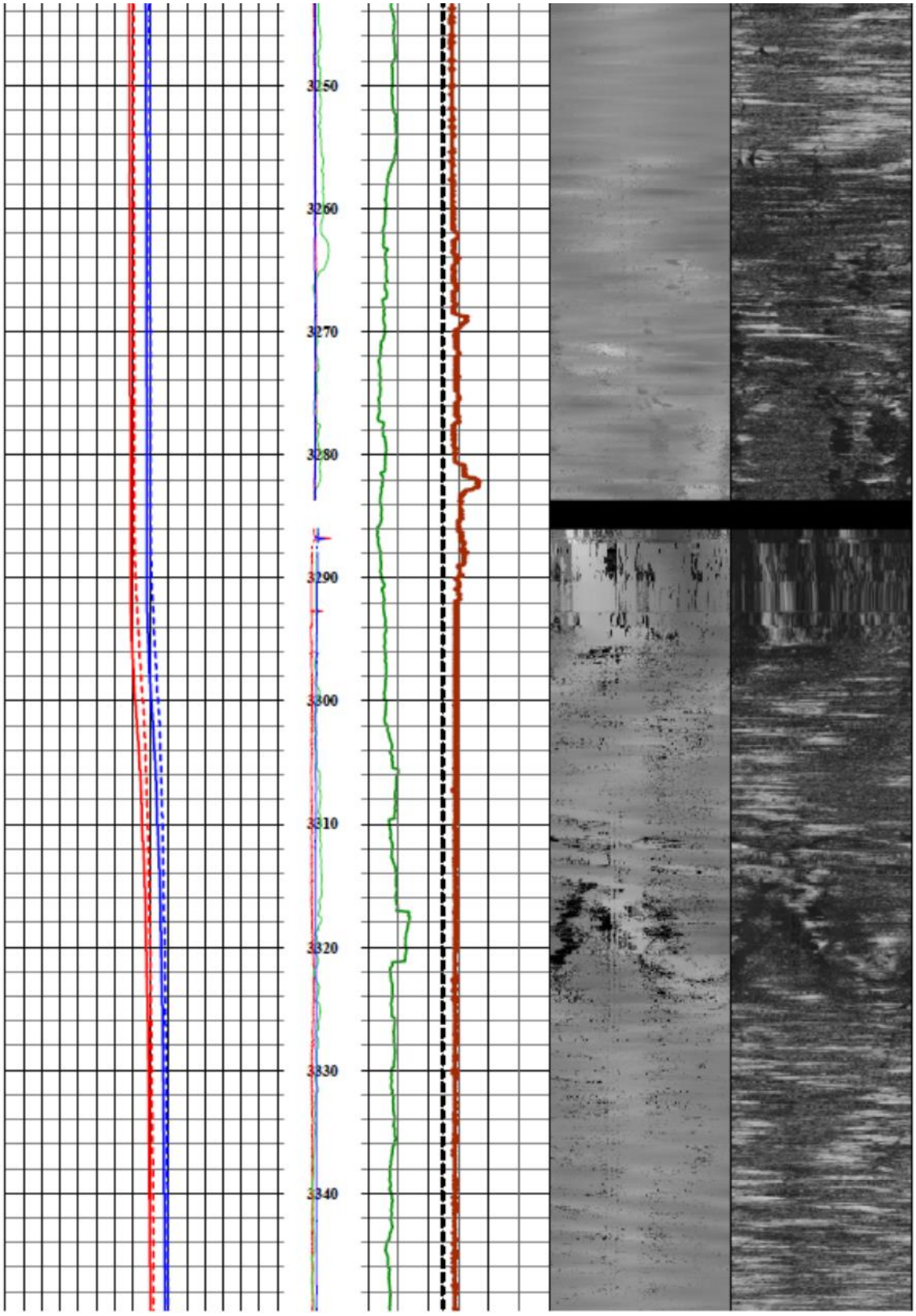
3250
3260
3270
3280
3290
3300
3310
3320
3330
3340

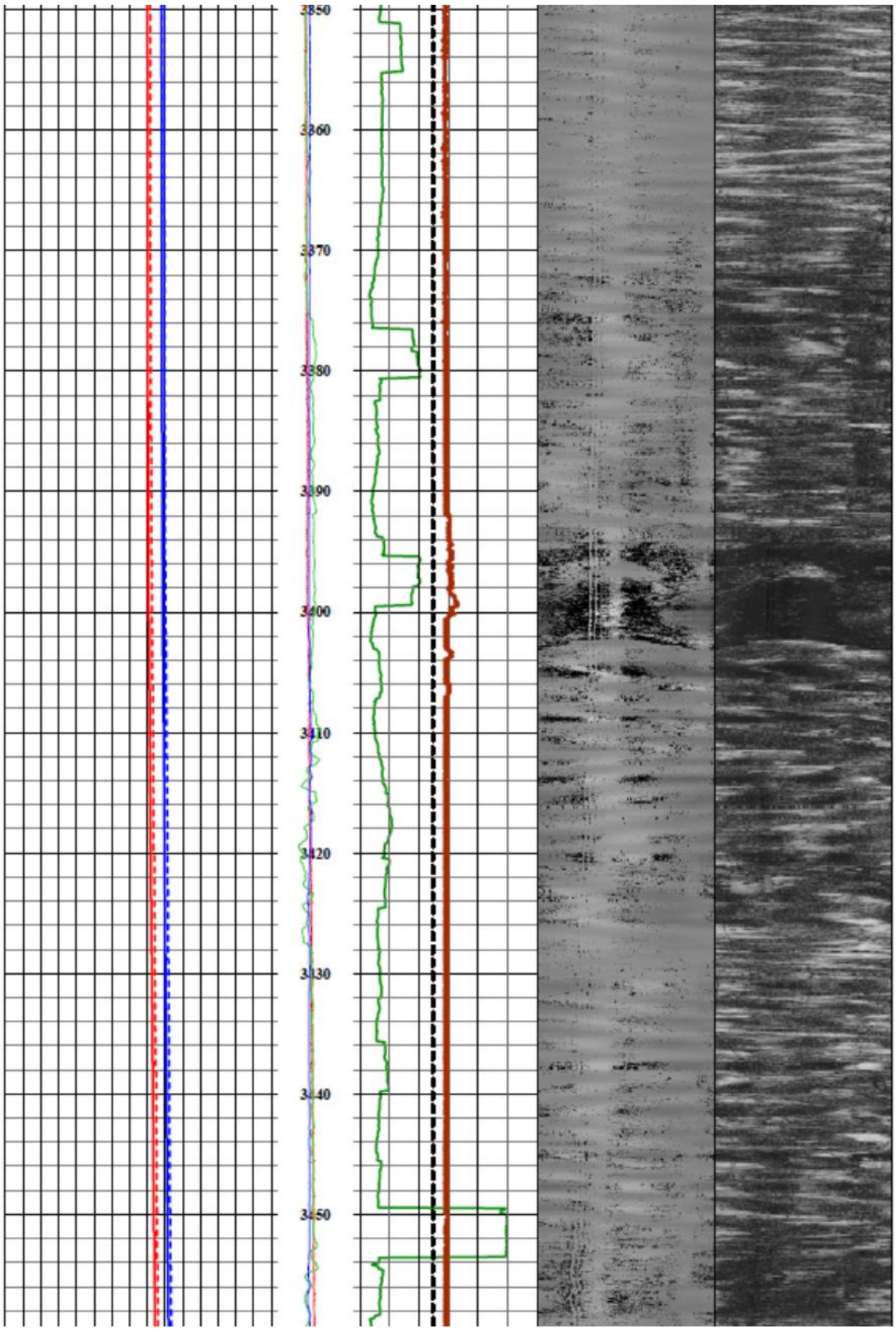
3350
3360
3370
3380
3390
3400
3410
3420
3430
3440
3450

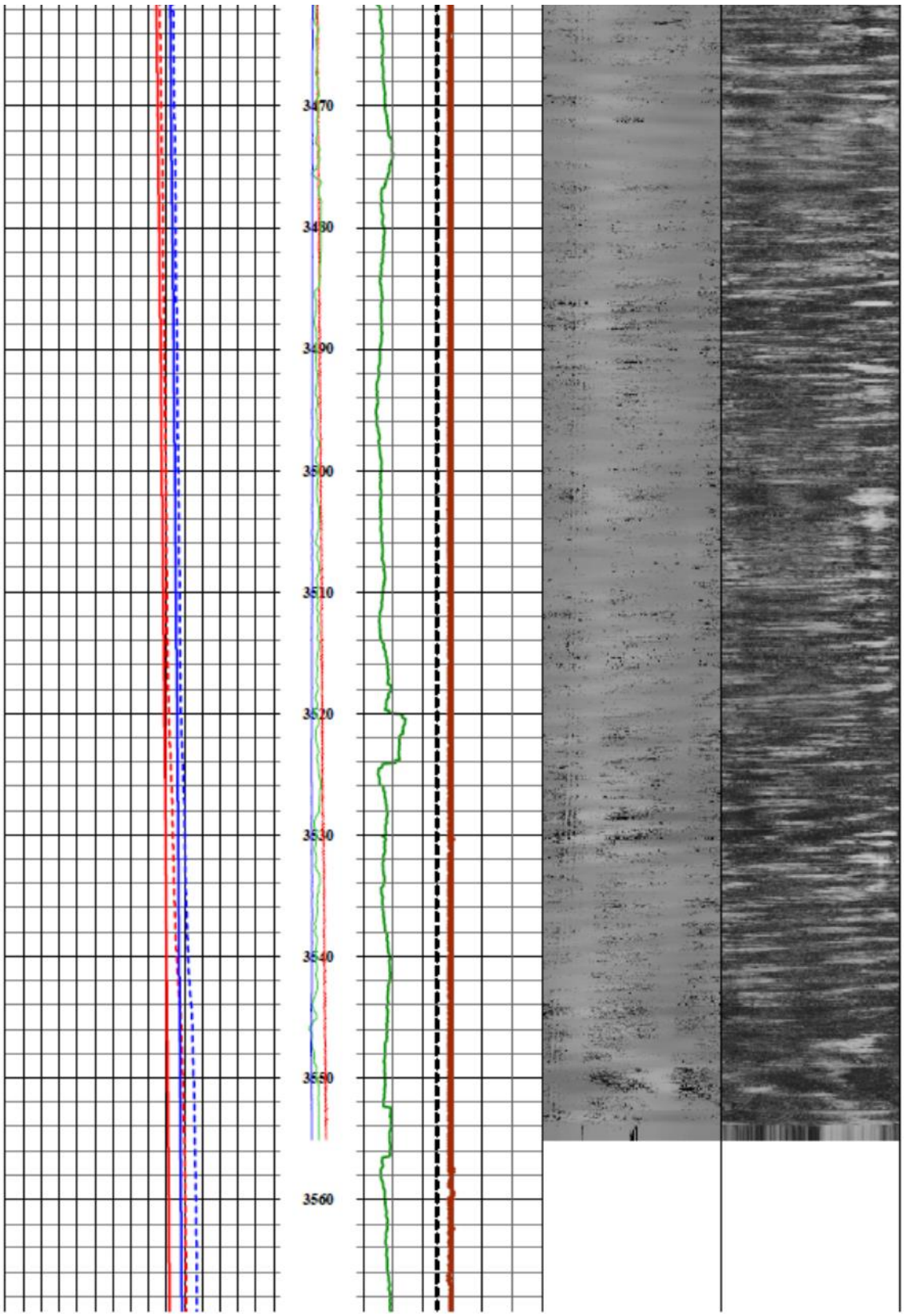
3470
3480
3490
3500
3510
3520
3530
3540
3550
3560

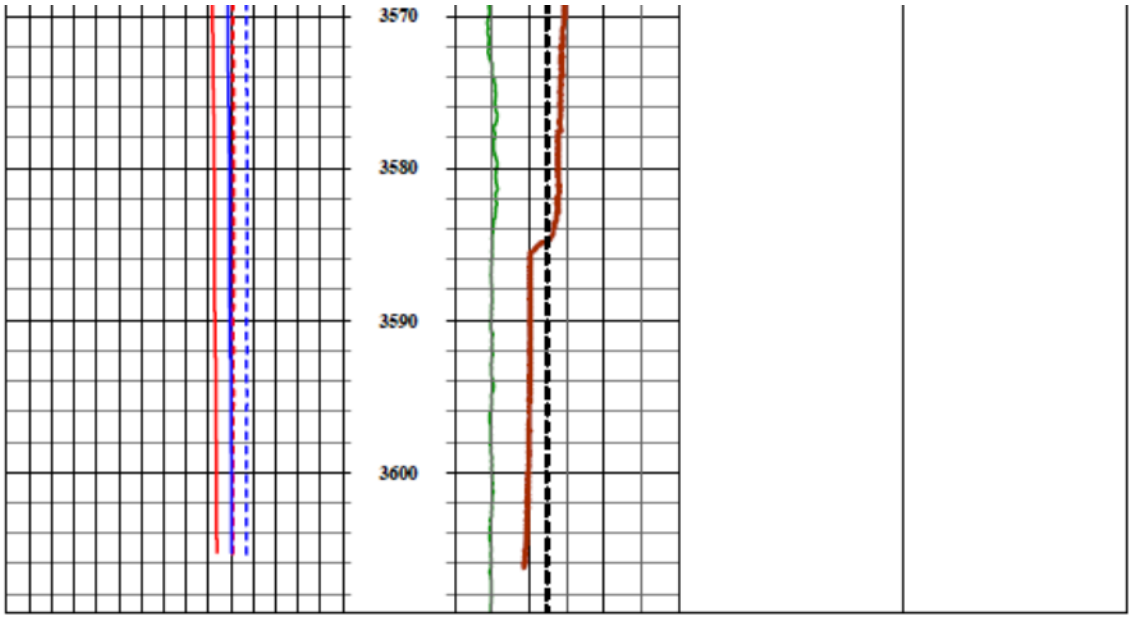
3570
3580
3590
3600

APPENDIX B:
WME-E1 Geophysical Interpreted Field Print

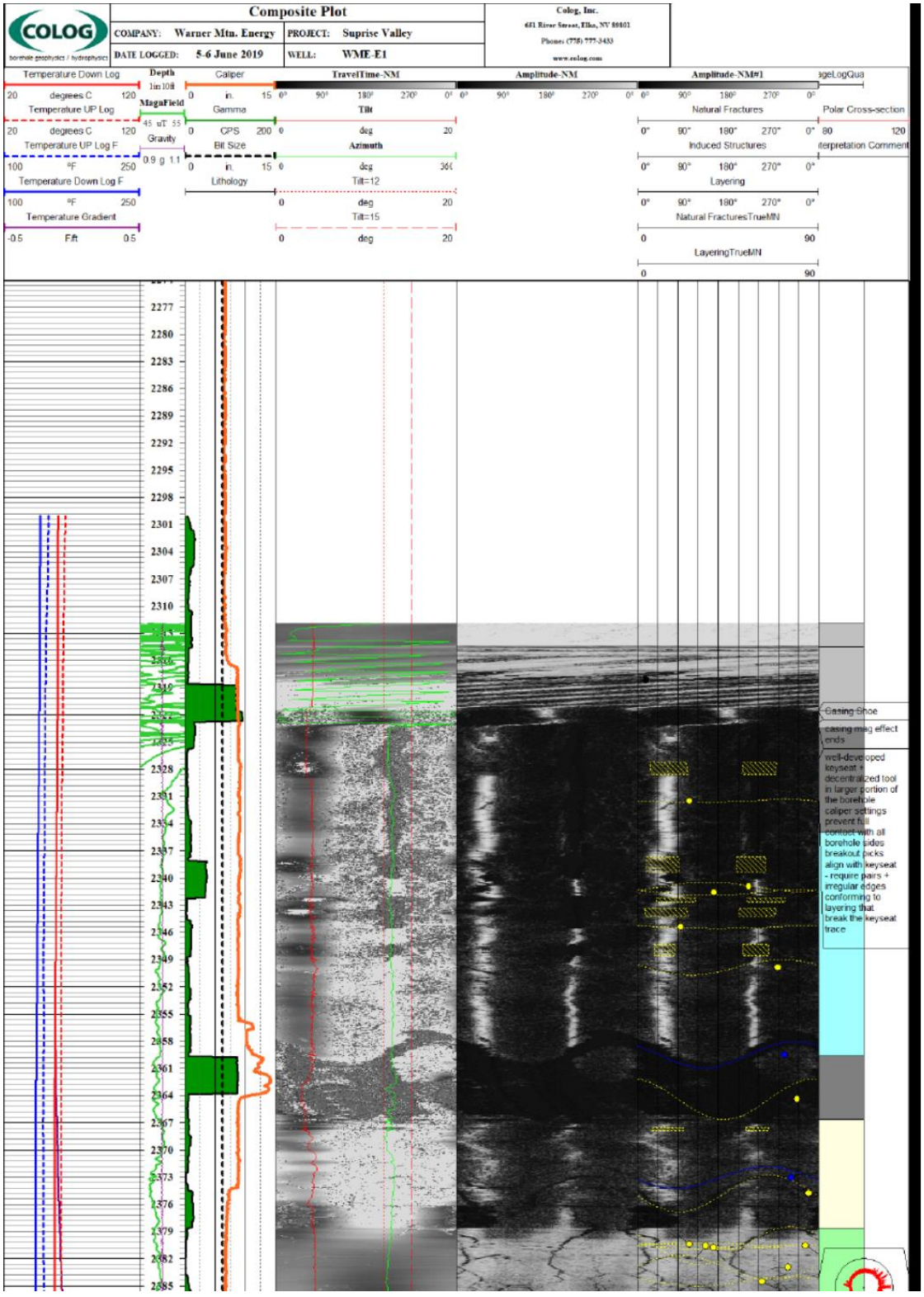

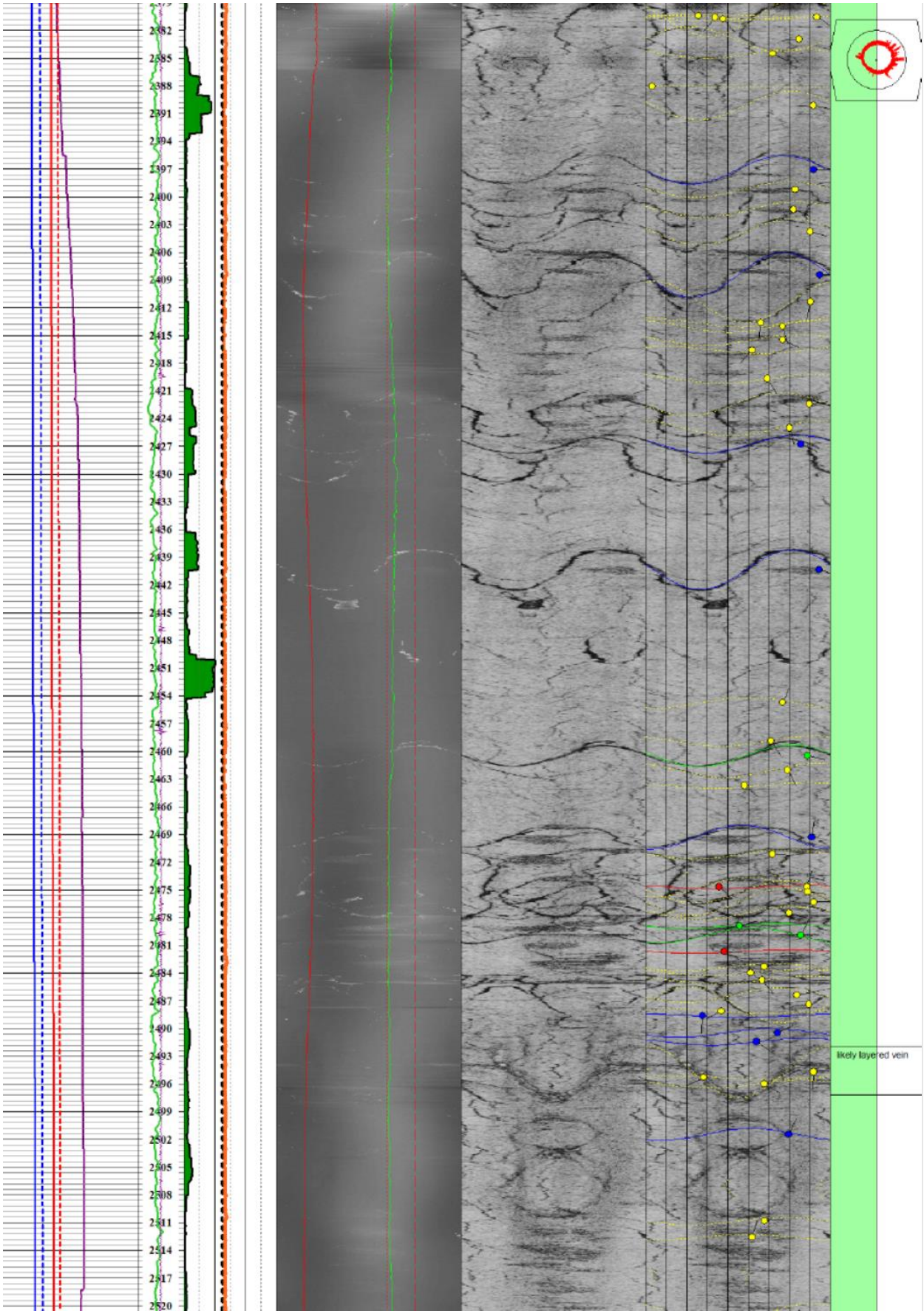

B-2

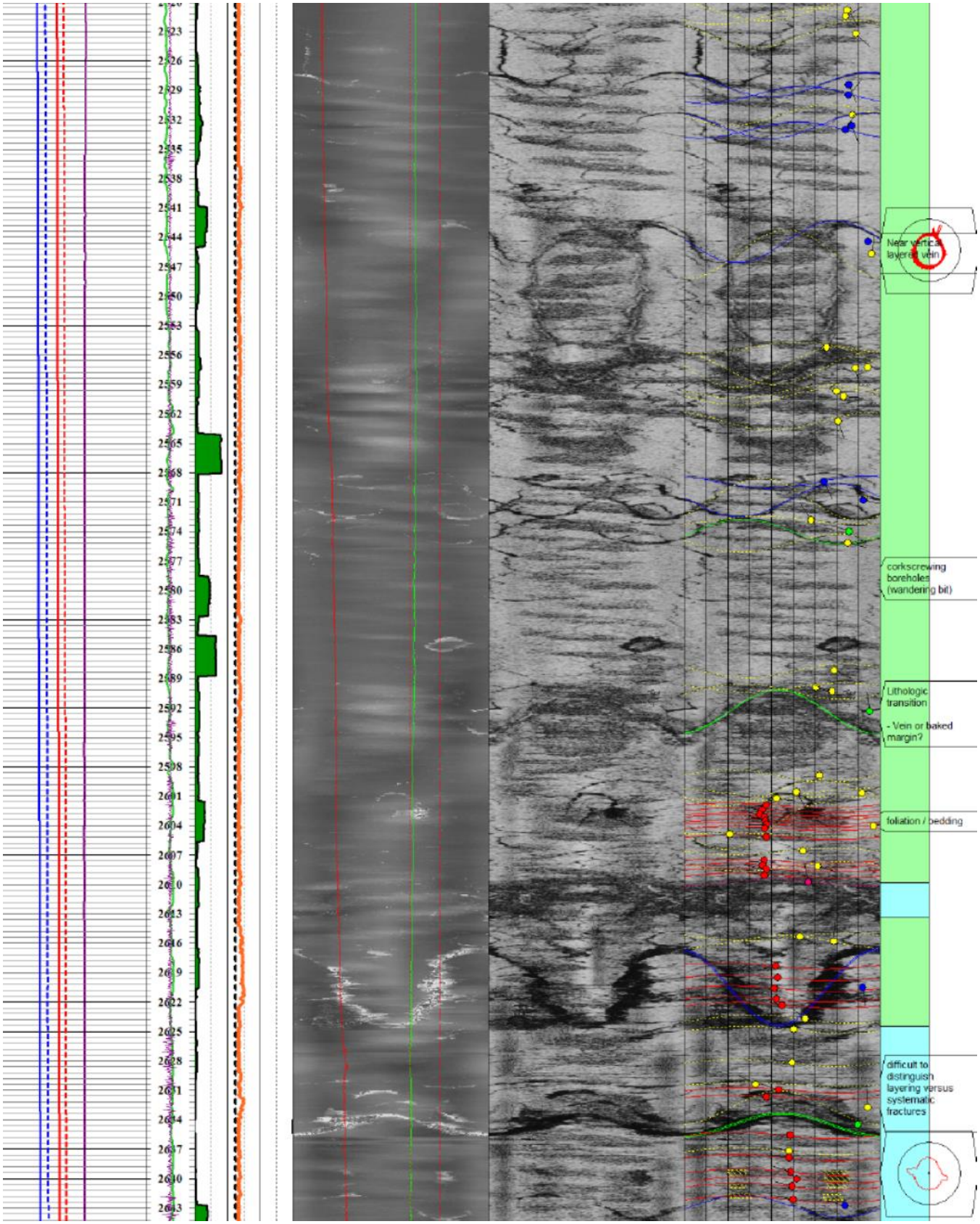
Near vertical layered vein
corkscrewing boreholes (wandering bit)
Lithologic transition
- Vein or baked margin?
foliation / bedding
difficult to distinguish layering versus systematic fractures

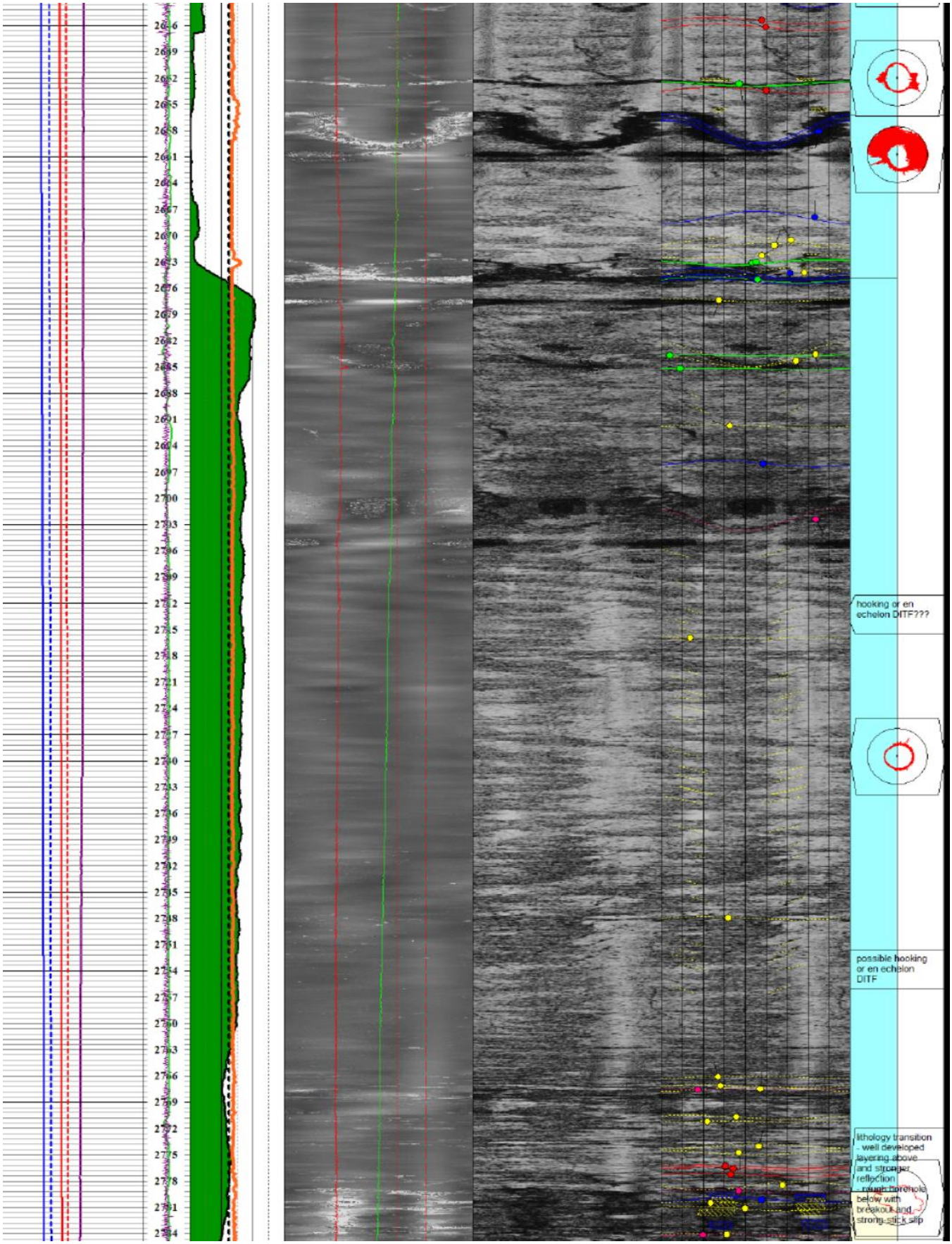
hooking or en echelon DITF???
possible hooking or en echelon DITF
lithology transition - well developed layering above and stronger reflection - rough borehole below with breakout and strong stick slip

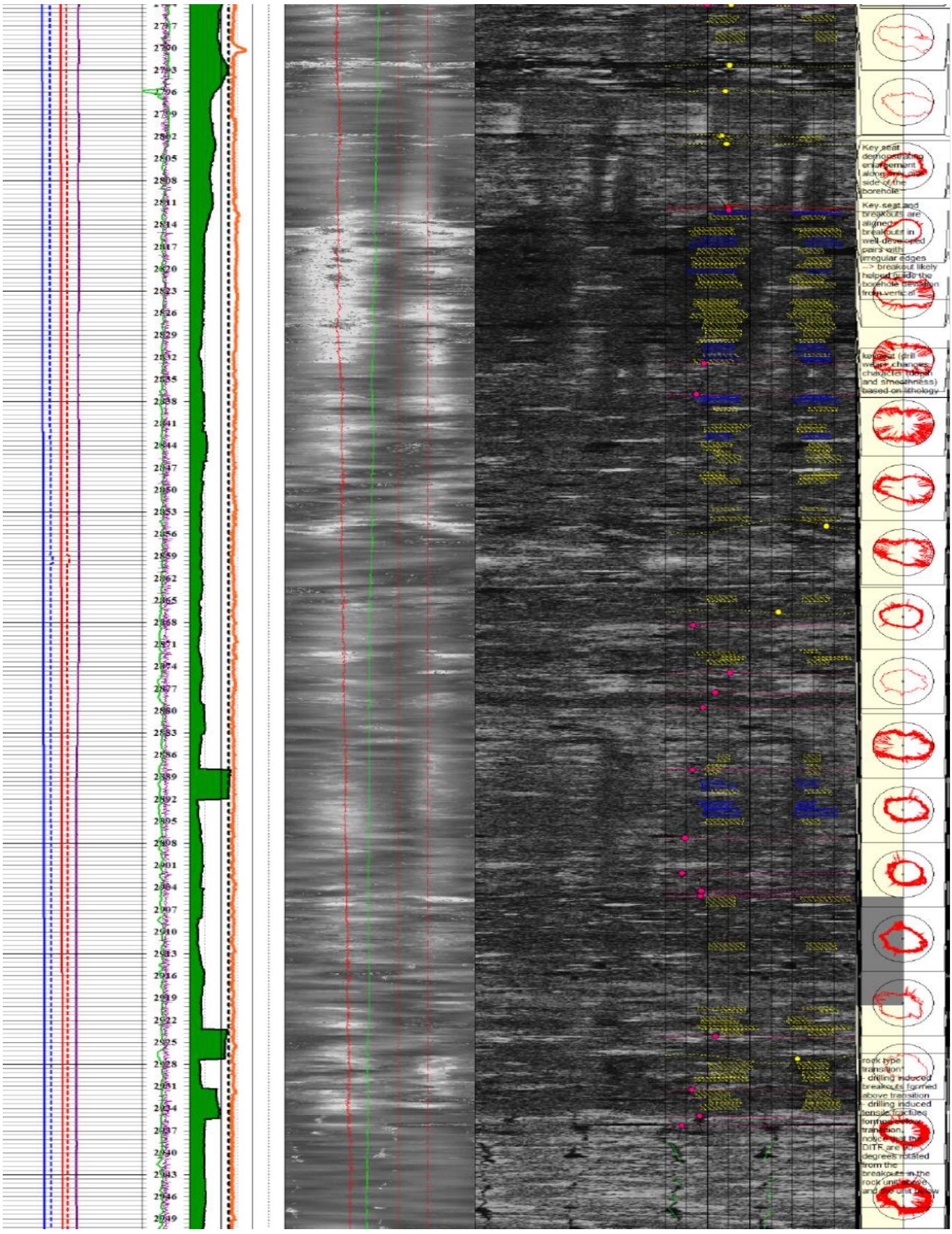
Key seat demonstrating enlargement along one side of the borehole
Key seat and breakouts are aligned
breakouts in well developed pairs with irregular edges
--> breakout likely helped guide the borehole deviation from vertical
rock type transition
- drilling induced breakouts formed above transition
- drilling induced tensile fractures formed below transition
notice that the DITF are 90 degrees rotated from the breakouts in the rock unit above and below

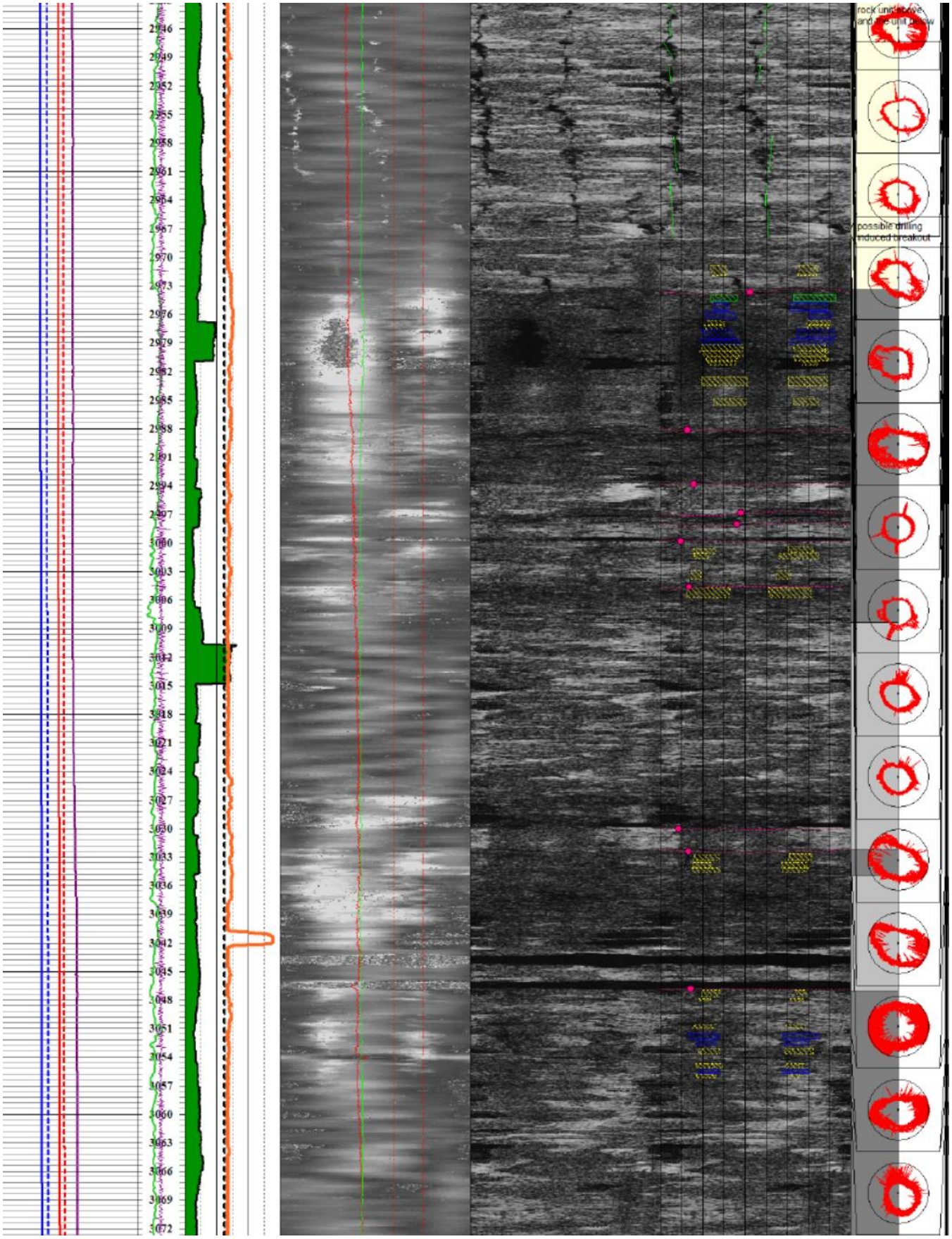
rock unit above
and die unit below
possible drilling
induced breakout

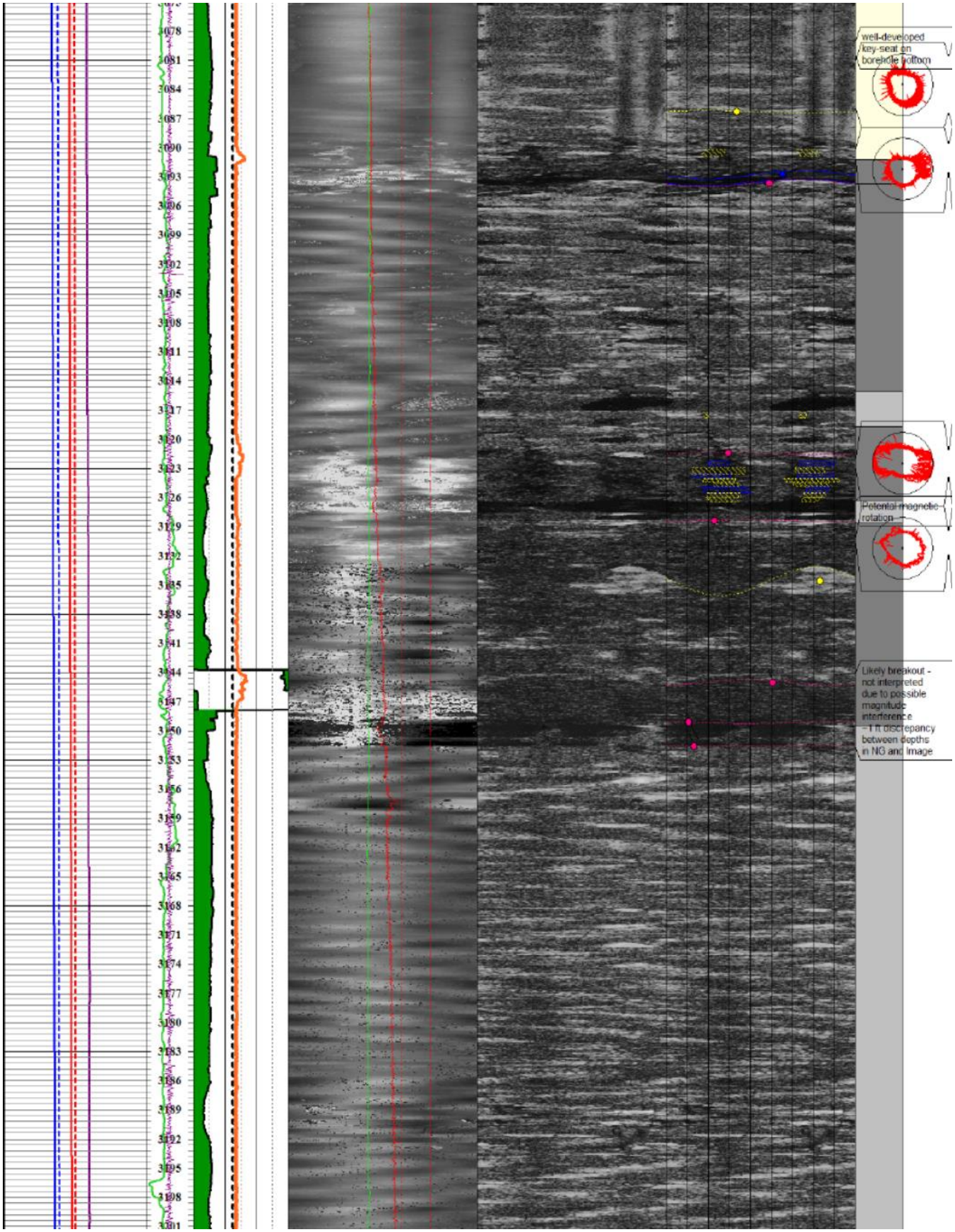
well-developed key-seat on borehole bottom
Potential magnetic rotation
Likely breakout - not interpreted due to possible magnitude interference - 1 ft discrepancy between depths in NG and Image

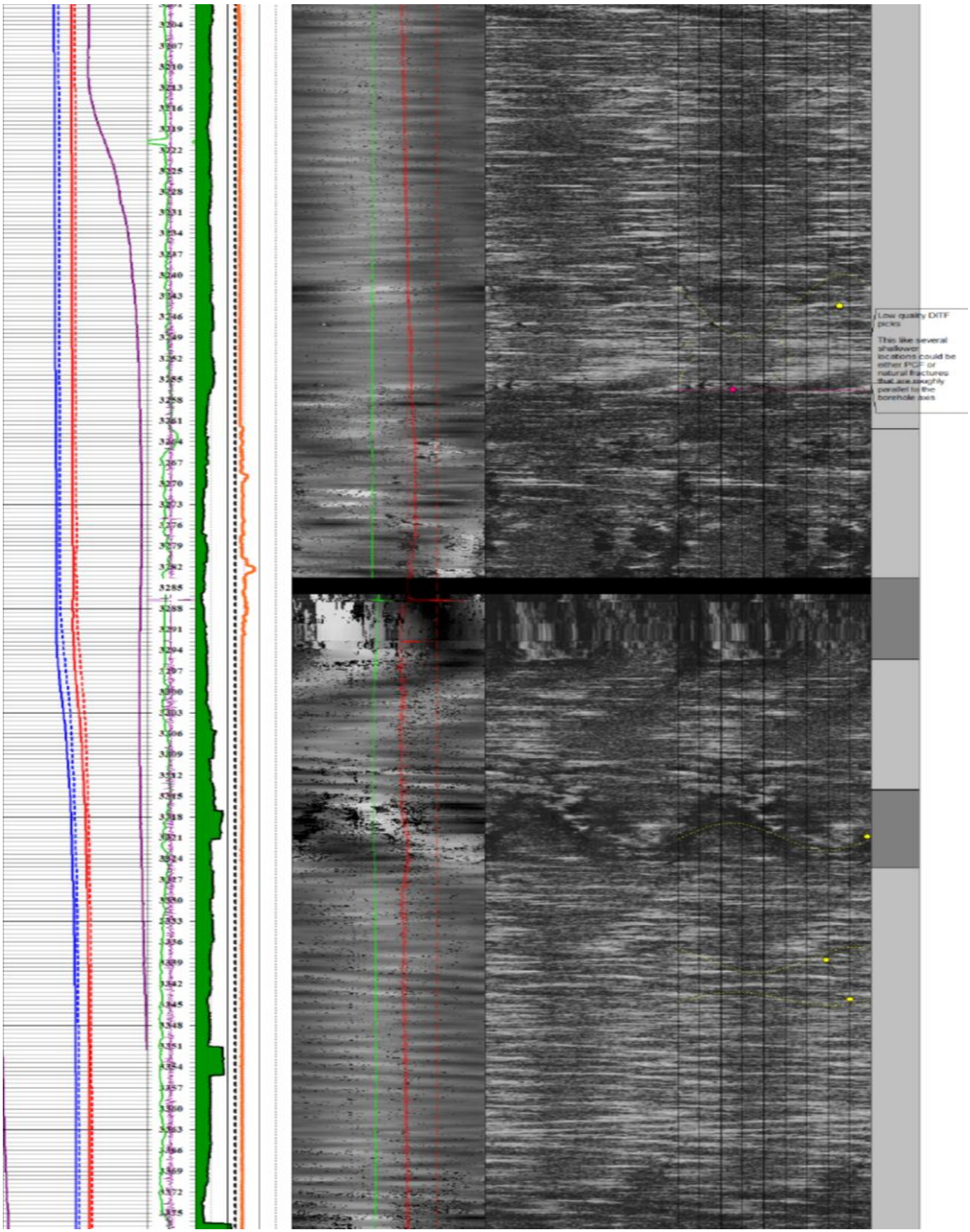
Low quality DITF picks
This like several shallower locations could be either PCF or natural fractures that are roughly parallel to the borehole axes

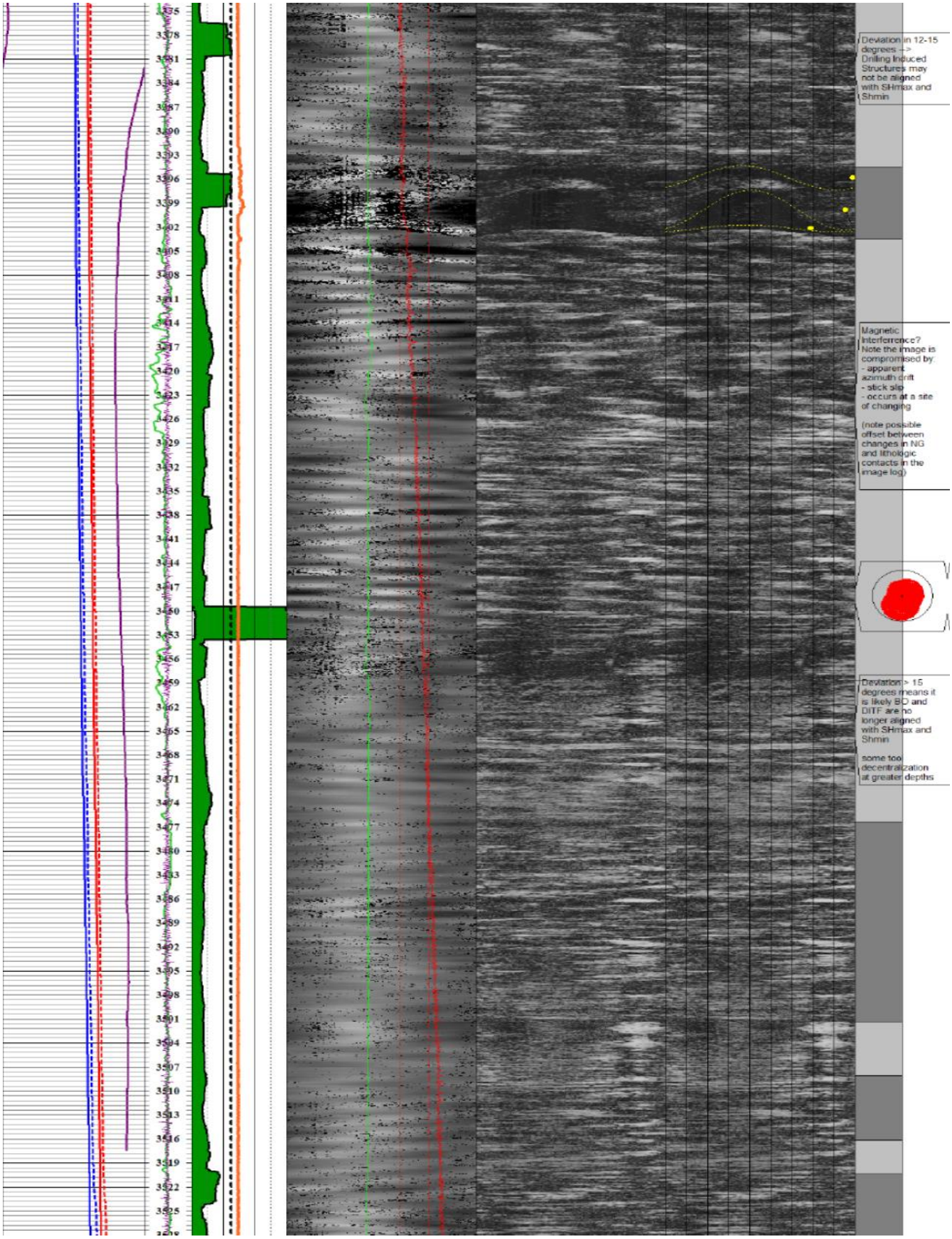
Deviation in 12-15 degrees --> Drilling Induced Structures may not be aligned with SHmax and Shmin
Magnetic Interferrence? Note the image is compromised by - apparent azimuth drift - stick slip - occurs at a site of changing
(note possible offset between changes in NG and lithologic contacts in the image log)
Deviation > 15 degrees means it is likely BO and DITF are no longer aligned with SHmax and Shmin
some too decentralization at greater depths

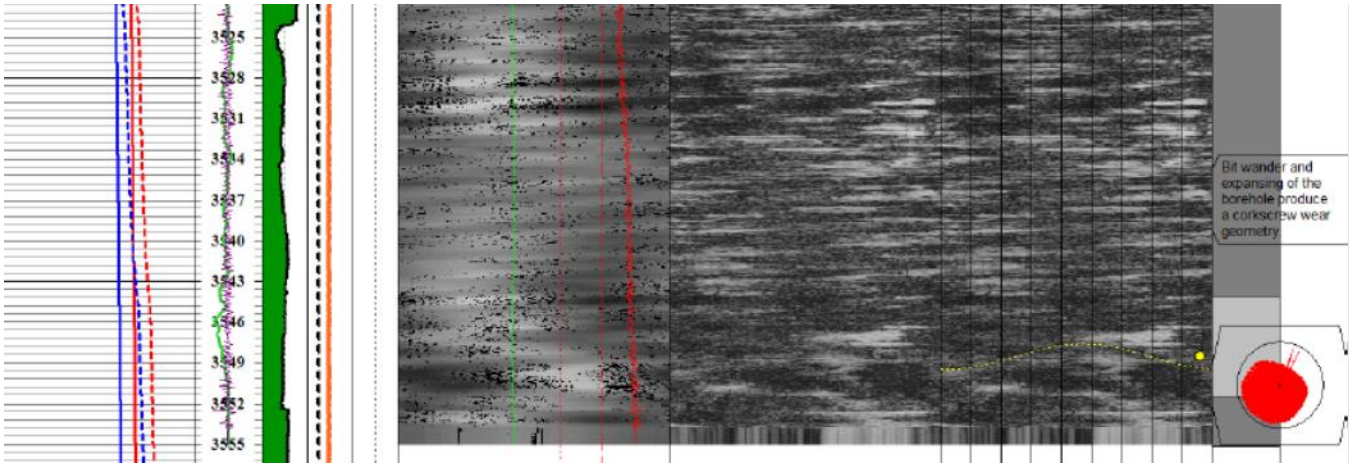
3525
3528
3531
3534
3537
3540
3543
3546
3549
3552
3555
Bit wander and expansing of the borehole produce a corkscrew wear geometry